ISTANBUL TECHNICAL UNIVERSITY ★ GRADUATE SCHOOL

BIOSYNTHESIS OF PIGMENT BY BACTERIA ISOLATED FROM ANTARCTICA

M.Sc. THESIS

Gülden AÇIL

Department of Polar Sciences

Polar Sciences Programme

DECEMBER 2025

ISTANBUL TECHNICAL UNIVERSITY ★ GRADUATE SCHOOL

BIOSYNTHESIS OF PIGMENT BY BACTERIA ISOLATED FROM ANTARCTICA

M.Sc. THESIS

Gülden AÇIL
(531221003)

Department of Polar Sciences

Polar Sciences Programme

Thesis Advisor: Prof. Dr. Fatma Elif GENCELİ GÜNER

DECEMBER 2025

ISTANBUL TEKNİK ÜNİVERSİTESİ ★ LİSANSÜSTÜ EĞİTİM ENSTİTÜSÜ

ANTARKTİKA'DAN İZOLE EDİLEN BAKTERİLERDEN PİGMENT BİYOSENTEZİ

YÜKSEK LİSANS TEZİ

Gülden AÇIL
(531221003)

Kutup Bilimleri Anabilim Dalı

Kutup Bilimleri Programı

Tez Danışmanı: Prof. Dr. Fatma Elif GENCELİ GÜNER

ARALIK 2025

Gülden AÇIL, a M.Sc student of ITU Graduate School, ID 531221003, successfully defended the thesis entitled "BIOSYNTHESIS OF PIGMENT BY BACTERIA ISOLATED FROM ANTARCTICA", which she prepared after fulfilling the requirements specified in the associated legislations, before the jury whose signatures are below.

Thesis Advisor : **Prof. Dr. Fatma Elif GENCELİ GÜNER** .....
Istanbul Technical University

Jury Members : **Assist. Prof. Dr. Ayşe Banu KOCAAĞA** .....
Istanbul Technical University

Assist. Prof. Dr. Cansu ÜLKER TURAN .....
Gebze Technical University

Date of Submission : 06 December 2025
Date of Defense : 25 December 2025

To Erdinç, my guiding light,

FOREWORD

Bacteria adapted to Antarctica's extreme conditions represent promising candidates for sustainable bio-pigment production. This study investigated the pigment production potential of Antarctic isolates and evaluated the biotechnological applications of these natural compounds. Their cold tolerance and metabolic diversity highlight their potential for future eco-friendly innovations.

It is with heartfelt appreciation that I extend my deepest gratitude to Prof. Dr. Fatma Elif GENCELI GÜNER, my esteemed advisor, whose unwavering support, understanding, and encouraging presence have profoundly shaped every stage of my graduate journey. I am also grateful to Prof. Dr. Sandra PUCCIARELLI from the Biotechnology Laboratory of the University of Camerino (UNICAM) for her support in my research on the two bacterial strains. I would like to express my sincere gratitude to my esteemed professor Assoc. Prof. Nil ÖZBEK for performing the FTIR analyses and to Assoc. Prof. Cüneyt Hüseyin ÜNLÜ for his invaluable support in the NMR and TLC analyses.

I sincerely thank Research Assistant Gamze NEŞE ÖZCAN, my first sister in science and life, for her invaluable support through every challenge and unforgettable shared experiences, including our time as housemates and travel companions in Italy. I also deeply appreciate Research Assistant Sena ALTUN, my second sister, whose integrity, warmth, and eagerness to share knowledge have greatly enriched this journey.

To my beloved husband Erdem AÇIL, whose strength, unwavering support, and calm presence have been my refuge in every difficult moment. Thank you for always being there, with patience, wisdom, and endless encouragement.

To my beloved brother, Erdinç KARA, every moment shared with you has been unparalleled in its meaning. I sincerely hope we continue to walk hand in hand through infinite lifetimes. You are my most precious treasure, and I extend my deepest gratitude for everything.

December 2025

Gülden AÇIL
(Polar Scientist)

TABLE OF CONTENTS

Page

ABBREVIATIONS

Adj MS : Adjusted mean square
Adj SS : Adjusted sum of squares
CHYB / CrtZ : β-carotene hydroxylase
CHYE : α-carotene ε-ring hydroxylase
Coef : Regression coefficient
CrtB : Phytoene synthase in bacteria and microorganisms
CRTISO : Carotenoid isomerase
DAB : 2,4-diaminobutyric acid
DF : Degrees of freedom
DHIR : 3,3'-dihydroxyisorenieratene
DPG : Diphosphatidylglycerol
DPPH : 2,2-diphenyl-1-picrylhydrazyl
FD&C : Food, drug, and cosmetic colorants
GGPP : Geranylgeranyl pyrophosphate
GL : Glycolipids
HPLC : High performance liquid chromatography
IPP : Isopentenyl pyrophosphate
IR : Isorenieratene
LYCB : Lycopene β-cyclase
LYCE : Lycopene ε-cyclase
MEP : Methylerythritol phosphate pathway
PDS : Phytoene desaturase
PG : Phosphatidylglycerol
PRESS : Predicted residual sum of squares
PSY : Phytoene synthase in plants
ROS : Reactive oxygen species
R-Sq : Coefficient of determination (%)
R-Sq (adj) : Adjusted coefficient of determination (%)
R-Sq (pred) : Predicted coefficient of determination (%)
SE Coef : Standard error of the coefficient

Seq SS **:** Sequential sum of squares

TLC **:** Thin layer chromatography

UV **:** Ultraviolet

UVA **:** Ultraviolet A (315–400 nm)

UVB **:** Ultraviolet B (280–315 nm)

UVC **:** Ultraviolet C (100–280 nm)

ZDS **:** ζ-Carotene desaturase

SYMBOLS

F	**:** Variance ratio
P	**:** Significance level (p-value)
R^2	**:** Coefficient of determination
R^2pred	**:** Predictive coefficient of determination
S	**:** Standard error of the regression
T	**:** t-statistic value

LIST OF TABLES

Page

LIST OF FIGURES

Page

BIOSYNTHESIS OF PIGMENT BY BACTERIA ISOLATED FROM ANTARCTICA

SUMMARY

Known as one of the world's most extreme environments, Antarctica is a region that has attracted researchers from around the world, boasting dozens of creatures, structures, and formations yet to be discovered. Human technology, as it has developed to date, has the capacity to gradually expand our horizons beyond the known by unlocking the mysteries of this continent. It serves as a guiding light for us in sustainable living and clean energy technologies, which are among the most important issues of our time, as well as in the protection of people and the planet. Every study done for this continent is a treasure, providing inspiration and ideas to advance deep research, learning and technology in every field, from microorganisms and metabolites to ocean life and its diverse habitats, from geological formations to the rich structure of its minerals. This study emerged as a result of interest and curiosity in the microorganisms living on this remarkable continent.

Antarctica hosts a diverse range of microbial communities, and the ways these communities adapt to extreme conditions compared to what we might call the world's normally temperate regions is being closely studied today. Due to the microorganisms' easy biodegradability, ease of controlled production in a laboratory setting, and rich variety of contents, scientific research on natural pigments derived from microorganisms has gained momentum in recent years as an alternative to synthetic pigment production. Many studies are focused on improving microbial pigments by bioengineering methods and generating scientific data on the adequate understanding of their metabolic formation pathways and on improving the biotechnological utilization of organic pigments. As a result, technologies based on chemical pigments, which harm humans and the ecosystem, are beginning to give way to natural solutions and transform.

In this study, pigment activities on *Rhodococcus fascians* isolated from ice cores from the Horseshoe, Hovgaard, and Nansen Islands of Antarctica, as well as *Brevibacterium* sp. and *Microbacterium* sp. isolated from the Ross Sea that belong to the Italian Maria Zucchelli Station, are analyzed experimentally. An optimization study (Plackett-Burman Design-PBD) was carried out to investigate the responses of bacteria to medium components and environmental factors, and appropriate pH and temperature values were investigated. To ascertain the chemical structure, FTIR, UV-Vis, NMR, and TLC analyses were carried out. The disk diffusion method was used to test its antibacterial activity, and DPPH (Free Radical Scavenging Test) tests were performed to determine its antioxidant capacity, and the results were shared in this study.

Spectroscopically, the pigment structure obtained from *R. fascians* shows the presence of a carotenoid-based pigment at 456 nm, as reported in the literature. The structure of isorenieratene, a carotenoid-derived pigment, at 405-408 nm in *Brevibacterium* sp., and neurosporene, a carotenoid-derived pigment also reported in previous studies, at

407-417 nm in *Microbacterium* sp., are strikingly similar. An optimization study was conducted to determine the most efficient production conditions for three different bacterial species. The highest total carotenoid concentration was obtained in *Rhodococcus fascians* (485.00 µg/g), followed by *Microbacterium* sp. (179.89 µg/g) and *Brevibacterium* sp. (63.62 µg/g). Pigments were extracted from the isolates and their antimicrobial activities were determined to inhibit both Gram (+) and Gram (-) bacteria. FTIR spectra for pigment production in these three Actinomycete bacterial species confirmed the presence of functional groups associated with carotenoid-like pigments. The FTIR analysis revealed strong O-H, C-H, and C=O stretching vibrations, which supported the pigment structures suggested by the UV-Vis data. DPPH was evaluated in detail for *Rhodococcus fascians* pigment by the free radical scavenging test. DPPH inhibition increased from 17.46% to 84.99%, indicating high antioxidant properties with IC_{50} value = 0.36 µg/µL based on linear regression analysis *(R^2=0.8817).* Further analysis of the chemical structure of the pigment obtained from *R. fascians* using Fourier transform infrared (FTIR) and nuclear magnetic resonance (NMR) spectroscopy revealed that it was a carotenoid pigment of the zeaxanthin and lutein varieties.

Microbial studies conducted in extreme environments like space and Antarctica demonstrate that microorganisms are more adaptable than their counterparts living under normal conditions. Researching Antarctic-origin microorganisms is very valuable in the search for solutions to existing problems in the space environment, from biofilm formation to natural polymers and the use of natural carotenoid pigments. Expeditions to the Moon and Mars will be able to make significant gains in the coming years, such as preventing infections, reducing cell decay, recycling waste, protecting against radiation, and improving food content, thanks to microorganism-based technological solutions.

ANTARKTİKA'DAN İZOLE EDİLEN BAKTERİLERDEN PİGMENT BİYOSENTEZİ

ÖZET

Antarktika, dünyanın en ekstrem koşulları olarak bilinen üzerinde henüz keşfedilmeyi bekleyen onlarca canlı, yapı ve oluşumuyla dünyanın her yerinden araştırmacının odak noktası olan bir bölgedir. Bugüne kadar gelişen insan teknolojisi, bu kıtanın sırlarının çözülmesiyle ufkumuzu adım adım bilinenin ötesinde bir aşamaya taşıma kapasitesi taşımaktadır. Günümüzün en önemli konularından sürdürülebilir yaşam ve temiz enerji teknolojileri ile insan ve gezegene ait koruma çalışmalarında bize yol gösterici bir ışık niteliği taşımaktadır. Mikroorganizmalardan, metabolitlere, okyanus yaşamı ve içerisindeki çeşitli habitatlara, jeolojik oluşumları ve madenlerinin zengin yapısına kadar her alanda bize derin bir araştırma, öğrenme ve teknolojiyi ileriye taşıyacak ilham ve fikirler sunan bu kıta için yapılan her bir çalışma hazine değeri taşımaktadır. Bu çalışma bu harika kıtada yaşayan mikroorganizmalara yönelik ilginin ve merakın bir sonucu olarak ortaya çıkmıştır.

Antarktika çok sayıda farklı mikrobiyal topluluklara ev sahipliği yapmaktadır. Normal koşullar diyebileceğimiz dünyanın farklı ılıman bölgelerine kıyasla ekstrem koşullara karşı oluşturdukları adaptasyonlar sayesinde günümüzde dikkatle incelenmektedirler. Mikroorganizmalardan elde edilen doğal yapılı pigmentler üzerinde yapılan bilimsel incelemeler, bu mikroorganizmaların biyolojik olarak kolay parçalanabilirliği, laboratuvar ortamında kontrollü üretim kolaylığı ve çeşitli zengin içerikleri sebebiyle son yıllarda sentetik yapılı pigment üretimi yerine alternatif olarak düşünülerek hız kazanmıştır. Birçok araştırma mikrobiyal kaynaklı pigmentlerin biyomühendislik yollarla iyileştirilmesi ve metabolik oluşum yollarının yeterince anlaşılabilmesi üzerine bilimsel veri üretmekte ve organik pigmentlerin bitoteknolojik yararlanım yollarını iyileştirmeye yönelmiştir. Bu sayede insana ve ekosisteme zarar veren kimyasal pigmentlere dayalı teknolojiler yerini doğal çözümlere bırakmaya ve dönüşme amacına gitmeye başlamıştır.

Günümüzde astaksantin, prodigiosin, viyolasein, piyosiyanin, zeaksantin ve aktinorhodin gibi çok sayıda bakteriyel pigment, modern tıpta yoğun biçimde araştırılmaktadır. Rekombinant DNA ve sentetik biyoloji yaklaşımları sayesinde, farklı doğal pigmentlerin bakteri konak hücrelerinde kontrollü biyosentezi pigment endüstrisinde mikrobiyal sentez çalışmalarını daha da güçlendirmektedir. Bu sayede pigment üretimi için geniş alanlara ve bakım zorlukları olan uzun süreli bitki yetiştirilmesine gerek kalmadan, laboratuvar ortamında bakteri kültürleri aracılığıyla benzer ürünler daha kısa sürede ve daha gelişmiş yapıda elde edilebilmektedir.

Yapılarındaki özel antifriz proteinler, düşük sıcaklıklarda aktif kalabilen enzimler ve esnek membran yapıları, UV ve oksidatif strese karşı dayanıklılıkları, özel EPS adı verilen bileşenleri ile biyopolimer yapıda ürüne dönüşebilme potansiyelleri gibi özellikleriyle kutup bölgelerinden izole edilen psikrofilik ve psikrotrofik organizmalar geleceğin teknolojik dönüşümünde çok önemli bir yere sahiptir.

Bakteriler tarafından sentezlenen karotenoid pigmentler, karbon iskelet uzunluklarına göre genel olarak C_{30}, C_{40} ve C_{50} sınıflarına ayrılmaktadır. β-karoten, likopen, β-kriptoksantin, zeaksantin, lutein, kantaksantin, astaksantin ve izorenieraten gibi bileşikler, dokuz izopren biriminden oluşan C_{40} tetraterpen iskeletine sahip karotenoidlerdir. Uzun konjuge çift bağ zincirleri sayesinde bu C_{40} karotenoidler güçlü antioksidan ve fotokoruyucu özellik göstererek hücreleri oksidatif ve foto-oksidatif strese karşı korumada önemli rol oynamaktadır. C_{30} karotenoidler, altı izopren biriminden türeyen daha kısa zincirli pigmentlerdir ve özellikle Gram-pozitif bakterilerde tanımlanan 4,4'-diapophytoene, 4,4'-diapophytofluene, 4,4'-diapo-ζ-carotene, 4,4'-diaponeurosporene ve bu iskelete bağlı türevlerden stafiloksantin (staphyloxanthin) bu sınıfa aittir. Bu pigmentler genellikle zar yapısının desteklenmesi ve oksidatif strese karşı ek bir koruma sağlamasıyla ilişkilendirilmiştir. C_{50} karotenoidler, on izopren biriminden oluşan daha uzun zincirli pigmentler olup daha nadir görülmekle birlikte özellikle ekstrem koşullara uyum sağlamış bakterilerde tanımlanmıştır. *Corynebacterium glutamicum*'un doğal sarı pigmenti olan dekaprenoksantin (decaprenoxanthin) C_{50} karotenoidlere klasik bir örnek teşkil eder; bu pigmentin, diğer C_{40} karotenoidler gibi plazma zarına entegre olduğu ve zar stabilitesi ile oksidatif strese karşı korunmada görev aldığı gösterilmiştir.

Bu çalışmada Antarktika'nın Horseshoe, Hovgaard ve Nansen adalarından elde edilen buzul karotlarından izole edilen *Rhodococcus fascians* ve İtalyan Maria Zucchelli istasyonuna ait Ross denizinden izole edilen *Brevibacterium* sp. ve *Microbacterium* sp. üzerinde pigment aktivitelerini analiz etmek adına deneysel çalışmalar yer almaktadır. Bakterilerin ortam bileşenleri ve çevresel faktörlere verdikleri tepkileri araştırmak adına optimizasyon çalışması (Placcket-Burman Design-PBD) yürütülmüş, uygun pH ve sıcaklık değerleri araştırılmıştır. Kimyasal yapıyı belirlemek adına FTIR, UV-Vis, NMR ve TLC analizleri yapılmıştır. Antibakteriyal aktivitesi disk difüzyon yöntemi ile test edilmiş ve antioksidan kapasitesi üzerine DPPH (Serbest Radikal Süpürme Testi) testleri yapılarak bu çalışmada sonuçlara ait veriler paylaşılmıştır. Ross Denizi'nden izole edilen *Brevibacterium* suşlarına ait altı adet 16S rDNA dizisinin filogenetik analizi, Jukes–Cantor modeline dayalı maksimum olabilirlik yöntemi kullanılarak gerçekleştirilmiştir. Elde edilen ağaçta en yüksek olabilirlik değerine sahip topoloji değerlendirilmiş ve ilgili dallardaki bootstrap yüzdeleri ile birlikte sunulmuştur. Analiz sonuçları, *Brevibacterium* izolatlarına ait dört dizinin *Brevibacterium anseongense* dalı içerisinde kümelendiğini, kalan iki dizinin ise ağacın geri kalanından belirgin biçimde ayrıştığını göstermiştir. Bu iki dizinin konumu, izolatların *B. anseongense*'ye yakın, ancak ondan ayrılan ve muhtemel yeni bir türü temsil edebileceğini düşündürmektedir. *Microbacterium* izolatının 16S rDNA dizisi ise filogenetik ağaçta *Microbacterium resistens* ile yakın bir akrabalık göstermektedir; ancak ilgili düğümdeki düşük bootstrap değeri , bu yerleşimin istatistiksel olarak zayıf olduğunu ve izolatın filogenetik konumunun kesinleştirilebilmesi için ek dizi verisine ihtiyaç duyulduğunu ortaya koymaktadır.Bu ön filogenetik bulgular ışığında, söz konusu izolatların taksonomik konumlarının daha ayrıntılı ve güvenilir biçimde aydınlatılabilmesi için tüm genom dizileme verilerinin elde edilmesi ve karşılaştırmalı genomik analizlerin gerçekleştirilmesi planlanmaktadır. TAE II seferi kapsamında Türkiye'ye getirilen buzul karotlarından izole edilen *Rhodococcus* suşunun 16S rRNA gen dizisi belirlenmiş ve GenBank veri tabanına PP563783 erişim numarasıyla kaydedilmiştir. Yapılan BLAST analizi, dizinin *Rhodococcus fascians* tip suşuna (NR_125492.1) karşı %98,44 oranında nükleotid benzerliği gösterdiğini ortaya koymuştur. 16S rRNA dizilerine dayalı filogenetik ağaç, MEGA 11.0.8 yazılımı

kullanılarak Maksimum Olabilirlik yöntemi ve Kamura-Tei modeli ile oluşturulmuş; dalların güvenilirliğini değerlendirmek amacıyla 100 bootstrap tekrarı uygulanmıştır.

Üç farklı bakteri türü için literatür taranarak uygun deney koşulları ve optimal ekstraksiyon yöntemleri belirlenmeye çalışılmıştır. *Brevibacterium* sp., *Microbacterium* sp. ve *Rhodococcus fascians* izolatları üzerinde yürütülen ön ekstraksiyon denemeleri sonucunda, görünür ışıkta inkübasyonun karanlık koşullara kıyasla bakteriyel biyokütleyi artırdığı, ancak elde edilen pigmentlerin ışığa maruz kaldıklarında fotostabilitelerinin azaldığı ve belirgin fotodegradasyona uğradıkları gözlemlenmiştir.

Spektroskopik olarak, *R. fascians* türünden elde edilen pigment yapısı için 456 nm'de literatürdeki karotenoid yapılı pigment varlığını göstermektedir. *Brevibacterium* sp. 405-408 nm dalga boyunda karotenoid türevi bir pigment olan isorenieraten yapısı ile ve *Microbacterium* sp. için 407-417 nm dalga boyunda önceki çalışmalarda da belirtilen karotenoid türevi bir pigment olan nörosporen yapılı pigment benzerliği dikkat çekmektedir. Üç farklı bakteri türü için en verimli üretim koşullarını belirlemek amacıyla bir optimizasyon çalışması yürütülmüştür. En yüksek toplam karotenoid konsantrasyonu *Rhodococcus fascians*'ta (485,00 µg/g) elde edilmiş, bunu *Microbacterium* türleri (179,89 µg/g) ve *Brevibacterium* türleri (63,62 µg/g) izlemiştir. İzolatlardan pigmentler çıkarılmış ve antimikrobiyal aktiviteleri hem Gram (+) hem de Gram (-) bakterileri inhibe ettiği belirlenmiştir.

Aktinomiset sınıfına ait olan bu üç bakteri türüne ait pigment çalışmalarında FTIR spektrumlarında 2920–2850 cm^{-1} aralığında alifatik C–H gerilmeleri, 1700–1730 cm^{-1} bölgesinde karbonil (C=O) ve 1600–1650 cm^{-1} civarında konjuge C=C bantlarının gözlenmesi, tüm pigmentlerin karotenoid iskeletine sahip olduğunu desteklemektedir. DPPH serbest radikal süpürme testi ile *Rhodococcus fascians* pigmenti için ayrıntılı olarak değerlendirilmiştir. DPPH inhibisyonu %17,46'dan %84,99'a yükselmiş, lineer regresyon analizi ile IC_{50} değeri =0,36 µg/µL ile yüksek antioksidan özellikler sergilemiştir (R^2=0,8817). *Rhodococcus fascians* pigment ekstraktının ^1H NMR spektrumunda 5–7 ppm aralığında yoğun vinilik proton sinyalleri, ^{13}C NMR'de ise 120–140 ppm aralığında belirgin sp^2 karbon sinyalleri gözlenmiş, bu da literatürde *Rhodococcus* türlerinden bildirilen karotenoid pigment karışımlarıyla uyumlu izoprenoid iskeletini desteklemektedir.

Uzay ortamı ve Antarktika gibi ekstrem ortamlarda yapılan mikrobiyal çalışmalar, mikroorganizmaların normal koşullara kıyasla adaptasyon yeteneklerini ortaya koymaktadır. Biyofilm oluşumundan, doğal polimerlere, doğal karotenoid özellikli pigmentlerin kullanım alanlarına kadar, uzay ortamında mevcut sorunlara çözüm arayışında Antarktika kökenli mikroorganizmaların araştırılması oldukça değerlidir. Önümüzdeki yıllarda Ay ve Mars'a gerçekleştirilecek seferlerde, mikroorganizmalara dayalı geliştirilecek teknolojik çözümler sayesinde enfeksiyonların önlenmesi, hücre bozunumunun azaltılması, atıkların geri dönüştürülmesi, radyasyona karşı korunma ve gıda içeriklerinin iyileştirilmesi gibi önemli kazanımlar elde edilebilecektir.

1. INTRODUCTION

Pigments are inorganic, organic and synthetic based. Inorganic pigments are chemically stable and durable substances that do not dissolve with solvents [1]. Chemical oxides, sulfates, chromates, silicates, borates, molybdates, phosphates, vanadates, iron cyanate, hydroxides, sulfides are inorganic pigments [2]. The source of natural pigments is plants, minerals, insects or microbial organisms [3].

The first synthetic pigment was discovered in 1856 by William Henry Perkin during his studies on an organic compound called aniline, a coal tar derivative. Perkin synthesized this compound and produced a synthetic purple pigment called mauveine. This synthetic dye created a major revolution, especially in the textile industry [4]. Although synthetic pigments have been used in the food, pharmaceutical, textile, and cosmetic sectors for many years due to their ease of use and high stability, the tendency towards natural pigments has increased, considering the damage they cause to humans and the environment, their high toxicity, and pollution potential [5]. Pigments can be classified in various ways according to their origin and chemical structure, as shown in Table 1.1.

Table 1.1 : Classification of pigments according to their origin and chemical structure.

	Pigment Type	Characteristics	Examples
According to Origin	Natural	Organic compounds obtained from plants, animals, and microorganisms	Carotenoids, Anthocyanins, Chlorophyll
	Synthetic	Compounds produced in vitro using chemical processes	FD&C (Food, Drug, and Cosmetic colorants)
	Inorganic	Inorganic compounds synthesized or found in nature	Lead chromate, Phthalocyanine blue, Chrome fast green

Carotenoids are isoprenoid pigments with long hydrophobic chains containing double bonds that make them soluble in lipid environments. Anthocyanins are oxygenated heterocyclic flavonoid compounds with a benzo-pyran ring that are water soluble.

They change color according to the pH. Chlorophyll is a pigment composed of tetrapyrrole rings and a central magnesium ion. Pigments can be classified based on their chemical structure, as shown in Table 1.2.

Table 1.2 : Classification of pigments according to their chemical structures.

According to the Structure	Tetrapyrrole Derivatives	Compounds with four pyrrole rings	Chlorophylls, Hem group
	Carotenoids	Isoprenoid derivatives; mostly polymeric structures	Lycopene, Carotene, Lutein, Capsanthin
	Non-Tetrapyrrolic Nitrogenous	Compounds containing nitrogen in their chemical structure	Purines, Pterins
	Heterocyclic Compounds	Ring structures containing nitrogen and/or oxygen	Flavins, Phenazines, Phenoxazines, Betalains
	Benzopyran Derivatives	Oxygenated heterocyclic compounds	Anthocyanins, Flavonoids
	Quinones	Compounds containing quinone groups	Benzoquinone, Naphthoquinone, Anthraquinone
	Melanins	Polymeric compounds derived from nitrogen-containing monomer	Eumelanin, Pheomelanin

An examination of Table 1.2 reveals that classifying pigments based on their chemical structures is an important step toward understanding their biological functions. Tetrapyrrole derivatives are essential to structures like the heme group and play a critical role in oxygen transport. Pigments that contain nitrogen but are not tetrapyrroles contribute to genetic material through their purine and pterine structures or are involved in redox balance. Heterocyclic compounds, such as phenazines and phenoxazines, are particularly antimicrobial. Betalains can be used to replace anthocyanins in certain plants. Quinone pigments contribute to energy production by participating in electron transport chains. Melanin's polymeric structures remove free radicals while also providing UV protection.

1.1 Chemical Structure of Pigments

Pigments are chemical compounds that absorb specific wavelengths of light in the visible light spectrum. The resulting color is due to a molecule-specific structure called

a chromophore, which can absorb energy and excite an electron to a higher orbit. The unabsorbed energy is reflected or refracted and detected by the eye and converted into neural signals, which are interpreted by the brain as a color [7]. In the case of natural pigments, color formation occurs when a polyene chain contains a minimum of six conjugated double bonds [8].

Natural pigments can be divided into various categories according to their structural properties. These include quinones, tetrapyrrole derivatives (heme and chlorophylls), benzopyran compounds (flavonoids and anthocyanins), melanins, isoprenoid derivatives (carotenoids and iridoids) and other N-heterocyclic compounds (betalains, phenazines, flavins, phenoxazines, purines, pterins) [7].

1.1.1 Structure and properties of carotenoids

Carotenoids are natural pigments produced by plants and microorganisms and are divided into two main groups: carotenes and xanthophylls. These pigments exist as hydrocarbons (e.g., lycopene, α-carotene, β-carotene) or their oxygen-containing derivatives (e.g., xanthophylls such as lutein, zeaxanthin, astaxanthin) [6].

These pigments have hues ranging from red to yellow and orange; their colors are determined by the length of their carbon skeletons and the number of conjugated double bonds. Carotenoids are C-40 isoprenoid pigments with at least 9 conjugated double bonds and colors ranging from yellow to red [7].

1.1.2 Carotenoid biosynthesis pathway

There are two main pathways for the biosynthesis of carotenoids: the methyl-erythritol-phosphate (MEP) and mevalonic acid pathways (MVA). These pathways produce a variety of carotenoids using precursor molecules such as isopentenyl pyrophosphate and dimethylallyl diphosphate [8]. The first step in carotenoid biosynthesis is the synthesis of C5 isoprenoid precursors via the MEP or MVA pathways [9], [10].

1.1.3 GGPP synthesis and phytoene formation

C5 isoprenoid precursors (IPP and DMAPP) lead to the formation of the GGPP (geranyl-geranyl pyrophosphate) molecule. Two molecules of GGPP are

enzymatically converted into phytoene by the enzyme phytoene synthase (PSY/CrtB) as illustrated by the following reaction;

GGPP → Phytoene *(Enzyme: Phytoene synthase, PSY/CrtB)*

1.1.4 Phytoene to all-trans-lycopene conversion in plants and bacteria

In plants, the conversion of phytoene to all-trans-lycopene is catalyzed by four distinct enzymes, whereas in bacteria, a single enzyme catalyzes all the steps of this transformation.

• *Phytoene → PDS → ZDS → CRTISO → all-trans-Lycopene*

1.1.5 Conversion of lycopene to cyclic carotenoids

Lycopene is converted into cyclic carotenoids by the action of cyclase enzymes

• *Lycopene → α-Carotene (enzyme: Lycopene ε-cyclase, LYCE)*

• *Lycopene → β-Carotene (enzyme: Lycopene β-cyclase, LYCB / CrtY)*

1.1.6 Hydroxylation of cyclic carotenoids

Cyclized carotenoids are converted to more functional derivatives by hydroxylase enzymes:

• *α-Carotene → Lutein (enzyme: α-carotene ring ε-hydroxylase, CHYE)*

• *β-Carotene → Violaxanthin (enzyme: β-carotene hydroxylase, CHYB / CrtZ)*

Carotenoids are divided into carotenes and xanthophylls based on their chemical structure and function. Figure 1.1 shows the chemical structures of different types of carotenoids [11].

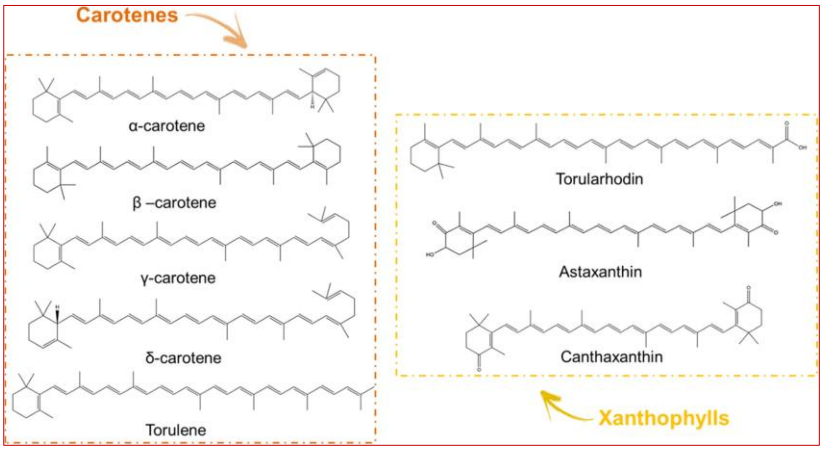

Figure 1.1 : Chemical structures of carotenoid types [11].

As shown in Figure 1.2, the biosynthesis of carotenoids in microorganisms occurs via the mevalonate (MVA) pathway [12].

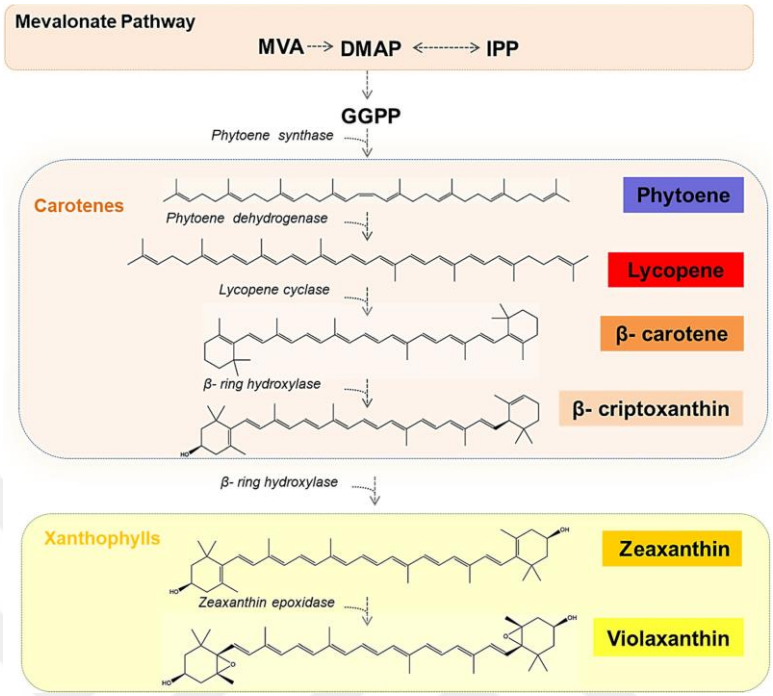

Figure 1.2 : Carotenoid biosynthesis through the MVA pathway in microorganisms.

The biosynthesis of carotenoids in microorganisms primarily occurs through the mevalonate (MVA) pathway. This pathway provides the essential isoprenoid precursors required for carotenoid formation [12]. Figure 1.3 illustrates the chemical structures of DHIR, IR, and lutein, highlighting their key functional groups and branched carbon skeletons relevant to their biological activity.

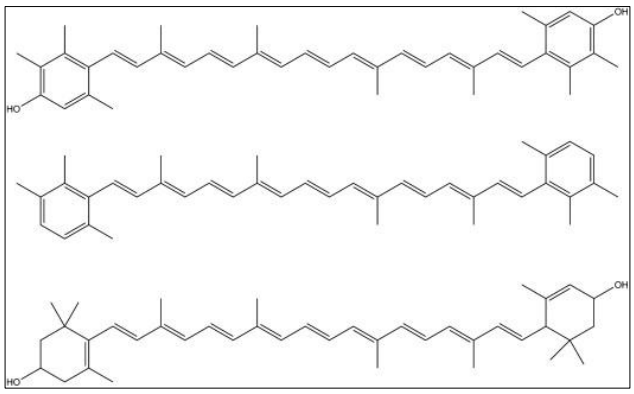

Figure 1.3 : Chemical structures of carotenoids DHIR, IR, and lutein.

Carotenoids include the structurally rare phenolic polyene 3,3'-dihydroxyisoreneniate (DHIR). DHIR and isoreniatene (IR) are aromatic carotenoids produced by *Brevibacterium linens* [13].

1.2 Spectral Properties of Carotenoids

1.2.1 Lycopene

Lycopene is a linear carotenoid that does not contain any rings. There are 11 conjugated double bonds, and it appears in red, which is associated with the expanded conjugation system. The UV-Vis spectrum shows absorption at longer wavelengths and a distinct spectral profile. Its conjugated structure enhances electron delocalization, thereby supporting the red tone [14].

1.2.2 α-Carotene

α-Carotene is an asymmetric carotenoid with β-ring and ε-ring. Although the ε-ring has a cyclic structure and a double bond, the location of the double bond and the geometry of the ring prevent conjugation from extending as efficiently as the β-ring. As a result, α-carotene has a shorter effective conjugation length than β-carotene, which affects its UV-Vis absorption [14].

1.2.3 γ-Carotene

γ-Carotene is a carotenoid with a single ring structure. It contains 11 conjugated double bonds and is structurally positioned between β-carotene and lycopene. It appears reddish-orange, and its UV-Vis absorption spectrum lies between that of lycopene and β-carotene. The presence of a single ring causes a slight disruption in electron resonance, placing its spectral characteristics in an intermediate position [14].

1.2.4 β-Carotene

β-Carotene is a symmetric carotenoid composed of two β-rings. Although it contains 11 conjugated double bonds, its cyclic structure results in a yellow-orange appearance. The UV-VIS spectrum shows a shift toward shorter wavelengths compared to lycopene, and its spectral absorption is generally less pronounced. The terminal rings slightly interrupt the conjugation, affecting its overall spectral behavior [14].

UV-VIS absorption spectra of lycopene, γ-carotene, and β-carotene have been compared by revealing the spectral features that distinguish their ring structures. The characteristic spectra of these three compounds are evaluated in terms of maximum wavelengths and absorption intensities and are presented in Figure 1.4.

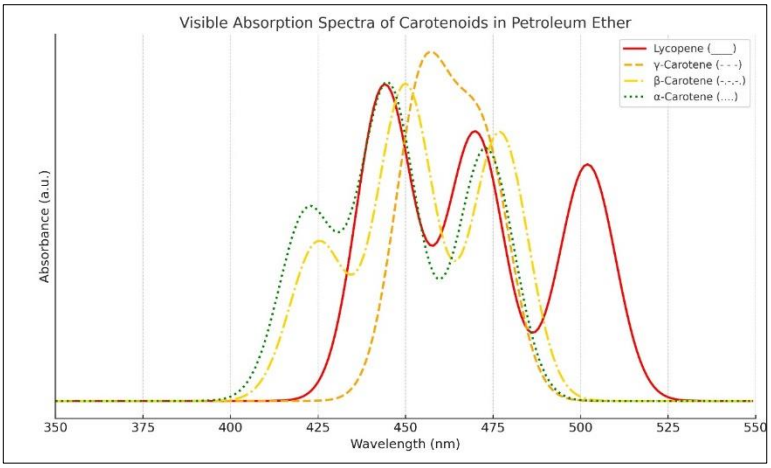

Figure 1.4 : The visible absorption spectra of lycopene, γ-carotene, β-carotene, and α-carotene measured in petroleum ether [14].

1.2.5 Isorenieratene

Isorenieratene is a C_{40} aryl carotenoid bearing aromatic φ-type rings at its ends [15]. Physically, isorenieratene, like other carotenoids, is an extremely hydrophobic, water-insoluble pigment found primarily in cell membranes. Its conjugated polyene chain provides significant antioxidant and photoprotective effects against photooxidative stress by scavenging reactive oxygen species such as singlet oxygen and hydroxyl radicals. Isorenieratene and its 3,3′-dihydroxy derivatives were found to significantly reduce UV-induced DNA damage and lipid peroxidation [13].

1.2.6 Neurosporene

Neurosporene, an acyclic carotene with a 7,8-dihydro-ψ,ψ-carotene skeleton and formula $C_{40}H_{58}$, is a polyene pigment that serves as a biosynthetic intermediate for lycopene and various bacterial carotenoids. In bacteria and fungi, neurosporene serves as an intermediate in the pathway from phytoene to phytofluene, ζ-carotene, neurosporene, and lycopene. Bacteria convert 15-cis-phytoene to phytofluene, ζ-carotene, and all-trans-neurosporene via a single CrtI-type 3-step phytoene desaturase. [16]. Functionally, neurosporene has been identified as an accessory pigment in light-harvesting complexes, a singlet oxygen quencher, an antioxidant that protects membranes from oxidative stress, and all of which are important steps in photooxidative stress adaptation [17].

1.3 Characteristics of Antarctic Bacteria

Antarctica, with its rich microbial diversity, is the source of many metabolites and compounds with high biotechnological potential that are waiting to be discovered. Bacteria discovered in Antarctica are notable for their remarkable adaptation to harsh conditions, including extreme cold, drought, UV radiation, and food scarcity. They are psychrophilic bacteria, meaning they can remain active at very low temperatures and have antifreeze proteins that prevent intracellular fluids from freezing. These bacteria are resistant to UV damage due to the presence of pigments or DNA repair mechanisms. Pigment properties of some bacterial species isolated from Antarctica are shown in

Table 1.3. Different bacteria harboring different pigment types, their biological activities, and color varieties have been compiled from studies.

Table 1.3 : Pigment content of some bacterial species isolated from Antarctica.

Pigment	Color	Biological Activity	Bacterial Identification	Isolation Source	Ref.
Carotenoid (α-carotene, echinenone, canthaxanthin, astaxanthin)	Orange	UVB resistance	*Microbacterium* sp. LEMMJ01	King George Island	[18]
Violacein	Violet	Antibacterial	*Janthinobacterium lividum* -ROICE173	Snow (King George-Island)	[19]
Flexirubin	Yellow/ orange	UV protector	*Flavobacterium* sp. Ant342	Land-locked freshwater lakes (Schirmacher Oasis)	[20]
Carotenoid (canthaxanthin)	Red	Photosensitive	*Hymenobacter* sp. A9A5	Soil (King George Island)	[21]

1.4 Literature Review

1.4.1 Studies on pigment production

Natural pigments contain many active ingredients that are environmentally friendly and beneficial to human health. For example, lutein pigment found in higher plants and microalgae has shown the ability to prevent and treat retinal damage, including age-related macular degeneration, glaucoma, and diabetic retinopathy [22]. Tetrapyrroles, carotenoids, flavonoids, curcuminoids, betalains, and quinones are common natural pigments obtained from plants, animals, and microorganisms [23].

Today, pigments of different types and shapes are widely used as additives or nutritional supplements in the food industry, cosmetics, pharmaceuticals, animal feed, and other fields. In the study conducted by Boo et al. (2012), antioxidant activities, total polyphenol and flavonoid contents and antimicrobial effects of some plant pigments were evaluated to be used in cosmetic products, and it was stated that these plant sources contain active functional components and can be used as excellent materials for natural cosmetics and food supplements [24]. Buttle et al. (2001) investigated the effects of astaxanthin and canthaxanthin pigments on pigment accumulation and color formation in the flesh of Atlantic salmon (*Salmo salar L.*) and conducted studies on how these pigments can be used in commercial feed formulations in fish farms. The study determined that the characteristic pink color of salmon meat is due to naturally accumulated carotenoid pigments. It was also determined that as the canthaxanthin content in the feed increases, the amount of canthaxanthin accumulated in fish meat also increases [25] . It has been shown in the study conducted by Hamano & Kilikian (2006) that the microorganism *Monascus ruber* supports the production of red pigments using agricultural industrial wastes such as corn soaking liquid. Corn soaking liquid provides a suitable nutrient medium for pigment production by *Monascus ruber*, with the nutrients it contains, such as nitrogen, amino acids, and vitamins. This finding is an important example of how agricultural waste can be utilized in biotechnological processes, especially in areas such as pigment production [26]. It was reported by Sopandi et al. (2013) that the fungus *Penicillium resticulosum* has the potential to produce fungal pigments by utilizing agricultural industrial wastes. The study revealed that this microorganism can increase pigment production by utilizing the nutrient content of agricultural wastes [27]. The biotechnological use of *Penicillium* species is also important in terms of environmental sustainability, as these fungi can obtain valuable products by bioconversion of waste. *Rhodotorula glutinis* is a microorganism used for carotenoid production. This microorganism promotes carotenoid production by using agricultural wastes such as hydrolyzed waste flour of mung bean as substrates. Carotenoids are compounds with important biological activities, and this process is an example of the transformation of waste into valuable biotechnological products. The activity of *Rhodotorula glutinis* in carotenoid production provides an important insight into how this microorganism can be used in biotechnological processes of agricultural waste [28].

1.4.2 Studies on the obtainment of bacterial pigments

Bacteria produce a variety of pigments, including carotenoids, melanin, prodigiosin, pyocyanin, actinorhodin, and zeaxanthin [29]. Many microbial pigments exhibit antioxidant, anti-inflammatory, or antimicrobial properties [30]. Carotenoids have a wide range of uses, including organic food coloring, animal feed, textile and paper dyeing, nutraceuticals, cosmetics and pharmaceuticals [31]. Melanin protects against UV radiation by absorbing a wide range of electromagnetic spectrum and preventing photo-induced damage. It also resists high temperatures and chemical stress. Melanin is widely used in cosmetics, sunscreens, eyeglasses and the safe containment of radioactive waste such as uranium [30]. Prodigiosin stands out as a powerful therapeutic molecule, especially due to its immune response suppression and anticancer effects. In addition, prodigiosin exhibits insecticidal, antifungal, antibacterial, and antimalarial properties [32]. Pyocyanin has been used as a biological control agent and is known for its antibacterial and antifungal activities [33]. Riboflavin (vitamin B2) is a water-soluble pigment with yellowish-green fluorescence. Riboflavin supplements are used in phototherapy applications for the treatment of neonatal jaundice. Additionally, riboflavin has been shown to be effective in relieving migraine headaches when used in conjunction with beta-adrenergic drugs [30]. One of the non-photosynthetic bacteria that produce carotenoid pigments is *Rhodococcus* sp. In a study conducted by Shimokata and Tsukamura in 1989, the carotenoid pigments of the *Rhodococcus* genus were examined in detail. As a result of the study, *Rhodococcus* species were divided into three groups according to the types of carotenes they contained: The first group produced beta-carotene, the second group produced gamma-carotene-like compounds; the third group did not produce any carotene [34]. In a study conducted by Osawa et al. (2011)**,** OH-chlorobacten glycoside, OH-γ-carotene glycoside, OH-4-keto-γ-carotene glycoside hexadecanoate, and OH-chlorobacten glycoside hexadecanoate compounds were isolated and identified as a new antioxidant carotenoid from *Rhodococcus* sp. It was reported that these compounds exhibited strong antioxidant activities [35].

1.4.3 Studies on pigment production from antarctic bacteria

Bacterial pigments have an extremely high potential in biotechnological applications due to their prevalence, species adapted to extreme conditions, especially in polar

regions, and the special biological mechanisms that allow these species to adapt to cold, as well as the potential new species that can be obtained from glaciers [36]. Microorganisms that can survive in the extreme conditions of Antarctica develop various morphological and biochemical strategies, such as the production of photoprotective compounds and protection mechanisms based on both enzymatic and non-enzymatic antioxidant systems [37]. Therefore, these microorganisms adapt themselves to cold by producing different pigments [38].Among the bacteria isolated from Antarctica, especially Gram (+), the genera *Staphylococcus, Bacillus, Mesobacillus, Kocuria, Gordonia, Rhodococcus, Micrococcus, Arthrobacter, Agrococcus* and *Salinibacterium* are common and mostly exhibit carotenoid pigment production [39], [40]. Correa-Llantén et al. (2012) studied the antioxidant potential of pigments produced by an Antarctic microorganism (*Pedobacter terrae*) isolated from Doumer Island [41]. The characterization of the pigment mixture produced by the microorganism determined that this mixture consisted of nine pigments belonging to the carotenoid group and showed a maximum absorption at 480 nm, as reported by Zhang et al. (1997) [42]. The analysis of the pigment mixture by mass spectrometry revealed the xanthophyll content. This study showed that the integration of the pigment mixture consisting of various carotenoids into liposome membranes reduced the degradation of lipids due to oxidative stress against UVB radiation and protected cell membranes from oxidative damage. It was stated that it has the potential to be used in biotechnological applications as an effective antioxidant, especially against high UVB radiation. In a study conducted by Dieser et al. (2010), it was found that pigments produced by microorganisms obtained from Antarctica reduced harmful oxygen derivatives called reactive oxygen species (ROS) formed in bacteria [43].

2. EXPERIMENTAL STUDIES

2.1 Materials

This section contains information about all of the materials and devices used in experimental studies.

2.1.1 Chemicals compounds used in the experiments

The chemical reagents used in the study, along with their product codes and packaging sizes, are listed in the table below. All reagents used were of analytical grade and were applied according to experimental protocols. Table 2.1 shows the chemical reagents used in pigment production, along with their product codes and packaging information.

Table 2.1 : Product codes and chemical reagents utilized in the experiment.

Chemical Name	Brand and Catalogue Number	Purity / Grade	Package Size
D (+) Glucose anhydrous	Carlo Erba - 454337	ACS Analytical Grade	1 kg
Mueller Hinton Agar II	Biolife - Mueller Hinton Agar II- 401740	—	500 g
Sodium Chloride, (NaCl)	Labkim - S.0165.08.17/ Carlo Erba - 479687	Extra pure	1 kg
Potassium dihydrogen phosphate (KH_2PO_4)	Merck - 1.04871.1000/ Baker Analyzed - 0240	Ph. Eur / Analytical Grade	1 kg/ 500 g
Peptone from Casein (pancreatic digest)	ITW Reagents - A2210	—	500 g
Peptone from meat, bacteriological	Millipore (Merck) - 91249-500G	—	500 g
Magnesium sulfate heptahydrate ($MgSO_4 \cdot 7H_2O$)	AFG Scientific - (M.W.246.47)	—	500 g
Ammonium sulfate ($(NH_4)_2SO_4$)	Merck - 101216.9029	Extra Pure	1 kg
25 mm PTFE hydrophilic syringe filter, 0.22 µm	ALWSCI Technologies -P/N MRZ0644	—	100 pcs/pack
Methanol, extra pure	Merck - 1.06008.2500	Extra Pure	2.5 L
DPPH (2,2-diphenyl-1-picrylhydrazyl)	Sigma-Aldrich – D9132-1G	≥ 95% (typical reagent grade)	1 g
Yeast Extract	Millipore (Sigma-Aldrich – 92144- 500G-F)	—	500 g
Hydrochloric Acid (HCl, 37%)	Baker Analyzed-6081	36–38% (w/w)/Analytical Grade	2.5 L
Ethanol Absolute Anhydrous (EtOH)	Carlo Erba - 414601	≥ 99.9%, Absolute Anhydrous, Analytical Grade	1 L

2.1.2 Laboratory equipments

The equipment listed below was obtained from the research laboratories of the University of Camerino, Faculty of Biology and Veterinary Medicine, and Istanbul Technical University, Faculty of Chemistry and Metallurgy, where the experimental studies were carried out. Table 2.2 provides an overview of the equipment, including model specifications and intended applications.

Table 2.2 : Model features of the equipment used in experimental studies and their purposes in research.

Equipment	Model	Application
Calculator	PHOENIX instrument-BTG-303	Calculation the contents of liquid media prepared for bacteria
Centrifuge	Eppendorf-5415 C	Pigment extraction/ 10,000 rpm
Centrifuge	OHAUS Frontier 5718R	Pigment extraction/ 7500 rpm
Shaking Incubator	ARGO LAB-SKI 4	Adjusting the temperature and agitation for bacteria incubation.
Magnetic Stirrer	LLG-Unistirrer 3	Ensuring a homogeneous mix of medium content
pH Meter	Giorgio Bormac S.r.l.-XS pH 50 VioLab	Calculation of different pH parameters
UV Spectrophotometer	VWR UV-1600PC	Detection of pigment absorbance bands, peaks, and levels
Water Bath	New Brunswick-Gyrotory Shaker G76	Pigments are extracted from bacterial cells using mechanical lysis.
Rotary Evaporatory	Heidolph Laborota 4000	Pigment concentration is accomplished by vacuum-removing organic solvents from pigment extracts.
Shaking Water Bath	Julaba-SW 23	Microorganisms are incubated at controlled temperatures.
Ultrasonic Homogenizer	Bandelin HD-4050	Using ultrasonic waves to disrupt cell suspensions, which provides mechanical lysis and pigment release.
FT-IR Spectrometer	Shimadzu 8300	Analysis of pigment functional groups and chemical structures using characteristic vibration bands in the infrared region.
Laboratory Drying Oven	Heraeus, Germany	Laboratory-type drying oven that can operate in a nitrogen atmosphere.
Freeze Dryer	Christ ,Alpha 1–2 LDplus, Germany	The freeze-drying (lyophilization) of pigment-containing samples results in dry products.

2.1.3 Bacterial strains used

The study's bacterial strains included three Antarctic isolates: *Brevibacterium* sp., *Microbacterium* sp., and *Rhodococcus fascians*. The structures and properties of these microorganisms are described in detail in the subheadings.

2.1.3.1 *Brevibacterium* sp.

Brevibacterium sp. cells can be morphologically rod-shaped or cocciform. These bacteria are obligate aerobes, meaning they require oxygen for growth. They are

chemoorganotrophic organisms that obtain energy from organic compounds. They act oxidatively or neutrally towards sugars and are catalase-positive [44]. Taxonomic classification of *Brevibacterium* species is important in terms of revealing the phylogenetic position and systematic relationships of these bacteria. The taxonomic levels to which *Brevibacterium* sp. belongs are presented in Table 2.3.

Table 2.3 : Taxonomic classification of *Brevibacterium* species.

Taxonomic Rank	Name
Domain	*Bacteria*
Phylum	*Actinobacteria (also referred to as Actinomycetota)*
Class	*Actinobacteria*
Order	*Micrococcales*
Family	*Brevibacteriaceae*
Genus	*Brevibacterium*

Colony morphology, pigment production, physiological and biochemical properties of *Brevibacterium* species are summarized in Table 2.4.

Table 2.4 : Colony and pigment characteristics in *Brevibacterium species* [45], [46].

Characteristics	*B. linens*	*B. iodinum*	*B. casei*	*B. epidermidis*	*B. mcbrellneri*	*B. otitidis*
Colony morphology and consistency	Smooth, creamy	Smooth, creamy	Smooth, creamy	Smooth, creamy	Contoured, friable, dry	Smooth, creamy
Pigment	Yellow-orange	Whitish-grayish	Whitish-grayish	Whitish-yellowish	Whitish-beige	Whitish-yellowish
Growth at 37°C	W	+	+	+	+	+
Nitrate reduction	+	+	V (-)	V (+)	-	-
β-Glucosidase activity	-	-	V	-	-	-
Xanthine hydrolysis	+	+	+	+	V	-
Utilization of:						
D-Arabinose	-	-	+	-	-	-
L-Arabinose	-	-	-	-	-	-
D-Arabitol	V (-)	-	-	+	-	-
Gluconate	-	-	+	+	-	-
Mannitol	V (-)	-	-	+	-	-

Symbols and Abbreviations:
+, positive; –, negative; V, variable; V (–), variable with most negative; V (+), variable with most positive; W, very weak growth. (Table adapted from Funke et al. (1997) [45]; Pascual and Collins (1999) [46].)

Most *Brevibacterium* species can hydrolyze casein, gelatin, and milk proteins. They grow well in media containing 8% NaCl. Their cell walls have a peptidoglycan structure based on meso-diaminopimelic acid (A2pm) and are cross-linked. In addition, complex teichoic acids consisting of neutral sugars, amino sugars, and sugar alcohols are found in the cell walls. The main polar lipids are diphosphatidylglycerol, phosphatidylglycerol, and dimannosyldiacylglycerol. The cells usually measure 0.6–

1.0 μm in diameter, and as the culture period is extended, they may transform into cocci. These bacteria show optimum growth in the temperature range of 20–37 °C and produce proteinase enzyme. These bacteria contain menaquinone (a derivative of vitamin K) [47].

Cadaverine and putrescine are biogenic amines formed by the degradation of lysine and ornithine. They are often associated with unpleasant odors but serve important functions for microorganisms. In *Brevibacterium* species, these two compounds are characteristic components of polyamines. Polyamines protect the cell membrane, interact with DNA and RNA, and ensure cell division.

Various optimization studies are available in the literature to increase pigment production in *Brevibacterium* species. Canthaxanthin, one of the pigments obtained from these species, stands out as an important carotenoid pigment due to its strong antioxidant properties and wide industrial application potential. In studies conducted to increase canthaxanthin production, different approaches have been shown to be effective. For example, in a study conducted on *Brevibacterium* sp. *KY-4313* strain; strategies such as obtaining a mutant strain, addition of carotenoidogenic chemicals, and optimization of culture conditions were applied. In this context, a 32% increase in pigment production was achieved in the mutant strain obtained by using N-nitrosomethylurea. In addition, canthaxanthin production was completed at the level of 9.3 mg/L in an innovative production medium containing fumaric acid and molasses, and this value reached the level of 7.2 mg/L in the fermentor with medium renewal [48]. In literature reviews, it is seen that the *Brevibacterium* genus is included in the *Corynebacterium* group in some sources. *Brevibacterium* and *Corynebacterium* are closely related groups, and in old classifications, *Brevibacterium* was considered to be part of the *Corynebacterium* group. For this reason, expressions such as "carotenoid-producing *Corynebacterium Brevibacterium linens*" are sometimes used in the literature. Some *Brevibacterium* species, such as *Brevibacterium vitarumen*, are not included in the 8th edition of Bergey's Manual, which is the main source for the classification of bacteria. However, this species name is included in the 1980 Approved Lists, where bacteria are officially recognized. Just like *Brevibacterium vitarumen*, it was thought that the species *B. liquefaciens* should actually be included in the Corynebacterium genus [49].

Guyomarc'h et al. (2000) found that *Brevibacterium linens* pigments absorb visible light in the 350-550 nm range. It was reported that adding NaOH to the methanol extract of *B. linens* pigments causes a pink-red color change with significant changes in the spectrum, resulting in a bathochromic shift and a shift in maximum absorbance to around 475 nm. While the pigment's color-changing properties can broaden potential application areas, they can also limit its use by reducing the molecule's stability [50]. The pigment's ability to absorb light in a broader spectrum allows it to capture light toward the red region, which can be particularly advantageous in applications such as photoprotection (protection against UV and visible light), sunscreens, and cosmetics. Furthermore, the color change to pink-red allows the pigment to be used as dye in various applications such as food, textiles, and biosensors. Furthermore, such observed shifts indicate increased conjugation in the pigment's structure and are generally associated with more stable colors. However, strong bases such as NaOH can ionize or fragment the pigment molecule, altering its natural structure, and therefore, the pigment's pH sensitivity can pose a potential stability problem in industrial applications.

2.1.3.2 *Microbacterium* sp.

The *Microbacteriaceae* family is a member of the Actinobacteria class and is classified as part of the Actinomycetales order [51]. Taxonomic classification of *Microbacterium* species is presented in Table 2.5.

Table 2.5 : Taxonomic classification of *Microbacterium* species.

Taxonomic Rank	Name
Domain	Bacteria
Phylum	Actinobacteria (Actinomycetota)
Class	Actinobacteria
Order	Micrococcales
Family	Microbacteriaceae
Genus	*Microbacterium*

The unique feature of the *Microbacteriaceae* family is that they contain group B peptidoglycan cell walls and unsaturated respiratory menaquinones (vitamin K2 derivatives) compounds [44]. Their existence has been demonstrated in various terrestrial and aquatic ecosystems, and isolated areas such as Antarctica [45], [52]. The group B peptidoglycan structure consists of a cross-link connecting the peptidoglycan

chains. This linkage is formed between the α-carboxyl group of D-glutamic acid and the D-alanine of the adjacent peptide chain. In addition, a diamino acid such as 2,4-diaminobutyric acid (DAB), lysine, or ornithine is often found in the peptidoglycan structures of these bacteria. This acid can be involved in both cross-links and can be found in the third position of the peptide chain. Colonies of the genus *Microbacterium* are usually yellow, white, or orange. These bacteria are generally non-motile, but some species may show limited motility. The main polar lipids found in cell membrane structures include diphosphatidylglycerol (DPG), phosphatidylglycerol (PG), and glycolipids (GL). In addition, the genomic G+C content of this genus ranges from 64% to 65% [44]. Protective abilities against ultraviolet rays have been detected in bacteria belonging to the *Microbacterium* genus. *Micrococcus luteus*, a pigmented bacterium from the Microbacteriaceae family, has been reported to produce UV-protective pigments [53].

2.1.3.3 *Rhodococcus fascians*

Rhodococcus is a genus of Gram-positive actinomycetes in the phylum Actinobacteria that contains mycolic acid, has a high G+C content, are obligatory aerobes, and do not form spores. According to studies, coccobacilli-rod shaped cells exist. Taxonomic classification of Rhodococcus species is presented in Table 2.6.

Table 2.6 : Taxonomic classification of *Rhodococcus* species [48].

Taxonomic Rank	Name
Domain	Bacteria
Phylum	Actinobacteria
Class	Actinobacteria
Order	Corynebacteriales
Family	Nocardiaceae
Genus	*Rhodococcus*

Most species can grow in a wide range of temperatures, pHs, and salts, and they are known for their metabolic versatility, oxidatively degrading a wide range of hydrocarbon compounds. They have nonmotile, urease-positive, slow-growing colonies that are creamy-yellow and orange in color. Rhodococcus colony coloration is primarily caused by carotenoid pigments embedded in the cell membrane and mycolic acid layer. These pigments are made up of a tetraterpene skeleton with long conjugated double bonds and cyclic or aromatic rings at the ends; some species also

contain hydroxylated keto-derivatives, sugar-linked glycosides, and fatty acid esters.[55]. Figure 2.1 shows Rhodococcus species colony morphology as well as bacterial morphology under SEM [56].

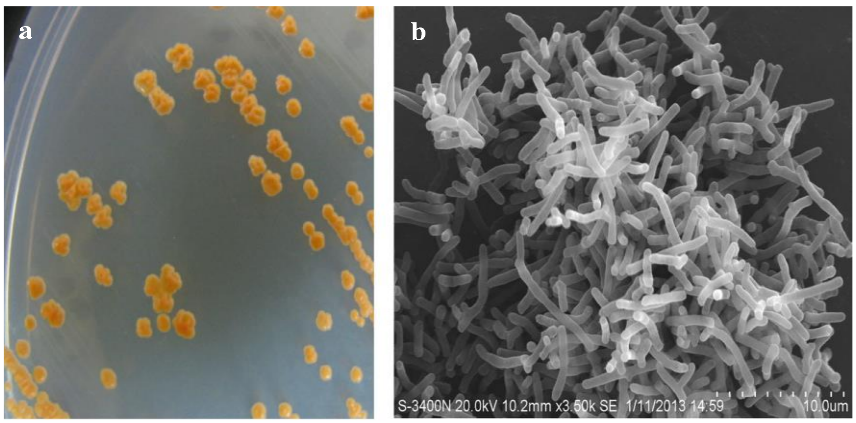

Figure 2.1 : The orange colonies of the *Rhodococcus* sp. A2-3 isolate observed in a Petri dish (a) and their cellular morphology determined by SEM image (b) are shown.

2.2 Experimental Setup

The experimental setup used in this study was configured to support bacterial growth, pigment extraction, optimization studies, and analytical characterization processes. All microbiological procedures were performed under sterile conditions in the Polar Laboratories of the ITU Department of Chemical Engineering.

2.2.1 Plackett-Burman experiment design (PBD)

In this study, a Plackett-Burman experimental design was used to identify the key factors influencing pigment production. The design included 12 conditions and three replicates, and it was carried out separately for three distinct bacterial isolates. The media components used in the study were D (+)-glucose anhydrous (Carlo Erba, 454337), Mueller Hinton Agar II (Biolife, 401740), sodium chloride-NaCl (Labkim S.0165.08.17; Carlo Erba 479687), potassium dihydrogen phosphate-KH_2PO_4 (Merck 1.04871.1000; Baker Analyzed 0240), peptone from casein, pancreatic digest (ITW Reagents, A2210), peptone from meat, bacteriological (Merck, 91249-500G), magnesium sulfate heptahydrate-$MgSO_4 \cdot 7H_2O$ (AFG Scientific, MW 246.47), ammonium sulfate-$(NH_4)_2SO_4$ (Merck, 1216) and yeast extract (Sigma-Aldrich, 92144-500G-F) were prepared at concentrations appropriate to the temperature and pH values specified in the design. The prepared cultures were grown in a controlled incubator environment.

2.2.2 Cultivation of bacterial cultures

Bacterial isolation and culture propagation were carried out in incubators (ARGO LAB SKI 4; Julaba SW 23) with precisely controlled temperature and shaking rate. To standardize the experimental conditions, the pH of the culture media was adjusted with a calibrated pH meter (Giorgio Bormac XS pH 50 VioLab).

2.2.3 Biomass collection and pigment preparation

The bacterial biomass was separated using high-speed centrifuges (Eppendorf 5415 C and OHAUS Frontier 5718R). The pigment was stabilized and made solvent-free by lyophilizing the resulting pellets using a freeze-drying system (Christ Alpha 1-2 LDplus, Germany).

2.2.4 Pigment extraction steps

Pigments were removed from cells using chemical and mechanical methods:

- Chemical solubilization involves the use of organic solvents such as methanol (Merck) and ethanol (Carlo Erba).
- Mechanical disruption of cells
    - Ultrasonic treatment (Bandelin HD-4050, 20 kHz, 40% amplitude, 8 minutes)
    - Shaking in a water bath (New Brunswick Gyrotory Shaker G76, 45°C, 130 rpm, 30 minutes)
- The pigment-containing supernatant collected at the end of extraction was concentrated in a rotary evaporator (Heidolph Laborota 4000) to remove the solvent.

2.2.5 Analytical pigment characterization

The chemical characteristics and structural elements of pigments were investigated using a variety of analytical techniques.

2.2.5.1 Pigment analysis with UV-Vis spectrophotometry

The pigment samples' characteristic absorption bands in the visible region were measured using a UV-Vis spectrophotometer (VWR UV-1600PC).

2.2.5.2 Fourier transform infrared (FT-IR) spectroscopy analysis

FT-IR spectroscopy (Shimadzu 8300) was used to determine the functional groups and molecular bond structures of the pigments. Characteristic peaks in the spectral regions were used to determine the pigment structure.

2.2.5.3 pH-dependent stability test

The maximum absorbance values of pigments at various pH levels, along with the resulting pigment concentration measurements, reveal the pigment's pH sensitivity. The experimental steps were taken from literature studies [59]. All three bacterial isolates received the medium and its components under the same conditions. Tryptic Soy Broth (TSB; Biolife -4021552) was used as the basal medium, and the cultures were incubated at 25°C with 140 rpm agitation [55].

2.2.5.4 Thin layer chromatographic (TLC) analysis

TLC analysis was used to separate pigments and compare Rf values. Analysis was performed using the CAMAG Twin Trough Chamber system with appropriate solvent mixtures.

2.2.5.5 DPPH antioxidant activity analysis

The antioxidant properties of the pigments were evaluated using a DPPH radical scavenging test. The spectrophotometric analysis was performed with the 2,2-diphenyl-1-picrylhydrazyl (DPPH) reagent (Sigma-Aldrich D9132-1G).

2.2.5.6 NMR (Nuclear magnetic resonance) analysis

Chemical structures of the pigments were confirmed using high-resolution NMR spectroscopy (Agilent VNMRS 500 MHz). The pigments' structural components were determined based on their ^{1}H and ^{13}C NMR spectra.

2.2.5.7 Antibacterial activity analysis

The pigments' biological activity was assessed using Mueller Hinton Agar II (Biolife, Cat. No. 401740). The pigments' antimicrobial activity was tested against both Gram-negative Escherichia coli and Gram-positive Staphylococcus aureus strains using the disk diffusion method [56][54].

2.3 Methods

The experimental methods used in the study are discussed in depth. Standard laboratory protocols were followed in the preparation of bacterial cultures, optimization studies using the Plackett-Burman design, pigment extraction, antioxidant activity analysis (DPPH), antibacterial activity tests, and analytical characterization techniques (UV-Vis, FT-IR, TLC, NMR).

2.3.1 Sample collection

Bacterial isolates were obtained from two distinct sources in Antarctica. *Brevibacterium* sp. and *Microbacterium* sp. isolates were obtained from coastal seawater samples collected near the Italian research base Mario Zucchelli Station (MZS; 74°41′42″ S, 164°07′23″ E) in the Terra Nova Bay region of Antarctica, along the coast of the Ross Sea. *Rhodococcus fascians* and *Arthrobacter psychrochitiniphilus* were obtained from ice core (glacial carot) samples collected during the II National Antarctic Science Expedition (TAE II) in 2018, covering three regions: Horseshoe (67°49′42″ S, 67°14′10.1″ W), Hovgaard (67°49′42″ S, 67°14′10.4″ W), and Nansen (64°33′05.2″ S, 62°05′32.3″ W) Islands.

Brevibacterium sp. and *Microbacterium* sp. were studied during an internship at Camerino University (UNICAM), as part of the Erasmus K131 program, whereas *Rhodococcus fascians* was transported under cold-chain conditions from Antarctica to the Department of Chemical Engineering, Istanbul Technical University, where they were maintained at low temperatures.

Figure 2.2 shows (a) the location of the Mario Zucchelli Station (MZS), the Italian Antarctic base situated in Northern Victoria Land (VL); (b) an aerial photograph of the station and its surrounding infrastructure, including 1: central buildings of the base, 2: fuel storage tanks, and 3: magnetic and astronomical observatories; and (c) a ground-level view of the base highlighting 4: laboratory buildings, 5: accommodation areas for both day and night use, 6: energy production units and water treatment facilities, 7: workshops, storage areas, and hangars, as well as 8: helipads [54].

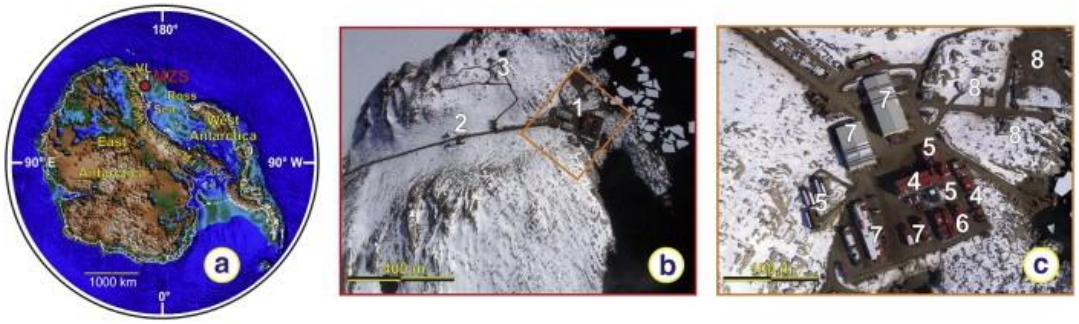

Figure 2.2 : The location of the Antarctic base Mario Zucchelli Station (MZS) in Northern Victoria Land (VL), where bacterial samples were taken [54].

Figure 2.3 shows images of the ice core samples at the time of collection during the II National Antarctic Science Expedition (TAE II).

Figure 2.3 : Images of the ice core samples at the time of collection during the II National Antarctic Science Expedition (TAE II).

Figure 2.3 shows the ice core sampling process, showing the field setup, core extraction, drilling steps, and temperature measurements.

2.3.2 Phylogenetic analysis of microorganisms used in the study

2.3.2.1 *Brevibacterium* sp. and *Microbacterium* sp.

Phylogenetic analysis using 16S rDNA sequences of six *Brevibacterium* and *Microbacterium* strains isolated from the Ross Sea allows the assessment of genetic relationships between congenic species. Evolutionary relationships were inferred using the Maximum Likelihood method based on the Jukes-Cantor model [55], and the phylogenetic tree was constructed with MEGA7 software [56]. For *Brevibacterium* sp. sequences, all positions containing gaps and missing data were eliminated, resulting in a final dataset of 1347 positions.

The analysis revealed that four *Brevibacterium* sequences clustered within the *B. anseongense* clade, while the other two sequences were located at a different position than existing strains, suggesting a potential new species. The *Microbacterium* isolate exhibited a close relationship to *Microbacterium resistens*, but the low bootstrap value at the corresponding node indicated that this placement had limited statistical support and required confirmation with additional sequencing data.

2.3.2.2 *Rhodococcus fascians*

The G-spin™ Total DNA Extraction Mini Kit (iNtRON Biotechnology, South Korea) was used to extract genomic DNA from pure bacterial isolates found in glacier cores containing *R. fascians*. PCR mixtures prepared with universal 16S rRNA primers (Sentobiolab, Turkey) were amplified using a standard program using Taq DNA polymerase (Thermo Scientific, EP0402). PCR products were analyzed on a 3.0% (w/v) agarose gel, purified with the EXO-SAP kit, and sequenced bidirectionally using the ABI 3500 XL Genetic Analyzer (Applied Biosystems, USA). The obtained forward and reverse sequences were edited using BioEdit (v7.2.5) to generate consensus sequences. The isolates' 16S rRNA gene sequences were compared to database reference sequences using the NCBI BLAST tool. The sequences of the relevant type and reference strains were obtained from NCBI, aligned with ClustalW, and phylogenetic trees were constructed in MEGA 11 using the Maximum Likelihood method and Tamura-Nei model (100 bootstrap repeats). The isolate's 16S rRNA gene sequence exhibited 98.44% similarity with the reference strain of *R. fascians* (GenBank accession number NR_125492.1), and the sequence acquired in this investigation was registered in GenBank with the accession number PP563783.

2.3.3 Bacterial cultivation

2.3.3.1 *Brevicacterium* sp. and *Microbacterium* sp.

These bacterial isolates were obtained from Antarctic seawater samples (*Brevibacterium* sp. and *Microbacterium* sp.). Samples were collected in sterile containers and transported to the laboratory under refrigerated conditions. Serial dilutions of seawater were prepared, and 100-µL aliquots were plated on appropriate media (e.g., R2A agar) using the spread plate method. Plates were incubated at 4°C for 4–6 weeks to allow colony growth. Colonies displaying distinct morphological characteristics were selected, and pure cultures were obtained using the streak plate

method. Pure isolates were mixed with a 15–20% glycerol solution and stored at -45°C in cryovials. When required for experiments, aliquots were transferred to agar plates or liquid media for further cultivation.

2.3.3.2 *Rhodococcus fascians*

Ice core samples with Rhodococcus fascians were isolated using modified procedures described by Butinar et al. (2007) and Cappa et al. (2014) [57][58]. Briefly, ice samples (40–90 mL) were aseptically thawed at room temperature and subjected to vacuum filtration through sterile 0.45 μm pore-size membranes. The membranes were then aseptically transferred to sterile falcon tubes filled with 18 mL of physiological saline solution (0.85% NaCl, w/v) and vortexed to ensure sample homogeneity. The resulting suspensions were serially diluted and spread on Tryptic Soy Agar (TSA; Merck, No. 1.05458, Darmstadt, Germany) and Reasoner's 2A Agar (R2A; Merck, No. 1.00416; Darmstadt, Germany). The plates were incubated for 3-6 weeks at temperatures ranging from 4°C to 25°C, in accordance with Singh et al. (2013) [59]. A light microscope was used to examine, purify, and observe emerging colonies at regular intervals. Pure cultures were stored at -40°C with 20% (v/v) glycerol until analysis.

2.3.4 Plackett–Burman design (PBD)

2.3.4.1 Plackett–Burman experimental design (PBD) for *Brevibacterium* sp.

Bacterial flasks were inoculated with 1% (v/v) of a 72-hour-old preculture, corresponding to a cell density of approximately McFarland 0.5 ($OD_{600} \approx 0.1$). The inoculated flasks were incubated at 25°C with continuous agitation at 145 rpm to ensure proper aeration and homogeneity. The inoculum volume for 1% (v/v) inoculation in 50 mL of culture medium was calculated as $50\ mL \times 0.01 = 0.5\ mL$. This procedure ensured a consistent starting cell density across all experimental runs, allowing reproducible assessment of bacterial growth and pigment production under the tested conditions shows an agar plate and liquid medium of *Brevibacterium* sp.; the colonies show distinct pigmentation.

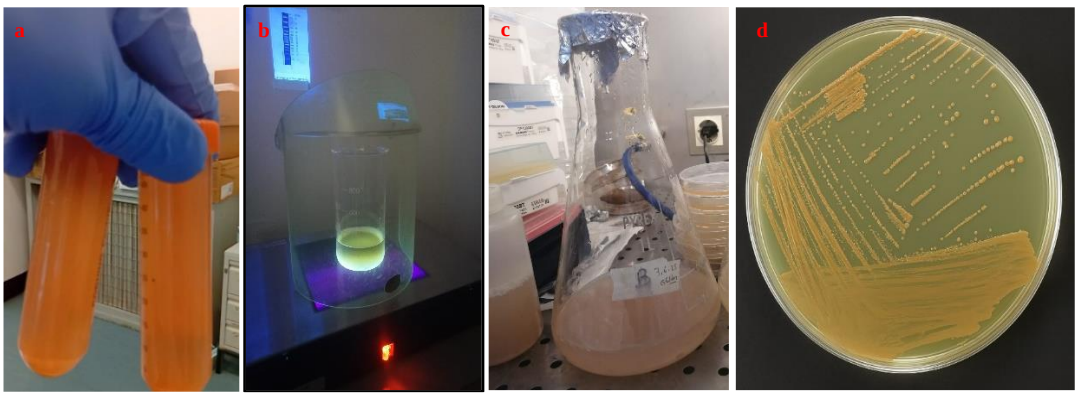

Figure 2.4 : Morphology of *Brevibacterium sp.* colonies on solid medium and appearance of the culture in liquid medium.

Based on information obtained from literature studies regarding the culture conditions of *Brevibacterium* sp., a preliminary optimization study was conducted, and the appropriate composition of the growth medium was determined as presented in Table 2.7-Table 2.9.

Table 2.7 : Basal medium composition used in the Plackett-Burman experimental design for *Brevibacterium* sp. cultivation.

Component	Amount
D (+) Glucose	20 g/L
Peptone	10g/L
Sodium Chloride (NaCl)	10 g/L
Yeast Extract	2 g/L
Potassium Dihydrogen Phosphate (KH_2PO_4)	1 g/L

In this study, the minimum and maximum values for *Brevibacterium* sp. culture medium components and conditions were determined according to the Plackett-Burman Design (PBD), as shown in Table 2.8.

Table 2.8 : Minimum and maximum values of culture medium components and conditions for *Brevibacterium* sp. determined according to the Plackett-Burman Design (PBD).

Component	Minimum Level (-1)	Maximum Level (+1)
D (+) Glucose	10	20
Peptone (g/L)	5	10
Sodium Chloride (NaCl) (g/L)	6	10
Yeast Extract (g/L)	2	5
Potassium Dihydrogen Phosphate (KH_2PO_4) (g/L)	1	3

The design for temperature and pH values, with minimum and maximum levels, is presented in Table 2.9.

Table 2.9 : Minimum and maximum values of temperature and pH used in the Plackett-Burman Design for *Brevibacterium* sp. cultivation.

Factor	Minimum Level (-1)	Maximum Level (+1)
Temperature (°C)	25	28
pH	6.9	7.5

2.3.4.2 Plackett–Burman experimental design (PBD) for *Microbacterium* sp.

Bacterial flasks were inoculated with 2% (v/v) of a 72-hour-old preculture, corresponding to 1.0 mL of inoculum per 50 mL of culture medium, with a starting cell density of approximately McFarland 0.5 ($OD_{600} \approx 0.1$). The inoculated flasks were incubated at 25 °C with continuous agitation at 145 rpm to ensure proper aeration and homogeneity. This standardized procedure provided a consistent initial bacterial load across all experimental runs, enabling reproducible assessment of both bacterial growth and pigment production under the tested conditions. Figure 2.5 shows an agar plate of *Microbacterium* sp.; the colonies show distinct pigmentation.

The basal medium used for the culture of *Microbacterium sp*. in the Plackett-Burman experimental design was formulated similarly to that used for *Brevibacterium* sp. (D(+) glucose 20 g/L, peptone 10 g/L, sodium chloride 10 g/L, yeast extract 2 g/L, and potassium dihydrogen phosphate 1 g/L). Based on the literature review, the design for temperature and pH levels was optimized, with minimum and maximum values as shown in Table 2.10.

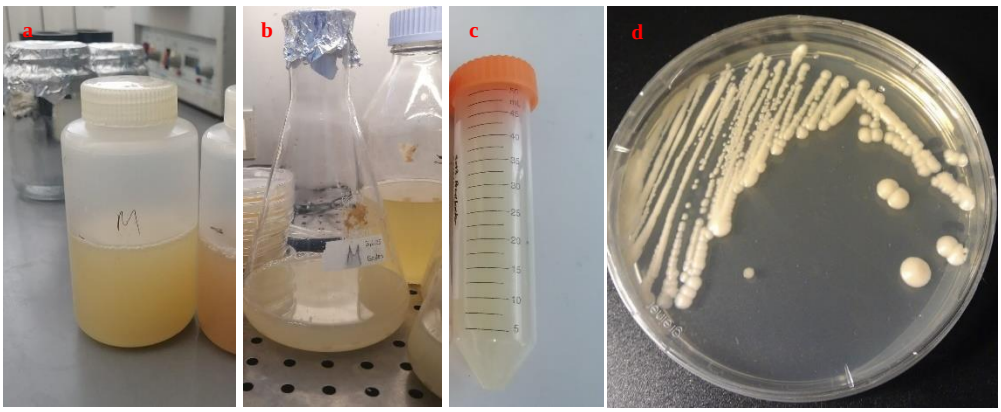

Figure 2.5 : Morphology of *Microbacterium* sp. colonies on solid medium and appearance of the culture in liquid medium.

Table 2.10 : Minimum and maximum values of temperature and pH employed in the Plackett-Burman design for *Microbacterium* sp. cultivation.

Factor	**Minimum Level (-1)**	**Maximum Level (+1)**
Temperature (°C)	25	30
pH	7	8

A 15-run Plackett-Burman design matrix was used to evaluate the effect of key media components and culture conditions (temperature and pH) on pigment yield. Different concentrations of glucose, peptone, NaCl, yeast extract, and KH_2PO_4 were tested.

Table 2.11 shows the minimum and maximum values of culture medium components and conditions for *Microbacterium* sp. determined according to the Plackett-Burman Design (PBD).

Table 2.11 : Min. and max. values of medium cmponent for *Microbacterium* sp.

Component	Minimum Level (-1)	Maximum Level (+1)
D (+) Glucose (g/L)	10	20
Peptone (g/L)	5	10
Sodium Chloride (NaCl) (g/L)	6	10
Yeast Extract (g/L)	2	5
Potassium Dihydrogen Phosphate (KH_2PO_4) (g/L)	1	3

2.3.4.3 Plackett–Burman experimental design (PBD) for *Rhodococcus fascians*

Bacterial plates were inoculated with 1% (v/v) of a 48-h preculture, corresponding to approximately the McFarland 0.5 standard (approximately $OD_{600} \approx 0.08–0.1$, $\sim 10^8$ CFU/mL). The inoculated plates were incubated at 25°C with shaking at 140 rpm to ensure proper aeration and homogeneity. For a 100 mL volume of culture medium, the 1% (v/v) inoculum volume was calculated as 1 mL (100 mL × 0.01 = 1.0 mL). This procedure ensured a consistent initial cell density across all experimental runs, allowing for reproducible assessment of bacterial growth and pigment production under the tested conditions. Figure 2.6 depicts the agar plate images and pigment colors of nine bacterial isolates purified from glacial ice cores collected during the Turkish Antarctic Expedition-II (TAE-II).

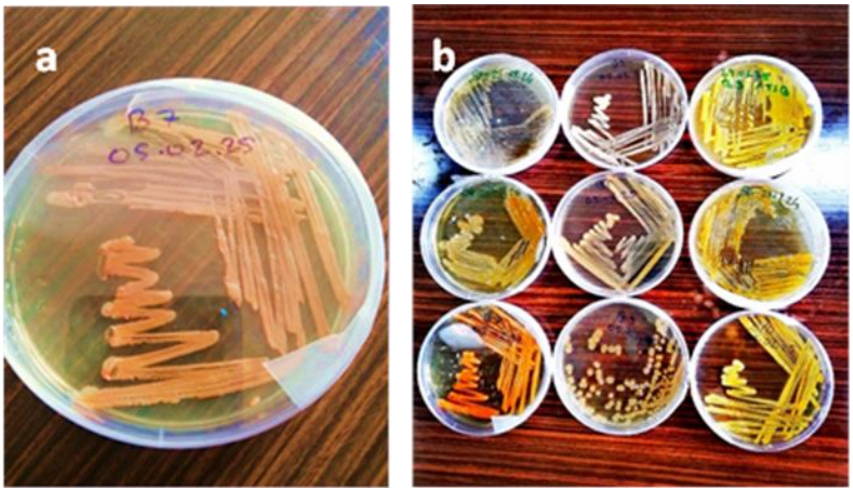

Figure 2.6 : Agar plate cultures of nine bacterial isolates obtained from Antarctic ice cores. (a) Agar plate of *Rhodococcus fascians* (b) Agar plates of nine different bacterial species and the pigmentation resulting from bacterial growth.

Utilizing data from previous studies on the culture conditions of *Rhodococcus fascians,* a preliminary optimization experiment was carried out to determine the minimum and maximum parameter ranges for the appropriate growth medium composition, as shown in Table 2.12. A Plackett-Burman experimental design with 15 runs was used to determine the major media components and culture conditions (temperature and pH) that influence pigment yield. In this design, 12 conditions contained experimental variables, and three conditions served as controls, with the factors run at intermediate values. The experiments evaluated various concentrations of glucose, peptone, yeast extract, NaCl, $MgSO_4 \cdot 7H_2O$, KH_2PO_4, and $(NH_4)_2SO_4$, as well as temperature (25-35 °C) and pH (6.5-7.2). Each factor was tested at two levels (-1, +1) to identify variables with a significant effect on pigment production.

Table 2.12 : Nutritional factors' concentrations at different levels in the Placket–Burman.

Component	Minimum Level (-1)	Maximum Level (+1)
(X_1) D(+) Glucose (g/L)	2	6
(X_2) Pepton (g/L)	4	6
(X_3) Yeast Ext (g/L)	2	6
(X_4) NaCl (g/L)	0.1	1.3
(X_5) $MgSO_4.7H_2O$ (g/L)	0.1	1
(X_6) KH_2PO_4 (g/L)	0.1	1.3
(X_7) $(NH_4)_2SO_4$ (g/L)	0.1	1
(X_8) Temperature (°C)	25	35
(X_9) pH	6.5	7.2

2.3.5 Pigment extraction procedure

2.3.5.1 Pigment extraction and quantification for *Brevibacterium* sp.

Pigment extraction was carried out according to the procedures outlined in the studies of Guyomarc'h, F., Binet, A. and Dufossé, L. (2000) according to the following steps [50]. Flasks containing 50 mL of production medium in 250 mL Erlenmeyer flasks were inoculated with 1 % (v/v) of a 72-hour pre-culture, corresponding to 0.5 mL of inoculum, and incubated at 145 rpm under the temperature and pH conditions specified in the Plackett–Burman experimental design. Following incubation, cells were harvested by centrifugation at 6000 × g for 15 min. The supernatant was inspected for residual cells or excreted pigments and discarded. The resulting cell pellet was rinsed with deionized water and centrifuged again under the same conditions, after which the supernatant was removed. Both wet and dry biomass weights were recorded. The washed biomass was suspended in 8 mL of 99.9 % ethanol and gently homogenized to prevent clumping. The extraction was repeated three times until the pellet was visibly bleached, using a total of 20 mL of ethanol**.** Samples were wrapped in aluminum foil to minimize light exposure and extracted at 50 rpm until the cells were visibly bleached, a process completed within approximately 2 h. The ethanol extract was separated from the biomass by centrifugation at 6000 × g for 15 min, and the pellet was examined for any remaining pigmentation before being discarded. To remove fine cellular debris, the extract was subjected to an additional centrifugation at 10 000 × g for 15 min. Pigment concentration in the clarified ethanol extract was finally quantified spectrophotometrically using the Beer–Lambert law. The dry pigment extract was stored at −20 °C for subsequent analyses.

2.3.5.2 Pigment extraction and quantification for *Microbacterium* sp.

Pigment extraction was carried out according to the procedures outlined in the studies of Patil, S. J., & Pendse, A. S. (2023) according to the following steps [60]. Erlenmeyer flasks containing 50 mL of medium adjusted to pH 7.0 were inoculated with a 2% (v/v) inoculum (approximately 1 mL) of an active culture with an optical density (O.D.) of 0.9 at 540 nm. The cultures were incubated for 72 hours under continuous light conditions at room temperature (RT) with shaking at 120 rpm. Following incubation, the cultures were centrifuged at 8000 rpm for 15 minutes to obtain biomass. The resulting cell pellet was suspended in distilled water, washed, and centrifuged at 4000 rpm for 15 minutes to remove any remaining medium components. The amounts of

wet and dry biomass were recorded before extraction. The washed cell pellet was suspended in 5 mL of methanol and vortexed for 1 minute. The mixture was then incubated in a 60°C water bath for 15 minutes to ensure complete dissolution of the pigment and then cooled to room temperature. Following cooling, the mixture was centrifuged at 4000 rpm for 15 minutes, and the pigment-containing supernatant was carefully collected. The supernatant was filtered through a 0.22 μm-pore membrane filter to remove cellular debris. The resulting methanolic pigment extract was analyzed by UV–Vis spectrophotometer to determine the characteristic absorption spectrum of the produced pigments. The pigment solution was dried and stored in amber vials at −20°C for later analysis.

2.3.5.3 Pigment extraction and quantification for *Rhodococcus fascians*

Pigment extraction was performed according to the protocol described by Silva et al. (2019) [61]. To obtain pure colonies, the isolated stock cultures were first placed on TSB agar and incubated at 25°C. *Rhodococcus fascians* colonies were then inoculated into LB broth and grown until they reached the 0.5 McFarland standard after 24 hours of incubation. This active preculture was added to the production medium at a 1% (v/v) concentration to serve as the initial inoculum in production experiments. For example, a 100-mL culture's inoculum volume was calculated to be 1 mL. The prepared active inoculum was then transferred to a production medium prepared in accordance with the Plackett-Burman experimental design. After 48 hours of incubation, 50-mL aliquots were collected from the cultures and centrifuged at 8000 × g. The resulting cell pellets were washed three times with 10 mL of distilled water and centrifuged under the same conditions. Cell pellets were washed, freeze-dried, and stored at -20°C for pigment extraction. Lyophilized cells were suspended in 20 mL of methanol and vortexed for 5 minutes to extract pigments. Subsequently, the suspension was incubated in a water bath at 40 °C for 30 minutes to facilitate mechanical disruption and enhance pigment solubilization. The pigment-containing supernatant was separated by centrifugation. The resulting supernatant was transferred to a round-bottom flask wrapped in aluminum foil, and the methanol was evaporated using a rotary evaporator at 40–45°C. The concentrated extract was then dried under a gentle stream of nitrogen, with all steps performed under light-protected conditions to prevent carotenoid degradation. Before analysis, the dry pigment extract was shaken in 4 mL of hexane for 10 minutes. After that, 2.3 mL of 10% (w/v) NaCl solution was added

to the mixture. The mixture was shaken for 15 minutes, then cooled to 4°C before the organic phase was carefully collected. The aqueous phase was re-extracted with a 3:1 (v/v) mixture of hexane: diethyl ether for 10 min before centrifugation at 2500 × g for 4 minutes. All organic phases were combined, transferred to 10 mL glass tubes, and completely dried under nitrogen flow at room temperature to obtain the final pigment extract.

2.3.6 Characterization analysis

2.3.6.1 UV-Vis spectrophotometric analysis

The absorption profiles of bacterial pigments were determined using UV-Vis spectrophotometric analysis. This technique provides important information about the chromophore structures of pigments and their maximum absorption values at different wavelengths. Using a UV-Vis spectrophotometer (VWR UV-1600PC), purified pigment extracts from three different bacteria were prepared in methanol, and wavelength-absorbance relationships were examined in detail [53]. Methanol was used to create a stock solution containing 12,5 mg/mL of dry pigment. This stock solution was diluted with 5% (v/v) methanol to produce working solutions with a final concentration of 1 mg/mL for UV-Vis measurements.

2.3.6.2 Fourier transform infrared (FTIR) analysis

The bacterial pigments' FTIR spectra were recorded using a Shimadzu FT-IR 8300 spectrometer in the range of 400-4000 cm^{-1} with a resolution of 4 cm^{-1}. The samples were analyzed using the ATR technique. Approximately 1–2 mg of dry pigment from each sample was used for analysis, and spectral data were exported to Microsoft Excel and presented graphically.

2.3.6.3 Thin-layer chromatography (TLC) analysis

The composition and purity of the bacterial pigments produced were evaluated using thin-layer chromatography (TLC). The protocol required for this study was chosen after reviewing the literature studies [62]. Pigment extracts (5–10 µL) were spotted onto TLC Silica gel 60 F_{254} aluminum sheets (20 × 20 cm; Merck, Darmstadt, Germany), used as the stationary phase. The plates were developed in a mobile phase that contained n-hexane and acetone (3:1, v/v). The solvent was dried at room temperature. The plates were then examined under visible and ultraviolet light (254

and 365 nm, respectively). Pigment bands were identified using their color and migration distances. For each band, the R_f value was calculated by dividing the band migration distance by the solvent front migration distance. The obtained Rf values were interpreted by comparing them to TLC profiles of bacterial carotenoids previously reported in literature. The study used a commercial β-carotene standard (Lucarotin® 1 CWD/Y, 1% β-carotene; BASF, Germany) as the control. The Rf (retention factor) value was calculated to determine the migration of bands in thin-layer chromatography (TLC) analysis.

2.3.6.4 DPPH Radical scavenging assay

The DPPH (2,2-diphenyl-1-picrylhydrazyl) radical test is a technique for determining an antioxidant molecule's ability to eliminate free radicals. The antioxidant activity of pure compounds is measured using a color change method. DPPH is a purple-colored stable radical that absorbs at 517 nm in methanol. The test works on the following principle: the antioxidant removes a hydrogen atom (H) from the DPPH radical, reducing DPPH to DPPH2 and changing the purple color to yellow; this change is accompanied by a decrease in absorbance at 517 nm. Color change is measured spectrophotometrically and used to determine antioxidant capacity [63]. The following formula, adopted from Koshti et al. (2022), was used to calculate the DPPH radical scavenging activity Equation 2.1 [53].

$$\text{DPPH scavenging activity (\%)} = \frac{A_{control} - A_{sample}}{A_{control}} \times 100 \qquad (2.1)$$

Figure 2.7 shows a representative color change caused by the antioxidant effect during the DPPH radical test. The purple color changes to yellow as the DPPH radical is reduced by the antioxidant molecule, indicating the presence of free radical removal and antioxidant capacity.

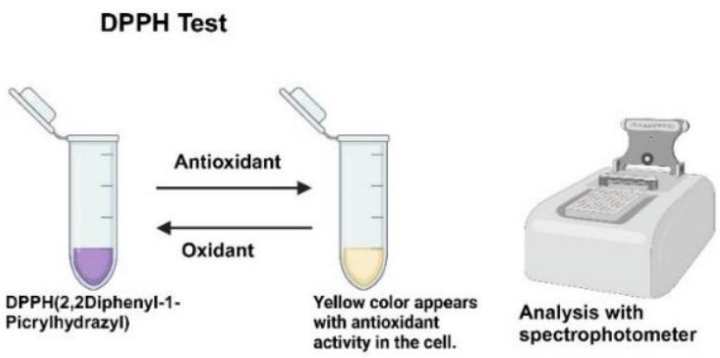

Figure 2.7 : Representative display of color change resulting from antioxidant effects in the DPPH radical test. Image prepared by the author using BioRender.com.

2.3.6.5 Nuclear magnetic resonance (NMR) analysis

The purified carotenoid-type pigment was analyzed structurally using ^{1}H and ^{13}C NMR (Agilent VNMRS 500 MHz, Agilent Technologies, USA). The ^{1}H NMR spectrum was recorded at 500 MHz, and the ^{13}C NMR spectrum was recorded at room temperature on an NMR spectrometer operating at 126 MHz. The solvent was $CDCl_3$, and the internal standard was TMS (tetramethylsilane). The data were analyzed to determine the chemical shift regions of the pigment's protons and carbon atoms, as well as its structural properties. Chemical shifts (δ) are expressed in ppm) Analysis. Due to the limited availability of pigment stocks from bacteria (*Brevibacterum* sp. and *Microbacterium* sp.) obtained from Italy, this analysis could only be performed on the pigment sample obtained from *Rhodococcus fascians*.

2.3.6.6 Antibacterial activity test

The antibacterial activity of the pigment extracts is evaluated using the disk diffusion method. The test microorganisms used are *Escherichia coli*, *Staphylococcus aureus*, for each bacterial strain, overnight cultures are prepared by transferring isolated pure colonies into sterile tubes containing 10 mL of sterile Nutrient Broth (NB) using a sterile loop, followed by incubation at 37°C for 16-18 hours. After incubation, bacterial density is standardized by preparing a suspension according to the McFarland standard using 0.85% NaCl (physiological saline) solution. For this purpose, 5 mL of sterile physiological saline is added to sterile tubes, and 1-2 drops of the overnight culture are transferred into these tubes. The turbidity of the suspension is visually adjusted to match the 0.5 McFarland standard (approximately 1.5×10^{8} CFU/mL). The standardized bacterial suspensions are evenly spread onto the surface of Mueller-Hinton Agar ((Biolife, 401740)) plates using sterile cotton swabs. Sterile white paper disks are carefully placed onto the agar surface after being impregnated with the pigment extract (approximately 10 µL per disk). Disks impregnated with only 10% methanol are used as controls. The prepared plates are incubated at 37°C for 24 hours. At the end of the incubation period, the diameters of the inhibition zones formed around the disks are measured in millimeters (mm) using a transparent ruler and recorded. These inhibition zone diameters are used to assess the antibacterial activity of the pigment extracts against the tested bacterial strains [64]. Figure 2.8 depicts experimental images of antibacterial activity tests performed using the disk diffusion method.

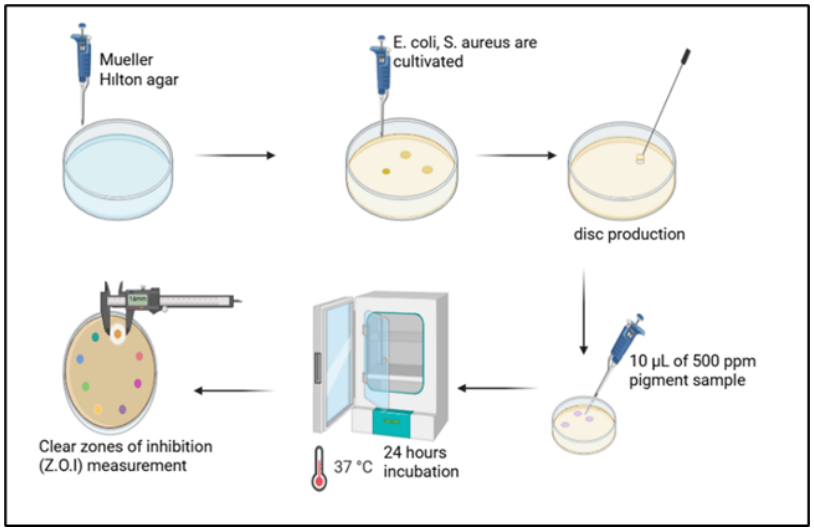

Figure 2.8 : Experimental images of the antibacterial activity of pigment.

3. RESULTS AND DISCUSSION

3.1 Plackett–Burman Optimization Results

Experimental setup for the three bacteria is provided in the following sub-headings, seperately.

3.1.1 *Brevibacterium* sp.

The culture medium composition and the Plackett-Burman experimental design (7 factors, 15 runs) used for *Brevibacterium* sp. are summarized in Table 3.1.

Table 3.1 : Plackett-Burman experimental design indicating the culture medium composition and experimental runs for *Brevibacterium* sp.

Run	Glucose (g/L)	Peptone (g/L)	NaCl (g/L)	Yeast Extract (g/L)	KH_2PO_4 (g/L)	Temp. (°C)	pH	Cell Weight/(g)	Total Carotenoid Concentration (µg/g)
1	15	7.5	8	3.5	2	26.5	7.2	0,231	26.525
2	10	10	6	2	1	28	7.5	0,159	50.761
3	10	5	10	5	3	25	7.5	0,197	50.761
4	10	5	6	2	1	25	6.9	0,250	21.12
5	15	7.5	8	3.5	2	26.5	7.2	0,247	26.531
6	10	10	10	5	1	28	7.5	0,469	63.62
7	20	5	6	2	3	28	7.5	0,452	27.07
8	20	10	6	5	1	25	6.9	0,405	6.324
9	20	10	10	2	3	28	6.9	0,381	9.02
10	10	5	6	5	3	28	6.9	0,273	28.321
11	10	10	10	2	3	25	6.9	0,186	51.182
12	20	10	6	5	3	25	7.5	0,546	8.791
13	20	5	10	2	1	25	7.5	0,537	17.139
14	15	7.5	8	3.5	2	26.5	7.2	0,156	26.489
15	20	5	10	5	1	28	6.9	0,572	0.56

In this study, a Plackett–Burman design consisting of 12 experimental conditions with 3 additional replicates (total of 15 runs) was applied to determine the primary media components and environmental parameters affecting pigment production. This design allows for rapid identification of the most influential factors with a limited number of experiments. The Plackett-Burman experimental design was used to conduct a preliminary screening of the factors affecting pigment production, and based on the

obtained results, the overall effect of the media components was examined. For more detailed optimization studies, the Box-Behnken Design (BBD) and Central Composite Design (CCD) methods can be used to determine the precise effects of each factor. Figure 3.1 shows the standardized effects of factors on pigment production in the Pareto chart. It shows which media component or environmental parameter has the strongest influence on pigment production overall.

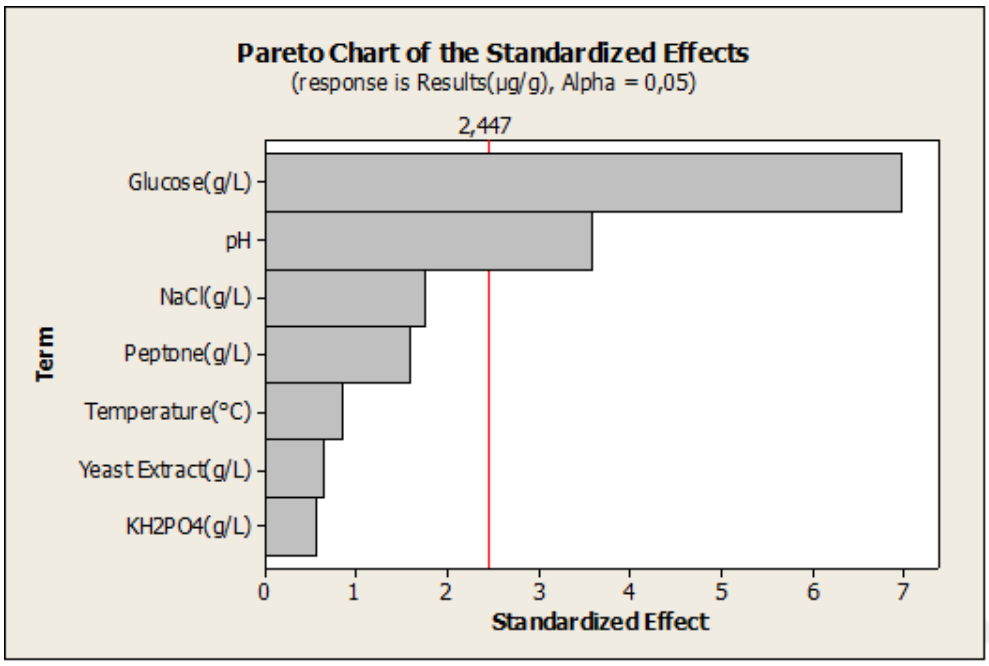

Figure 3.1 : Pareto chart of the Plackett-Burman design for *Brevibacterium* sp.

The Pareto chart depicts the standardized effects of the independent variables on pigment production. In the chart, the red line (2.447) represents the 95% confidence level's statistical significance threshold. Factors that fall to the right of this threshold are considered statistically significant.

The findings revealed that glucose concentration (g/L) had the greatest influence on pigment production. Increased glucose levels were found to reduce pigment yield, implying that excess carbon sources may inhibit secondary metabolite synthesis. *(Effect = –32,81; T = –6,95; F = 48,31; p < 0,001).* The second significant variable was pH. Changes in pH had a positive and statistically significant effect on pigment production *(Effect = 16.94; T = 3.59; F = 12.87; p = 0.012).* This finding demonstrates that acidic and basic environments have a significant impact on microorganism metabolism. Other variables, such as peptone (p = 0.165), NaCl (p = 0.129), yeast extract (p = 0.550), KH_2PO_4 (p = 0.601), and temperature (p = 0.429), showed higher

effect values for peptone and NaCl, indicating that these factors may play a secondary role in pigment production.

Table 3.2 shows the effects of independent variables on pigment production (µg/g) in coded units. The coded units make it easier to compare the effects of variables in different units.

Table 3.2 : Estimated effects and coefficients for results (µg/g) (coded units).

Term	Effect	Coef	SE Coef	T	P
Constant	-	27,89	2,360	11,82	0,000
(X_1)-Glucose(g/L)	-32,81	-16,41	2,360	-6,95	0,000
(X_2)-Peptone(g/L)	7,45	3,73	2,360	1,58	0,165
(X_3)-NaCl(g/L)	8,32	4,16	2,360	1,76	0,129
(X_4)-Yeast Extract (g/L)	-2,99	-1,49	2,360	-0,63	0,550
(X_5)-KH_2PO_4(g/L)	2,60	1,30	2,360	0,55	0,601
(X_6)-Temp(°C)	4,01	2,00	2,360	0,85	0,429
(X_7)-pH	16,94	8,47	2,360	3,59	0,012
Ct Pt	-	-1,37	5,278	-0,26	0,803

Model fit statistics: S = 8.17603; PRESS = 3609.76; R^2 = 91.92%; R^2 (adj) = 81.15%; R^2 (pred) = 27.30%.

Effects of independent variables on pigment production (µg/g) in coded units. Using coded units allows direct comparison of the relative effects of variables at different scales. The standard error (S) of the model was calculated as 8.17603 µg/g, which reflects the mean deviation between observed pigment yields and model-predicted values. Experimental data were analyzed using the multiple linear regression method in Minitab 16.0 software, and the general form of the model was expressed as follows:

In this model, Equations 3.1 and 3.2 represent the pigment concentration (µg/g), and Xi represents the coded levels of the relevant factors.

$$Y = \beta_0 + \sum_{i=1}^{7} \beta_i X_i \tag{3.1}$$

$$Y = \beta_0 + \beta_1 X_1 + \beta_2 X_2 + \beta_3 X_3 + \beta_4 X_4 + \beta_5 X_5 + \beta_6 X_6 + \beta_7 X_7 \tag{3.2}$$

The regression equation obtained using the coded units as a result of the analysis is presented in Equation 3.3.

$$\text{Results (µg/g)} = 27.89 - 16.41X_{Glucose} + 3.73X_{Peptone} + 4.16X_{NaCl} - 1.49X_{Yeast} + 1.30X_{KH_2PO_4} + 2X_{Temp} + 8.47X_{pH} \tag{3.3}$$

The model's coefficient of determination (R^2 = 91.92%) explains approximately 92% of the observed variance. The adjusted R^2 (R^2(adj) = 81.15%) indicates the model's high explanatory power. Examination of the regression coefficients in the table reveals that glucose concentration has a statistically highly significant ($p < 0.001$) and strong negative effect on pigment production (Effect = –32.81; Coefficient = –16.41). This result indicates that increasing the carbon source suppresses pigment biosynthesis. pH has a positive and statistically significant effect (Effect = 16.94; Coefficient = 8.47; p = 0.012). This finding indicates that pigment synthesis is supported at maximum pH. Other variables such as peptone (Effect = 7.45; p = 0.165) and NaCl (Effect = 8.32; p=0.129) tend to increase pigment production. Yeast extract, KH_2PO_4, and temperature factors had limited effects. Selecting glucose, peptone, and NaCl as variables with significant effect coefficients and examining them under different experimental conditions during further optimization stages may help better understand their potential roles. The center point (Ct Pt) result (-1.37 µg/g) indicates acceptable reproducibility of the experiments and largely maintains the linearity assumption. Equation 3.4 shows the regression equation generated with the experimental factors' actual units. This model is used in practical evaluations because it allows for the interpretation of the variable's physical quantities.

$$Y = -188.444 - 3.281X_1 + 1.491X_2 + 2.079X_3 - 0.995X_4 + 1.302X_5 + 1.335X_6 + 28.226X_7 \quad (3.4)$$

These findings show that the two models developed using coded and real units are compatible, and that glucose and pH are the primary factors influencing pigment production.

3.1.2 *Microbacterium* sp.

The culture medium composition and the Plackett-Burman experimental design (7 factors, 15 runs) used for *Microbacterium* sp. are summarized in Table 3.3. A 12-run Plackett-Burman design (with 3 additional replicates a total of 15 runs) was applied to identify the key media components and culture conditions influencing pigment production in *Microbacterium* sp. This approach enables rapid screening of the most significant variables with a limited number of experiments. The design allowed a preliminary evaluation of factors affecting pigment yield and the overall impact of each medium component.

Table 3.3 : Plackett-Burman experimental design indicating the culture medium composition and experimental runs for *Microbacterium* sp.

Run	Glucose (g/L)	Peptone (g/L)	NaCl (g/L)	Yeast Extract (g/L)	KH_2PO_4 (g/L)	Temp. (°C)	pH	Cell Weight/(g)	Total Carotenoid Concentration (µg/g)
1	10	5	6	2	1	25	7	0,314	126.75
2	10	5	6	5	3	30	7	0,184	179.89
3	10	10	6	2	1	30	8	0,275	107.63
4	20	5	6	2	3	30	8	0,425	35.764
5	10	10	10	2	3	25	7	0,215	125.306
6	20	10	6	5	3	25	8	0,398	73.11
7	10	5	10	5	3	25	8	0,300	89.66
8	15	7.5	8	3.5	2	27.5	7.5	0,098	62.03
9	15	7.5	8	3.5	2	27.5	7.5	0,098	62.01
10	20	10	6	5.0	1	25.0	7	0,225	88.646
11	20	5	10	2.0	1	25.0	8	0,104	9.615
12	20	5	10	5.0	1	30.0	7	0,247	48.987
13	15	7.5	8	3.5	2	27.5	7.5	0,101	60.22
14	10	10	10	5.0	1	30.0	8	0,398	77.319
15	20	10	10	2.0	3	30.0	7	0,406	34.729

For more detailed optimization, Box-Behnken (BBD) or Central Composite Design (CCD) methods can be employed. Figure 3.2 illustrates the standardized effects of these factors in a Pareto chart, highlighting those with the greatest influence on pigment production.

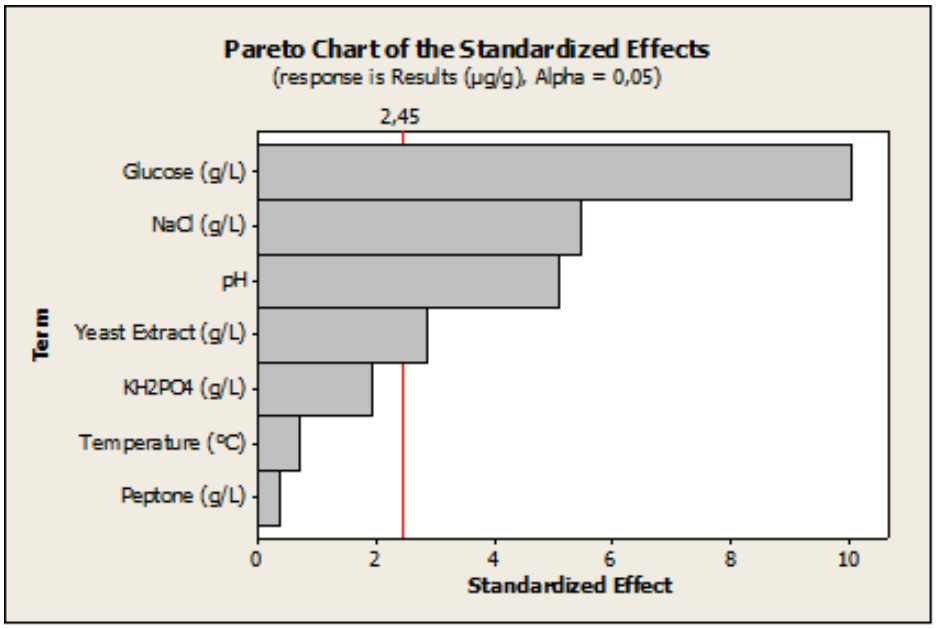

Figure 3.2 : Pareto chart of the Plackett-Burman design for *Microbacterium* sp.

Based on the Pareto chart derived from the Plackett-Burman design, the effects of various medium components and environmental factors on pigment production were investigated.

The Pareto analysis revealed that glucose concentration exerted the most pronounced negative effect on pigment biosynthesis (Effect = –69.28; $p < 0.001$). This finding suggests that an excess carbon source can suppress secondary metabolite formation, consistent with reports of catabolite repression in related Actinobacteria. Similarly, NaCl displayed a significant negative influence (Effect = –37.70; $p = 0.002$), implying that elevated salinity may reduce pigment accumulation rather than promoting osmotic-stress–induced secondary metabolism. Conversely, yeast extract contributed a positive and statistically significant effect (Effect = 19.64; $p = 0.029$), indicating that additional complex nitrogen sources may stimulate pigment formation, possibly by supplying growth factors or vitamins that enhance biosynthetic pathways. KH_2PO_4 also showed a positive tendency (Effect = 13.25; $p = 0.103$), suggesting that phosphate availability could play a supportive role, although the effect did not reach the conventional 95 % significance threshold. Among the physical factors, pH had a clear negative effect (Effect = –35.20; $p = 0.002$), showing that higher pH lowered pigment yield. Temperature showed a small negative trend (Effect = –4.79; $p = 0.513$), and peptone gave a slight positive effect (Effect = 2.68; $p = 0.711$), but these were not statistically significant in the tested range. The estimated effects and coefficients of the results and the effects of the independent variables on pigment production (μg/g) are shown in Table 3.4.

Table 3.4 : Estimated effects and coefficients for results (μg/g) (coded units).

Factor	Effect	Coeff.	SE Coeff.	T-value	P-value
Constant	-	83,12	3,446	24,12	0,000
(X_1) Glucose (g/L)	-69,28	-34,64	3,446	-10,05	0,000
(X_2)Peptone (g/L)	2,68	1,34	3,446	0,39	0,711
(X_3)NaCl (g/L)	-37,70	-18,85	3,446	-5,47	0,002
(X_4)Yeast Extract (g/L)	19,64	9,82	3,446	2,85	0,029
(X_5)KH_2PO_4 (g/L)	13,25	6,63	3,446	1,92	0,103
(X_6)Temp (°C)	-4,79	-2,40	3,446	-0,70	0,513
(X_7) pH	-35,20	-17,60	3,446	-5,11	0,002

Model fit statistics: S = 11,9358, PRESS = 7678,39, R-Sq = 96,73% R-Sq(pred) = 70,63% R-Sq(adj) = 92,37%.

The screening model captured over 96% of the variance in pigment production, highlighting glucose, NaCl, yeast extract, and pH as the main drivers of variability. In this model Equations 3.1 and 3.2. The regression equation obtained using the coded units as a result of the analysis is presented in 3.5.

$$Y = 83.13 - 34.64X_{Glucose} + 1.34X_{Peptone} - 18.85X_{NaCl} + 9.82X_{Yeast} + 6.63X_{KH_2PO_4} - 2.46X_{Temp} - 17.6X_{pH} \quad (3.5)$$

Equation 3.6 shows the regression equation generated using the actual units of the experimental factors. This model is used in practical evaluations because it enables the interpretation of the variable's physical quantities.

$$Y = 512.638 - 6.92840X_1 + 0.53580X_2 - 9.42392X_3 + 6.54544X_4 + 6.62600X_5 - 0.95893X_6 - 35.2017X_7 \quad (3.6)$$

These findings show that the two models developed with coded and real units are compatible, and that glucose, NaCl, yeast extract, and pH are the main factors influencing pigment production. These results provide a solid basis for subsequent optimizations, such as Box-Behnken designs, by focusing on the most influential factors identified in this preliminary study. According to the Optimization Plot data obtained as a result of the experimental optimization performed with the Plackett–Burman design (Minitab 16.0), the medium components and culture conditions that provided the highest level of pigment production were determined as glucose 20 g/L, peptone 5.0 g/L, NaCl 6 g/L, yeast extract 5.0 g/L, KH_2PO_4 3.0 g/L, temperature 30 °C and pH 7.0, respectively.

3.1.3 *Rhodococcus fascians*

The culture medium composition and the Plackett-Burman experimental design (9 factors, 15 runs) used for *Rhodococcus fascians* are summarized in Table 3.5. To identify environmental factors influencing pigment production, a nine-factor Plackett-Burman (PBD) experimental design was used. The following factors were assessed: glucose, peptone, yeast extract, NaCl, $MgSO_4 \cdot 7H_2O$, KH_2PO_4, $(NH_4)_2SO_4$, temperature, and pH. The design consisted of 15 conditions (12 baseline conditions and 3 center points). The experiment's pigment concentrations (µg/g) were analyzed using Minitab 16.0 software for multiple linear regression.

Table 3.5 : Plackett–Burman design for 12 variables and 3 dummy variables (runs 4, 10, and 15) coded to complete the 15-run design.

Run	Glucose (g/L)	Peptone (g/L)	Yeast extract (g/L)	NaCl (g/L)	$MgSO_4.7H_2O$ (g/L)	KH_2PO_4 (g/L)	$(NH_4)_2SO_4$ (g/L)	Temp (°C)	pH	Cell Weight(gr)	Total Carotenoid Concentration (µg/g)
1	2	4	6	1.3	1	0.1	1	35	6.5	0.147	42.17
2	2	4	2	1.3	1	1.3	0.1	35	7.2	0.222	27.92
3	2	6	2	0.1	0.1	1.3	1	35	6.5	0.285	31.22
4	4	5	4	0.7	0.55	0.7	0.55	30	6.85	0.218	42.20
5	6	4	6	1.3	0.1	1.3	0.1	25	6.5	0.045	200.00
6	6	6	2	1.3	0.1	0.1	0.1	35	7.2	0.039	220.00
7	6	4	6	0.1	0.1	0.1	1	35	7.2	0.074	452.70
8	2	6	6	1.3	0.1	1.3	1	25	7.2	0.087	485.00
9	2	6	6	0.1	1	0.1	0.1	25	7.2	0.281	61.56
10	4	5	4	0.7	0.55	0.7	0.55	30	6.85	0.230	43.91
11	6	6	2	1.3	1	0.1	1	25	6.5	0.060	180.00
12	6	6	6	0.1	1	1.3	0.1	35	6.5	0.069	95.16
13	6	4	2	0.1	1	1.3	1	25	7.2	0.069	255.07
14	2	4	2	0.1	0.1	0.1	0.1	25	6.5	0.161	93.16
15	4	5	4	0.7	0.55	0.7	0.55	30	6.85	0.225	40.88

The overall regression model is expressed as Equation 3.7.

$$Y = \beta_0 + \sum_{i=1}^{9} \beta_i X_i \tag{3.7}$$

The pigment concentration is denoted by Y, while the coded levels of the factors are represented by X_i.

The regression equation obtained using the coded units as a result of the analysis is presented in Equation 3.8.

$$\begin{aligned} Y = 178.7 + 55.2X_1 + 0.2X_2 + 44.1X_3 + 13.9X_4 - 68.3X_5 + \\ 3.7X_6 + 62.4X_7 - 33.8X_8 + 71.7X_9 \end{aligned} \tag{3.8}$$

The regression model in which the factors are expressed in real experimental units is given in Equation 3.9.

$$\begin{aligned} Y = -1234.53 + 27.5789X_1 + 0.1595X_2 + 22.0511X_3 + \\ 151.888X_5 + 6.2186X_6 + 138.586X_7 - 6.76023X_8 + 204.889X_9 \end{aligned} \tag{3.9}$$

A Plackett-Burman experimental design with 15 runs was used to determine the major media components and culture conditions (temperature and pH) that influence pigment yield. In this design, 12 conditions contained experimental variables, and three conditions served as controls, with the factors run at intermediate values. The

experiments evaluated various concentrations of glucose, peptone, yeast extract, NaCl, $MgSO_4 \cdot 7H_2O$, KH_2PO_4, and $(NH_4)_2SO_4$, as well as temperature (25-35 °C) and pH (6.5-7.2). Each factor was tested at two levels (-1, +1) to identify variables with a significant effect on pigment production.

Figure 3.3 illustrates the standardized effects of these factors in a Pareto chart, highlighting those with the greatest influence on pigment production.

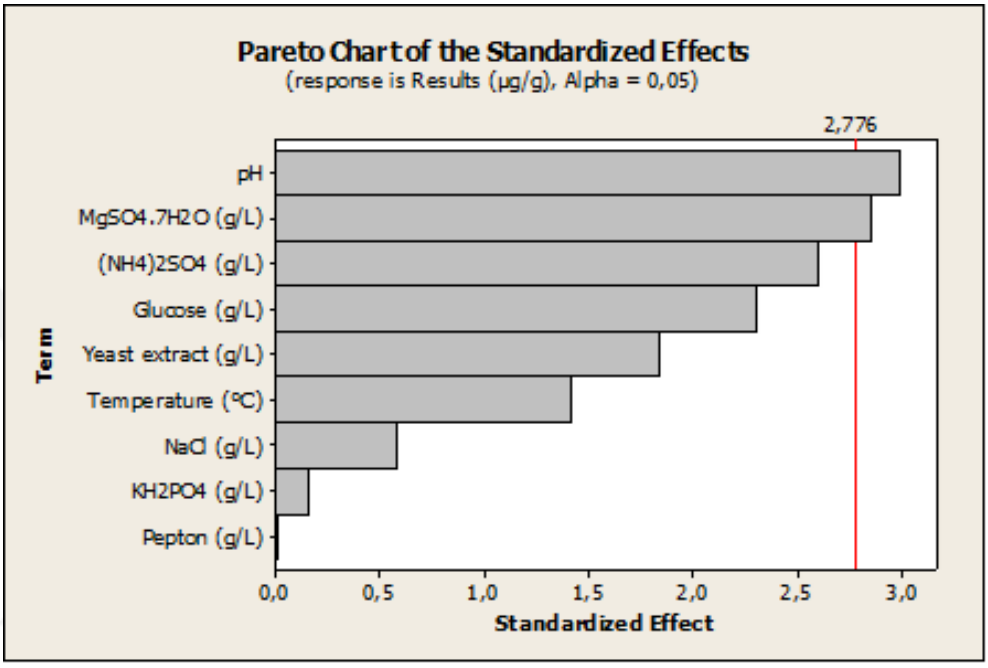

Figure 3.3 : Pareto chart of the Plackett-Burman design for *Rhodococcus fascians.*

Each factor's relative impact on pigment production is represented by horizontal bars in the graph; the length of the bar indicates the effect size, and the red vertical line denotes a significance level of $\alpha = 0.05$. The graph indicates that the factors with the greatest effects on pigment production are pH and $MgSO_4 \cdot 7H_2O$. Positive standardized effects indicate that pigment yield increases, whereas negative effects indicate that it decreases. Nutrients like $(NH_4)_2SO_4$ and glucose have significant effects, but not as much as pH and $MgSO_4 \cdot 7H_2O$. Other factors with lower effect values include yeast extract, temperature, NaCl, KH_2PO_4, and peptone. These findings suggest that pH and magnesium salt concentration are critical for pigment production and should be prioritized in production optimization.

Table 3.6 presents the impact of the independent variables on pigment production (µg/g) expressed in coded units, which facilitates comparison of the effects across variables with different measurement scales.

Table 3.6 : Estimated effects and coefficients for results (µg/g) (coded units).

Factor	Effect	Coefficient	SE Coefficient	T-value	P-value
Constant		178,7	23,96	7,46	0,002
Glucose (g/L)	110,3	55,2	23,96	2,3	0,083
Peptone (g/L)	0,3	0,2	23,96	0,01	0,995
Yeast Extract (g/L)	88,2	44,1	23,96	1,84	0,140
NaCl (g/L)	27,7	13,9	23,96	0,58	0,594
$MgSO_4,7H_2O$ (g/L)	-136,7	-68,3	23,96	-2.85	0,046
KH_2PO_4 (g/L	7,5	3,7	23,96	0,16	0,884
$(NH_4)2SO_4$ (g/L)	124,7	62,4	23,96	2,60	0,060
Temperature (°C)	-67,6	-33,8	23,96	-1.41	0,231
pH	143,4	71,7	23,96	2.99	0,040
Ct Pt		-136,3	53,59	-2,54	0,064
S = 83,0147	*PRESS = 992211*				
R-Sq = 91,18%	*R-Sq(adj)=69,14%*				

The factorial regression results between pigment production (µg/g) of *Rhodococcus fascians* and different medium components and culture conditions are shown in the above table. The "Effect" and "Coef" values in the table indicate the direction and magnitude of each variable on pigment yield. Positive values represent an increasing effect on pigment production, while negative values represent a decreasing effect. According to the analysis results, pH and $(NH_4)_2SO_4$ show increasing effects on pigment production, while $MgSO_4 \cdot 7H_2O$ stands out as a significant factor reducing pigment production. The effects of other nutritional sources, such as glucose and yeast extract, are more limited and less statistically significant. The R^2 value of the model is 91.18%, explaining a large portion of the model data variance. These results emphasize that pH and magnesium salt concentration are particularly critical parameters for optimizing pigment production.

Optimization plot data obtained from experimental optimization using the Plackett-Burman design (Minitab 16.0) revealed that *Rhodococcus fascians* produced the most pigment at low $MgSO_4 \cdot 7H_2O$ and NaCl concentrations, high yeast extract, and moderate ammonium sulfate levels. Experimental data revealed that pigment synthesis reached its highest level at pH 7.20 and an incubation temperature of 25°C. In the study, it was found that the highest pigment yield (485 µg/g) was obtained with 2 g/L glucose, 6 g/L peptone, 6 g/L yeast extract, 1.3 g/L NaCl, 0.10 g/L $MgSO_4 \cdot 7H_2O$, 1.3 g/L KH_2PO_4, 1.0 g/L $(NH_4)_2SO_4$, 25°C and pH 7.20. This medium composition was presented as the experimental optimum culture formulation discovered for *Rhodococcus fascians* pigment production in the scope of the study. The three center points used in this study were incorporated into the design to evaluate experimental

error and potential curvature. The Plackett-Burman design only estimates main effects and cannot analyze interactions between factors, resulting in a relatively low R^2(adj) value. Some variables, such as glucose and $(NH_4)_2SO_4$, were included in the analysis despite not being significant at $p<0.05$ due to their biological significance and effects near $p<0.10$. Multifactorial and non-replicated screening designs may result in lower adjusted R^2 values, but the model still explains a significant portion of the data. The fact that the residual distributions resemble a normal distribution suggests that the model is consistent with the statistical assumptions.

3.2 Characterization Analysis Results

3.2.1 Effect of pH on the pigment stability for *Brevibacterium* sp.

Absorbance measurements performed with UV spectrophotometry at different pH values reveal the pigment's chemical stability and pH sensitivity. These analyses help determine the pigment's optimum pH and the pH range at which its color or absorbance is maximized. UV-Vis spectrophotometric analyses of *Brevibacterium* sp. pigments reveal significant changes in their absorbance properties depending on pH. Figure 3.4 shows the UV-Vis absorbance values of pigments measured in *Brevibacterium* sp. bacteria grown at different pH values in TSB (Tryptic Soy Broth) at 25°C with an agitation speed of 110 rpm.

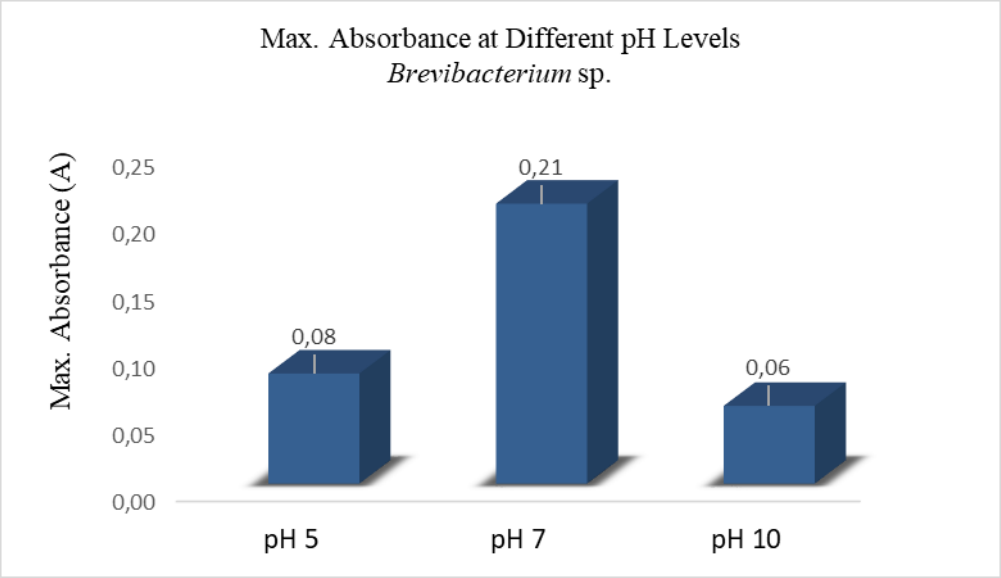

Figure 3.4 : UV-Vis absorbance of pigments produced by *Brevibacterium* sp. at different pH values.

The figure indicates that the absorbance is 0.082 at pH 5 (maximum wavelength 397nm), 0.209 at pH 7 (427nm) and 0.060 at pH 10 (372nm). These findings reveal that the pigment exhibits the highest light absorption and therefore maximum stability under neutral pH conditions (pH 7). The low absorbance in an acidic environment (pH 5) indicates that the light absorption of the pigment has decreased and the color form may have partially changed. The fact that the absorbance is low again in a basic environment (pH 10) suggests that structural changes have occurred in the pigment molecules and that stability has decreased. These decreases are due to the changes in the electronic structure and conjugation system of the pigment due to excessive protonation (acidic environment) or deprotonation (basic environment). Therefore, according to these three different pH conditions, the optimum stability and maximum light absorption of the pigment was observed at pH 7; Acidic and basic environments negatively affected the photostability of the pigment. The effects of different pH values on pigment concentration in *Brevibacterium* sp. are shown in Figure 3.5.

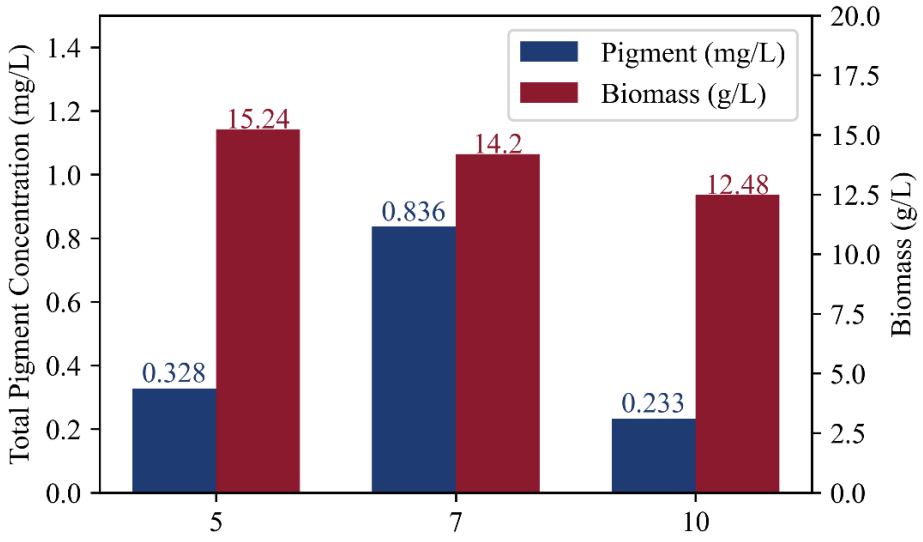

Figure 3.5 : The impact of various pH levels on pigment concentration.

The analysis results showed that pigment concentrations peaked at neutral pH (pH 7). Pigment concentrations decreased significantly in both acidic (pH 5) and basic (pH 10) conditions. These results suggest that the pigment is more stable in neutral environments, but its stability decreases at extreme pH values due to structural degradation or fragmentation.

3.2.2 Effect of pH on the pigment stability for *Microbacterium* sp.

The pH-dependent absorbance properties of *Microbacterium* sp. pigments were investigated using a UV-Vis spectrophotometer. Figure 3.6 shows the growth conditions of *Microbacterium* sp. at 407 nm wavelength under different pH conditions. According to different pH conditions, optimum pigment stability and maximum light absorption were observed at pH 7; acidic and basic environments negatively affected pigment photostability. Acidic environments had the most negative effect on pigment stability, while pH 7 achieved the optimum effect.

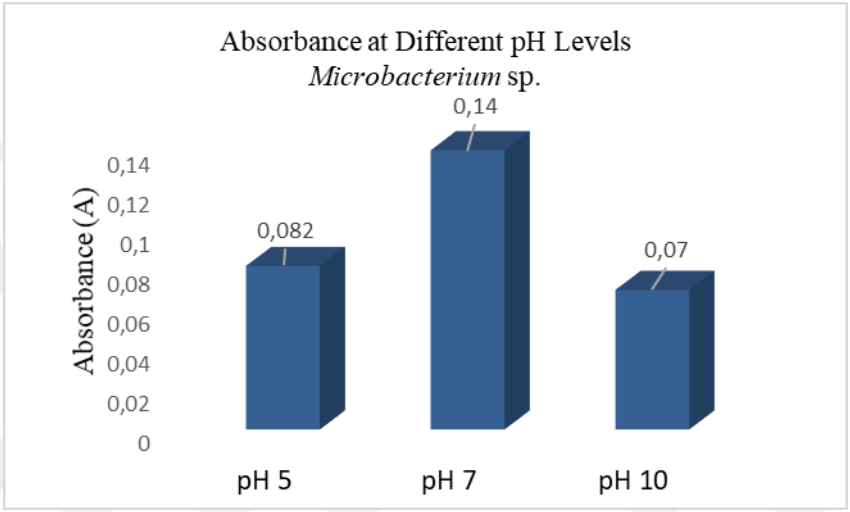

Figure 3.6 : UV-Vis absorbance of pigments produced by *Microbacterium sp.* at different pH values.

The effects of different pH values on pigment concentration in *Microbacterium* sp. are shown in Figure 3.7.

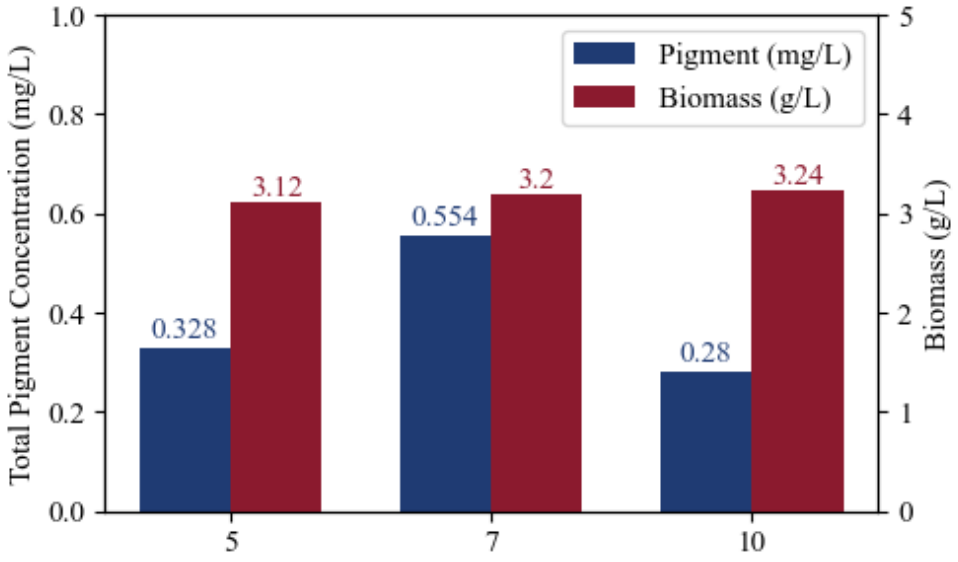

Figure 3.7 : The effect of various pH levels on pigment concentration.

Pigment concentration varied significantly between pH conditions. At pH 7, the highest pigment concentration was observed (0.554 mg/L) and remained at a moderate level in acidic environments (pH 5), while there was a significant decrease in alkaline environments (pH 10). These findings show that the pigment is sensitive to both low and high pH conditions, with pigment yields remaining most consistent in the neutral range.

3.2.3 Effect of pH on the pigment stability for *Rhodococcus fascians*

The stability of *Rhodococcus fascians* pigment was assessed under various pH conditions using both total pigment concentration and measured absorbance values. The findings indicate that pigment production and stability are pH dependent, with the optimal range being close to neutral. In Figure 3.8 , absorbance measurements were used to assess pigment stability. At pH 7, the highest absorbance value was 0.217 Å, while at pH 7.5 and 6 it was 0.15 Å and 0.079 Å respectively. At pH 9, the min. absorbance was 0.05 Å.

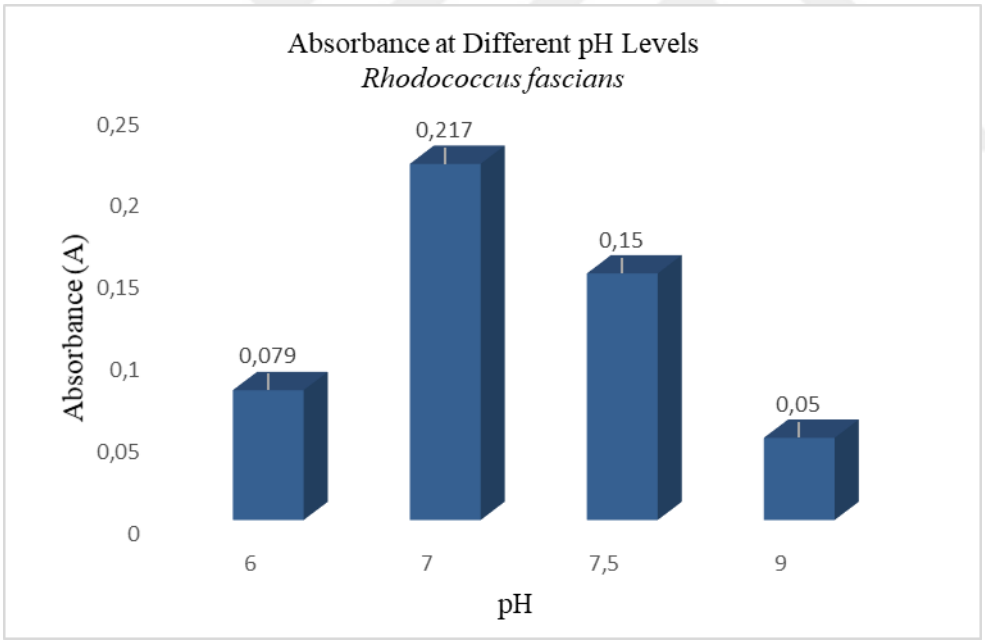

Figure 3.8 : Effect of pH on the pigment stability of *Rhodococcus fascians* based on absorbance measurements.

These findings show that pigment stability peaks at neutral pH and degrades in both acidic and alkaline conditions. Overall, the data show that *Rhodococcus fascians* pigment is more stable in the neutral pH range (pH 7-7.5) and performs best in terms of both production and optical absorbance. Shifting the pH to more extreme levels, such as 6 and 9, has a negative impact on the pigment's synthesis and structural

stability. Figure 3.9 shows the total pigment concentration and biomass values obtained at various pH levels.

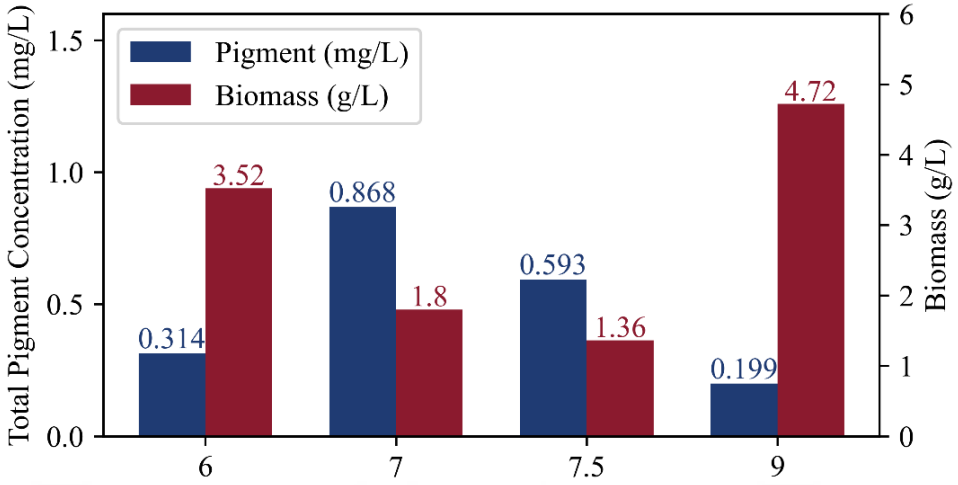

Figure 3.9 : Total pigment concentration and biomass values at various pH levels.

The figure shows that total pigment concentration peaked at pH 7, reaching 0.868 mg/L. Cellular biomass reached 1.8 g/L at this pH. At pH 7.5, pigment concentration decreased slightly to 0.593 mg/L, while biomass production was relatively low at 1.36 g/L compared to pH 7. Under low pH (pH 6) conditions, pigment production decreased significantly (0.314 mg/L), while biomass increased to 3.52 g/L. Pigment production decreased to its lowest level (0.199 mg/L) in an alkaline environment (pH 9), while biomass production reached its highest level (4.72 g/L).

This is a result of bacteria shifting their metabolic resources in different directions in response to stress conditions. Pigment production is mostly a secondary metabolite, while biomass increase is a product of primary metabolism. The fact that pigment production peaked at pH 7, at 0.868 mg/L, is a result of the max. activity of carotenoid biosynthesis enzymes within the optimal pH range. Key enzymes involved in the synthesis of carotenoid pigments (e.g., phytoene synthase, desaturase, and cyclase) are most active at a specific pH. Therefore, based on these data, the enzymes required for pigment production achieved the ideal ionization state between pH 7 and 7.5. In other words, metabolic progression shifted to pigment production. However, low and high pH ranges stressed these bacteria and activated their primary defense mechanisms. Therefore, metabolic energy was directed not toward pigment production but toward maintaining essential vital processes and growth.

Extraction results performed to evaluate the solubility of the pigment produced by *Rhodococcus fascians* in different solvents are presented Figure 3.10. Extraction

studies in four different solvents show that the pigment's dissolution behavior is influenced by solvent polarity. According to the findings, the pigment had the highest solubility in methanol, with a relative absorbance value of 100%. Methanol was the most prevalent, followed by diethyl ether (75.5%) and ethanol (66.5%). In contrast, the pigment's solubility in ethyl acetate was extremely low, with a relative absorbance value of only 36%. These findings suggest that the pigment is extracted more efficiently in medium to high polarity solvents, with methanol, in particular, showing compatibility with the pigment's structural features (possibly oxygen-containing functional groups or xanthophyll-like character).

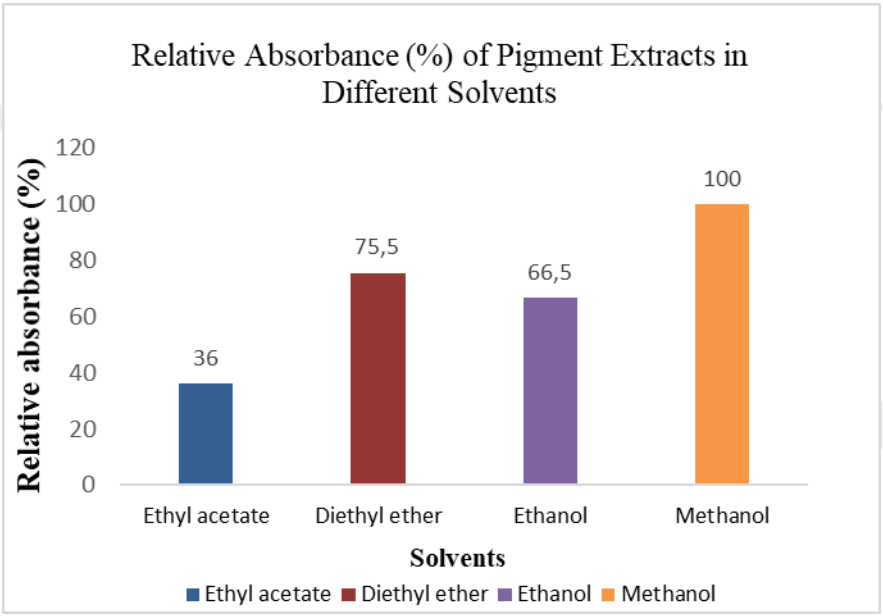

Figure 3.10 : Comparative relative absorbance (%) of *Rhodococcus fascians* pigment extracted with four different solvents.

3.2.4 Fourier transform infrared (FT-IR) spectroscopy of pigments

3.2.4.1 FT-IR analysis of the pigment extract from *Brevibacterium* sp.

According to the literature, secondary amide groups can replace the free N–H stretching band by forming dimers (cis configuration) or polymers (trans configuration) through hydrogen bonding. The prominent band in the 2922 cm^{-1} region in the spectrum represents asymmetric aliphatic C-H stretching vibrations (CH_2-CH_3 stretching), typical of carotenoid structure [65]. This band, which indicates the presence of long isoprenoid chains, has been frequently observed in bacterial carotenoids. This vibration originating from the isoprene chain supports the pigment's aliphatic hydrocarbon backbone.

The resulting FTIR spectrum (Figure 3.11) contain vibrational ranges that indicated the pigment's carotenoid or isoprenoid nature.

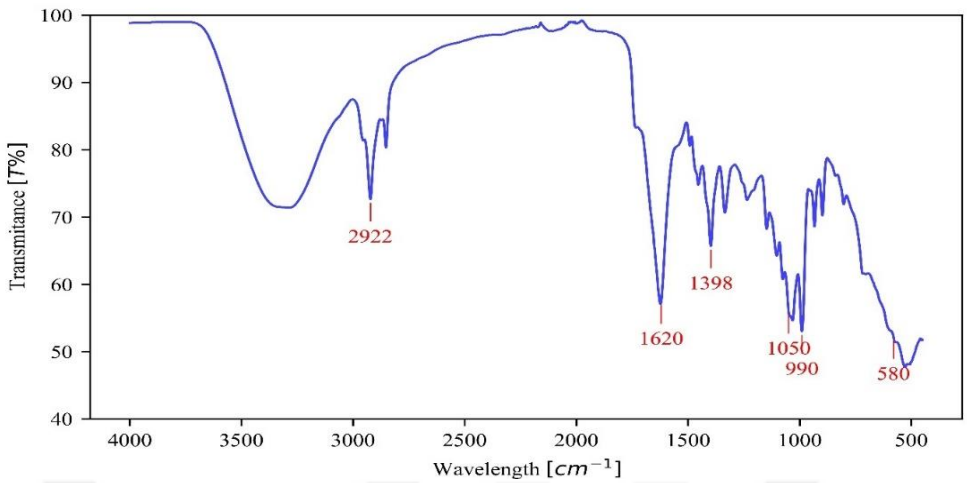

Figure 3.11 : Structural FTIR interpretation of the *Brevibacterium* sp. pigment

The broad band observed between 3500–3000 cm^{-1} may be due to phenolic or aliphatic O–H stretching vibrations and N–H stretching vibrations of the secondary amide. UV-Vis analysis revealed that *Brevibacterium* sp. pigment has maximum absorption in the 407-412 nm range, which is consistent with pigments with medium-length conjugated π-electron chains in the carotenoid class. According to the FTIR spectrum, the conjugated C=C stretching vibration band appears at a higher frequency than linear carotenoids [66]. While the C=C stretching band is typically observed in the 1500-1520 cm^{-1} range in linearly conjugated carotenoids (e.g., β-carotene), the fact that this band becomes more pronounced around 1550-1580 cm^{-1} in *Brevibacterium* pigment suggests that the conjugation of the pigment does not form a completely linear chain, but rather has the structural behavior seen in aryl carotenoids containing aromatic rings. The FTIR spectrum shows bands corresponding to aromatic C=C vibrations in the 1480-1600 cm^{-1} range, indicating the presence of aromatic rings within the pigment structure. Aromatic C-H bending vibrations in the 700-900 cm^{-1} range also support the aryl character. The 580 cm^{-1} band in the low-frequency region of the spectrum indicates the presence of three-ring conjugation or heavy-atom bonds. This region can be interpreted as indicating the presence of ringed or rigid units in the pigment's structure.

3.2.4.2 FTIR analysis of the pigment extract from *Microbacterium* sp.

The FTIR spectrum of the pigment from *Microbacterium* sp. shows characteristic vibration bands consistent with carotenoidisoprenoid structures. The main absorption

peaks are observed at 2920, 1620, 1398, 1050 and 514 cm^{-1} and in a broad region between 3000-3500 cm^{-1}. The FTIR profile of *Microbacterium* sp. Figure 3.12 exhibits diagnostic vibrational features indicative of an isoprenoid, carotenoid-like pigment.

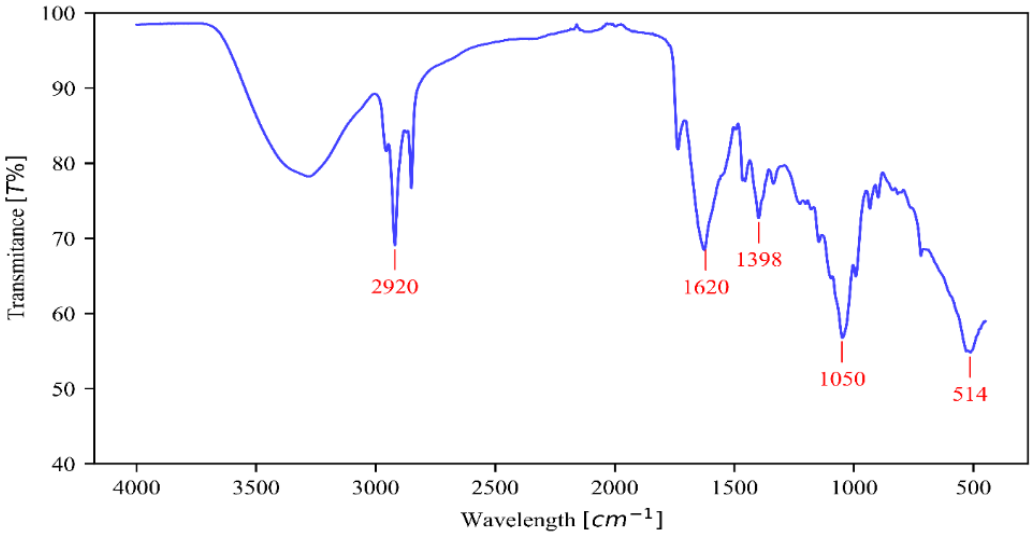

Figure 3.12 : FTIR analysis of the pigment extracted from *Microbacterium* sp.

The broad band between 3000–3500 cm^{-1} in the FTIR spectrum generally corresponds to the O–H stretching vibration and indicates structures containing hydroxyl groups, such as alcohols, phenolic compounds, or hydroxylated carotenoid derivatives. Indeed, a distinct broad O–H band in this region has been reported in the literature in pigments produced by *Microbacterium oxydans* [67]. The peak observed in the spectrum around 2920 cm^{-1} is consistent with the asymmetric stretching vibration of aliphatic CH_2-CH_3 groups and frequently occurs as a strong absorption in carotenoids with long isoprene chains [65]. Conjugated double bonds typically exhibit C=C stretching vibrations at 1500-1650 cm^{-1} [68]. The band at 1620 cm^{-1} in this study suggests that the pigment has a short or medium-length conjugation chain. An aryl ring or a peripheral ring unit in the structure may participate in conjugation to some extent. This frequency range is supported by the fact that *Microbacterium* species produce primarily yellow-orange pigments.

3.2.4.3 FTIR analysis of the pigment extract from *Rhodococcus fascians*

The 1600–1650 cm^{-1} range is a critical region in the FTIR characterization of carotenoids and confirms that the pigment contains conjugated double bonds [69]**.** The 1399 cm^{-1} band is associated with CH_3 bending vibrations of methyl groups in the isoprene chain, according to literature [70]. This region represents the methylation

pattern found in carotenoids and contains information about the pigment's isoprenoid skeleton.

The FTIR spectrum of *Rhodococcus fascians* (Figure 3.13) reveals characteristic absorption bands associated with the structural features of the pigment.

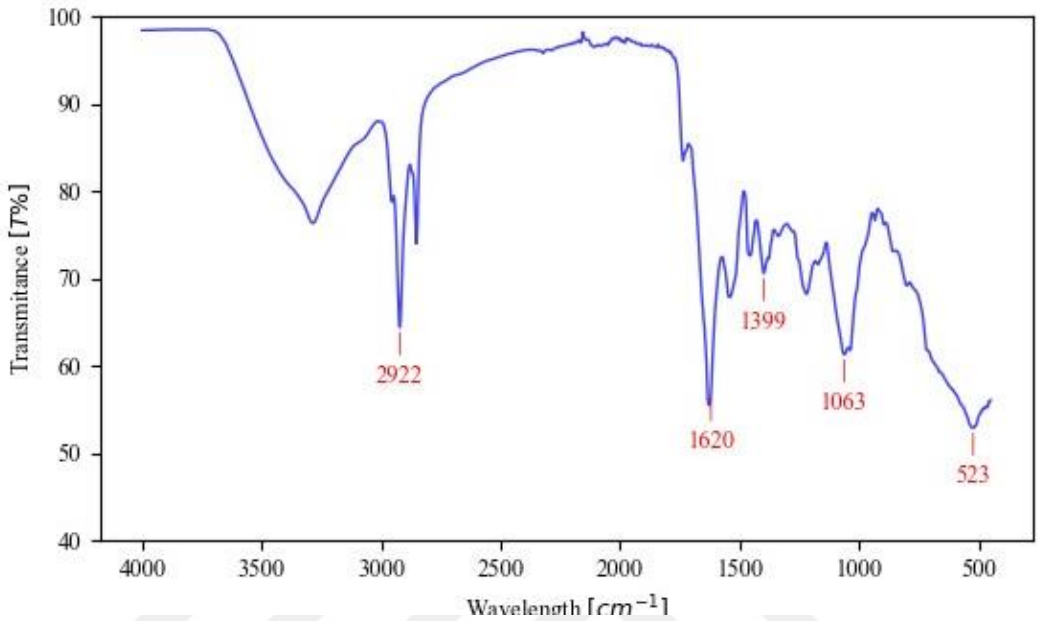

Figure 3.13 : FTIR analysis of the pigment extracted from *Rhodococcus fascians.*

A study in the literature reported that the symmetric N-H_2 stretching vibrations of amide groups in the FTIR spectrum formed a distinct peak around 3261 cm^{-1}. C-H stretching vibrations of alkane and alkane-derived isopropyl and ethyl side chains were observed at 2949 cm^{-1}, C-N stretching vibrations at 1151 cm^{-1}, and C-H convex vibrations of aromatic rings at 711 cm^{-1}, respectively [71]. These bands provide important vibrational information about the structural properties of the *Rhodococcus fascians* pigment, indicating that it has a mixed molecular structure with both aliphatic and aromatic components. In addition, the pigment's high solubility in methanol (MeOH) suggests that the structure may be a xanthophyll-type carotenoid with oxygen-containing functional groups rather than a pure β-carotene skeleton.

Additionally, the presence of pigment from *Rhodococcus fascians* is demonstrated in Figure 3.14 using a scanning electron microscopy (SEM) image.

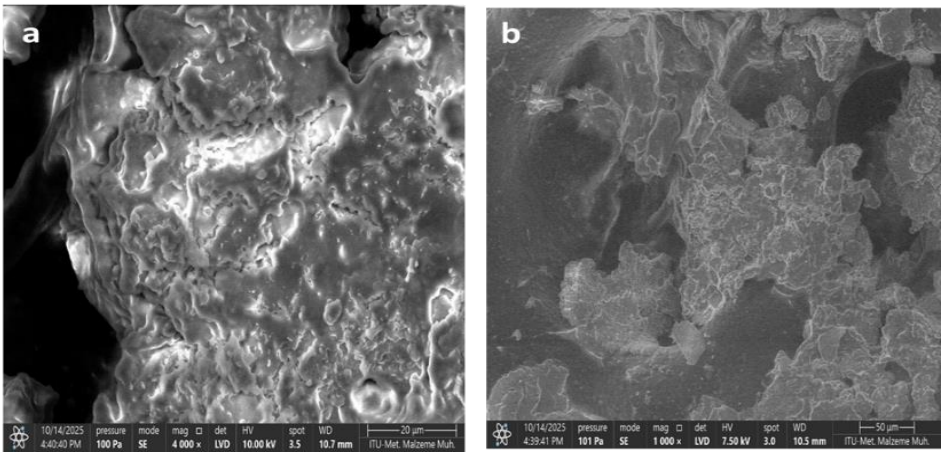

Figure 3.14 : The pigment extracted from *Rhodococcus fascians* was imaged by SEM, showing (a) a 20 µm and (b) a 50 µm scale, at the ITU Faculty of Chemical and Metallurgical Engineering.

3.2.5 UV-Vis spectrophotometric analysis

UV-Vis spectrophotometric analysis was performed to determine the absorption profile of the bacterial pigments. Distinct peaks observed in the UV and visible regions indicate the presence of extended double-bond systems within the pigment molecules. Figure 3.15 shows the λ_{max} absorbance and wavelength in UV-vis spectrophotometry of the ethanolic pigment solution obtained from *Brevibacterium* sp.

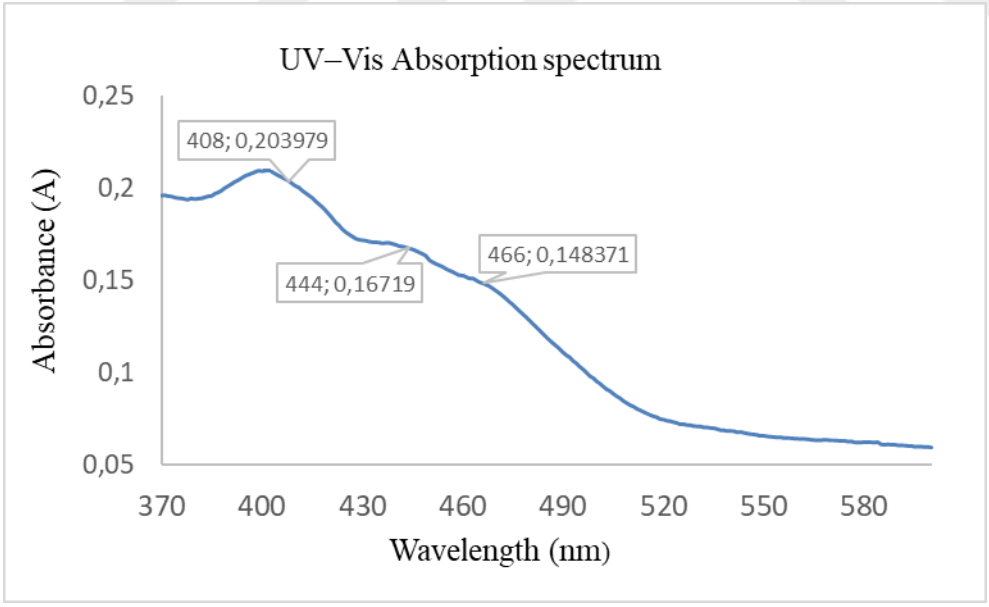

Figure 3.15 : UV–Vis absorption spectrum of *Brevibacterium* sp. pigment extract.

The maximum absorption wavelength (λ_{max}) of the colored supernatant obtained after pigment extraction was determined using UV/Visible spectrophotometer. The spectrum of the *Brevibacterium* sp. pigment extract revealed a main maximum at 407 nm (A_max = 0.21). Previous studies have shown that three carotenoid pigment

fractions isolated from *Brevibacterium linens* cells exhibit nearly identical electronic absorption spectra [53], [76]. They later determined that the pigments with these spectral properties were isorenieratene, 3-hydroxyisorenieratene, and 3,3′-dihydroxyisorenieratene. These findings imply that the pigment isolated from the *Brevibacterium* sp. strain in our study also contains a carotenoid-structured chromophore and may have a structure similar to isorenieratene and its derivatives described in the literature. Figure 3.16 shows the UV-Vis spectral analysis data for *Microbacterium* sp. pigments. UV-Vis spectral analysis of pigments from *Microbacterium* sp. revealed λ_{max} at 407, 441, and 469 nm.

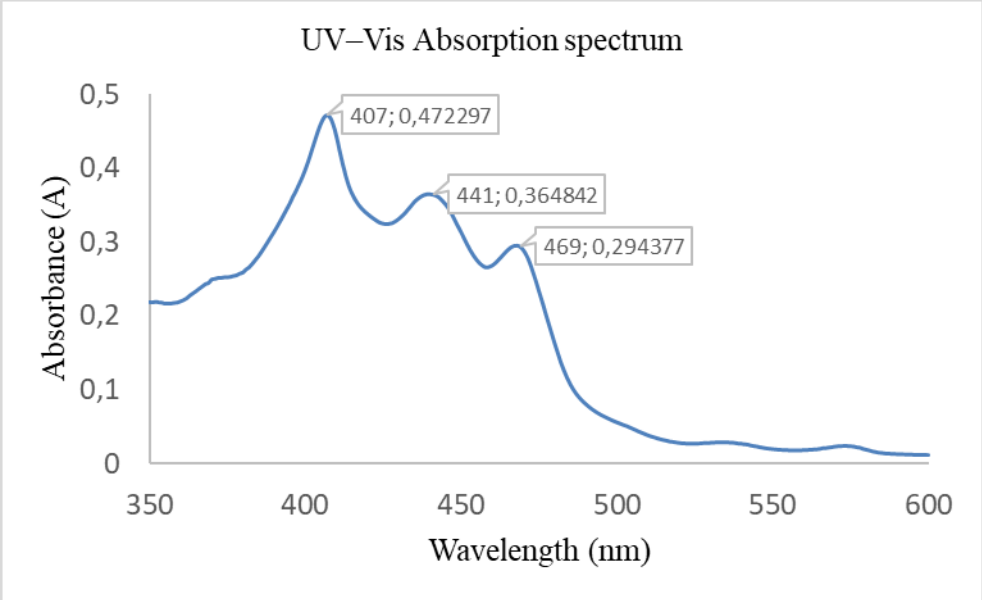

Figure 3.16 : UV–Vis absorption spectrum of *Microbacterium* sp. pigment extract.

Literature studies suggest that the pigment structure may be a neurosporene-type C40 carotenoid or its derivative derivative [47], [72]. Neurosporene typically exhibits three absorption maxima at approximately 410–420 nm, 435–440 nm, and 465–470 nm, consistent with a C_{40} carotene containing nine conjugated double bonds. Figure 3.17 shows the UV-Vis spectral data for *Rhodococcus fascians* pigments. The spectrum has a broad band structure in the visible region (300-600 nm), with three distinct absorption peaks at 428, 457, and 490 nm.

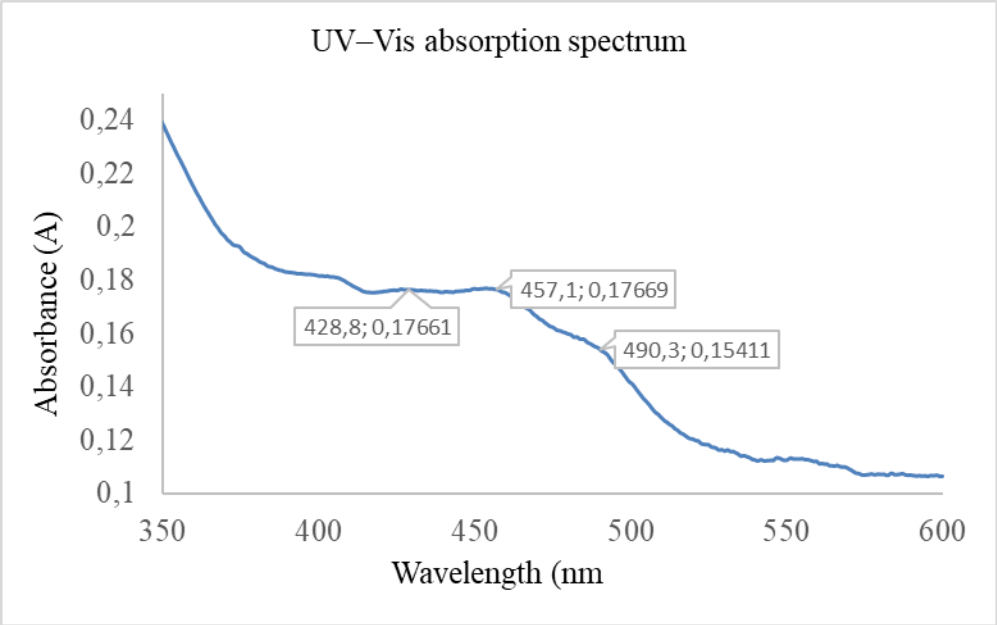

Figure 3.17 : UV-Vis absorption spectrum of *Rhodococcus fascians* pigment extract.

When combined with the TLC analysis data from this study, the absorption peaks in the UV-Vis spectrum indicate a carotenoid/xanthophyll structure for the pigment, as studies in the literature have shown that xanthophylls such as lutein and zeaxanthin have similar multiband absorption profiles in the UV-Vis range [34], [73].

3.2.6 Thin-layer chromatography (TLC) of pigment extracts

The pigment diversity and band profiles were evaluated using thin layer chromatography. 5–10 µL of pigment solutions were applied as spots onto silica gel 60 F_{254} aluminum plates (20 × 20 cm; Merck, Darmstadt, Germany), which served as the stationary phase.

As a result, two bands were found in the TLC analysis of *Rhodococcus fascians* pigment extract, with Rf values of 0.84 and 0.31, respectively. The Rf value for the band corresponding to the Lucarotin® 1 reference pigment was calculated as 0.92.

In the literature, Rf values reported for xanthophylls in TLC studies are approximately 0.38 for zeaxanthin, 0.35 for violaxanthin, and 0.74-0.81 for lutein [74]. When the Rf values obtained for the *Rhodococcus fascians* pigment extract in this thesis (0.31 and 0.84) are compared to these ranges, it is discovered that the band with Rf = 0.31 indicates a more polar, xanthophyllic carotenoid fraction, similar to the Rf values reported for zeaxanthin and violaxanthin. In contrast, the band with Rf = 0.84 is located in a region very close to the Rf range reported for lutein and the Rf = 0.92 value of the β-carotene standard used as a control in this study, representing a lower-polarity,

carotene-like pigment fraction. According to TLC results, at least two carotenoidic components with distinct polarities are present in the pigments produced by *R. fascians*.

3.2.7 DPPH (2,2-diphenyl-1-picrylhydrazyl) analysis

DPPH solution turns from purple to yellow after 15 and 30 minutes of antioxidant interaction. After incubation, the absorbance of all mixtures was measured with a UV-Vis spectrophotometer in the 517 nm wavelength range (bandwidth 1-2 nm). A 200 μM DPPH stock solution was prepared for use in the analyses. For this purpose, 2 mg of DPPH (M = 394.32 g/mol) was placed in a 50 mL volumetric flask. A small amount of methanol was added to completely dissolve it, and the volume was made up to 25 mL with methanol. The prepared DPPH stock solution was stored in an amber bottle at 4°C and protected from light. The pigment stock solution was prepared at a concentration of approximately 1.2 μg/μL. For this purpose, 12 mg of purified pigment were dissolved in 10 mL of methanol. The stock solution concentration was 1,2 mg/mL (1.2 μg/μL), and all working concentrations were obtained by extracting appropriate volumes of this stock solution. For the DPPH experiment, six different pigment concentrations (0.24, 0.36, 0.48, 0.60, 0.72, and 0.84 μg/μL) were prepared in each Eppendorf tube, totaling 1 mL (1000 μL). For this purpose, 200, 300, 400, 500, 600, and 700 μL of the stock pigment solution were taken, respectively, and the volume of each tube was completed to 1 mL with 200 μM DPPH solution. Thus, the ratio of the stock pigment solution in the tubes was varied between 20–70% to obtain the working concentrations. All tubes used in the experiment were gently mixed and incubated in the dark at room temperature for 30 minutes. During this period, the pigment reacted with the DPPH radical, causing a decrease in the purple color of the solution. For 30 minutes, the reaction mixtures were incubated at room temperature and in the dark. The percentage of DPPH radical scavenging at each concentration was calculated using Equation 2.1. Experimental observations of antioxidant interaction and color change from purple to yellow after 15 and 30 minutes are displayed in Figure 3.18.

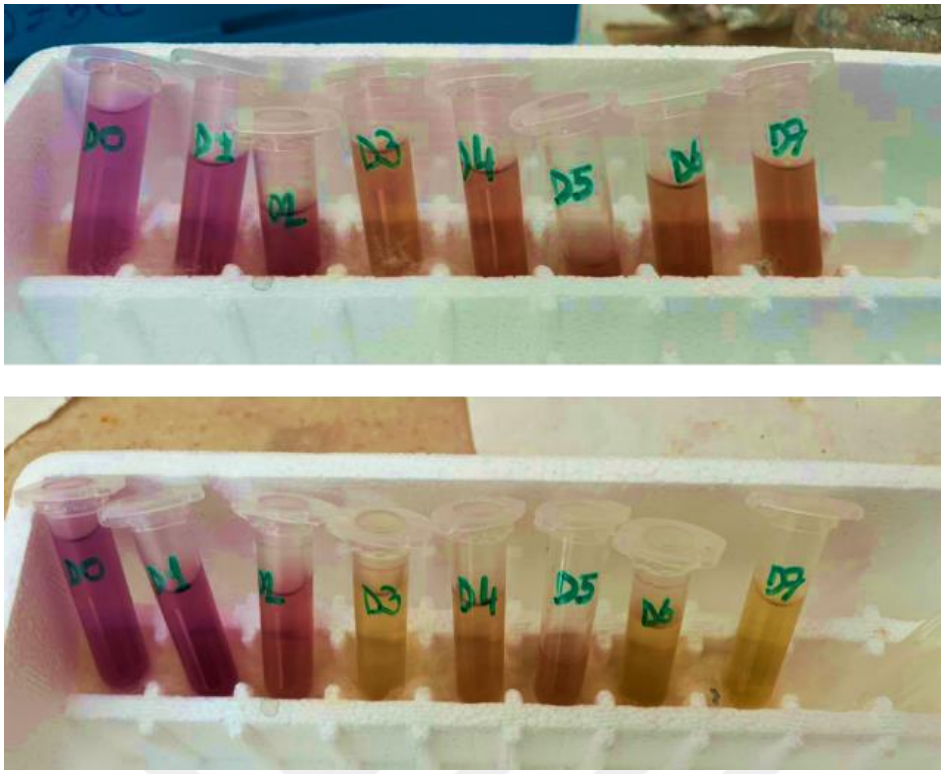

Figure 3.18 : DPPH solution turns from purple to yellow after 15 and 30 minutes of antioxidant interaction.

A_{517} absorbances and calculated percentage inhibition values of the tubes used in the DPPH experiment are given in Table 3.7.

Table 3.7 : Solution volumes, pigment concentrations, A_{517} absorbances and calculated percentage inhibition values of the tubes used in the DPPH experiment.

Sample	Pigment Solution (µL)	Pigment concentration (µg/µL)	Absorbance (A)	Inhibition %
D_2	200	0.24	0.501	17.46
D_3	300	0.36	0.302	50.19
D_4	400	0.48	0.219	63.92
D_5	500	0.6	0.206	66
D_6	600	0.72	0.127	79.08
D_7	700	0.84	0.091	84.99

In this study, the control group (D_0) was made up entirely of DPPH solution and methanol, with no pigment. The absorbance value of this control solution measured at 517 nm (A_{517} = 0.607) was used as a reference in calculating the DPPH radical scavenging percentage for all samples. To quantify DPPH radical scavenging activity, the pigment concentration with 50% inhibition (IC_{50}) was calculated. This study used the two dose-response curve points closest to 50%: 0.24 µg/µL (D_2), which provided 17.46% inhibition, and 0.36 µg/µL (D_3), which provided 50.19% inhibition. As a

result, the pigment extract's IC_{50} value was calculated to be 0.36 µg/µL. A linear model was used in this study to determine the correlation between pigment concentration and DPPH radical scavenging percentage. Figure 3.19 depicts the association between pigment concentration and DPPH inhibition.

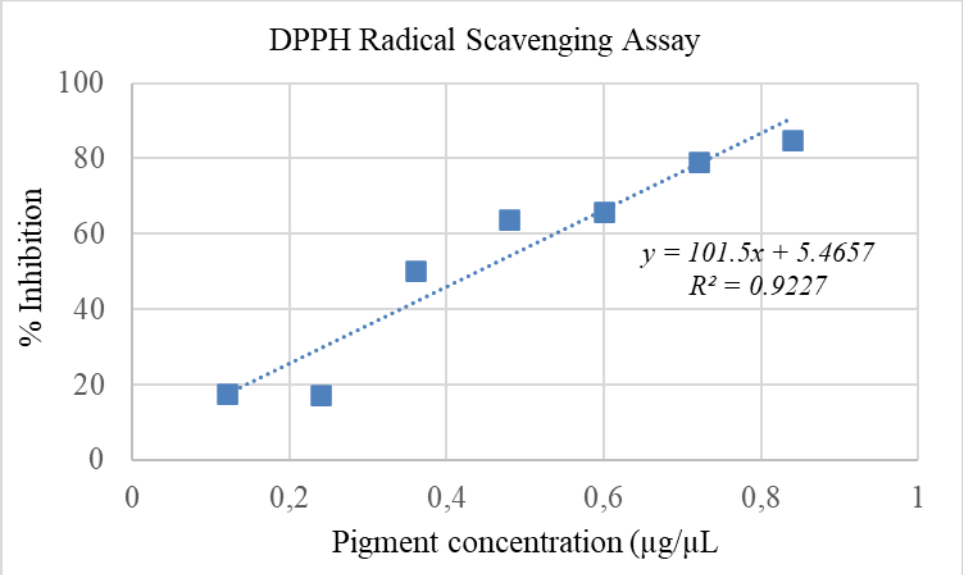

Figure 3.19 : DPPH radical scavenging activity of the pigment extract from *Rhodococcus fascians* as a function of concentration.

The pigment concentration (µg/µL) and the percentage of DPPH radical scavenging are represented by x and y, respectively. A positive slope indicates that increasing the pigment concentration significantly increases the percentage of DPPH radical scavenging. The linear model explains 92% of the variance in the data, with a strong linear relationship between concentration and percentage inhibition in the studied concentration range ($R^2 = 0.92$). Therefore, the relevant regression equation was used with confidence to estimate inhibition values for intermediate concentrations and to calculate IC_{50}.

3.2.8 Nuclear magnetic resonance (NMR) Analysis

The purified carotenoid-type pigment was analyzed structurally using ^{1}H and ^{13}C NMR. The ^{1}H NMR spectrum was recorded at 500 MHz, and the ^{13}C NMR spectrum was recorded at room temperature on an NMR spectrometer operating at 126 MHz. The solvent was $CDCl_3$, and the internal standard was TMS (tetramethylsilane). The data were analyzed to determine the chemical shift regions of the pigment's protons and carbon atoms, as well as its structural properties. Chemical shifts (δ) are expressed in ppm. *Brevibacterium* sp. and *Microbacterium* sp. microorganisms studied at the

University of Camerino in Italy were unable to undergo NMR, TLC, SEM and DPPH analyses due to a lack of sufficient pigment stock and the inability to transport culture samples to Turkey. Pigment extraction for both bacterial species was performed using only pure ethanol due to the lack of alternative organic solvents in the University of Camerino's laboratory. Therefore, a comparison of extraction efficiencies with different solvents was not possible. Figure 3.20- Figure 3.21 shows ^{1}H (500 MHz, $CDCl_3$) and spectra of the pigment isolated from *Rhodococcus fascians*. The upper right and lower left panels show expanded regions of the aromatic (δ 7.5–5.5 ppm) and aliphatic (δ 1.8–0.4 ppm) proton signals, respectively.

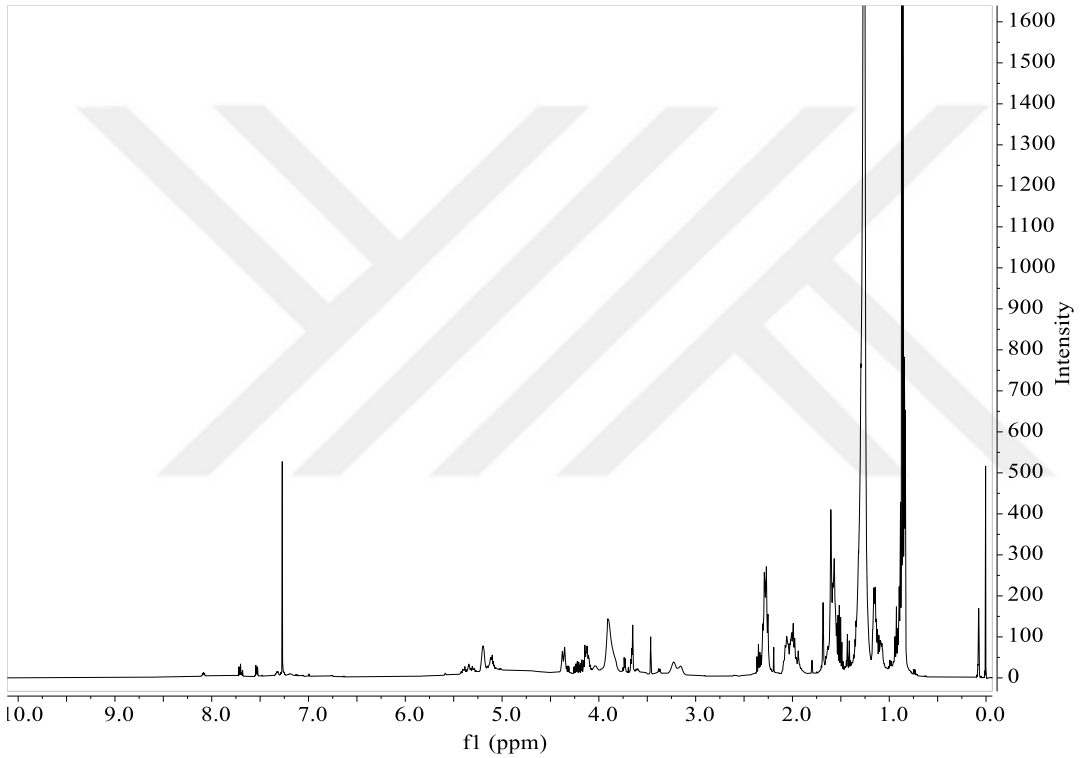

Figure 3.20 : ^{1}H spectra of the pigment isolated from *Rhodococcus fascians.*

^{1}H NMR gives information about the hydrogen environment and molecular arrangement, while ^{13}C NMR shows the carbon skeleton of the molecule. The presence of oxygenated proton signals in the 3–4 ppm region is the key NMR feature detecting xanthophylls from carotenes.

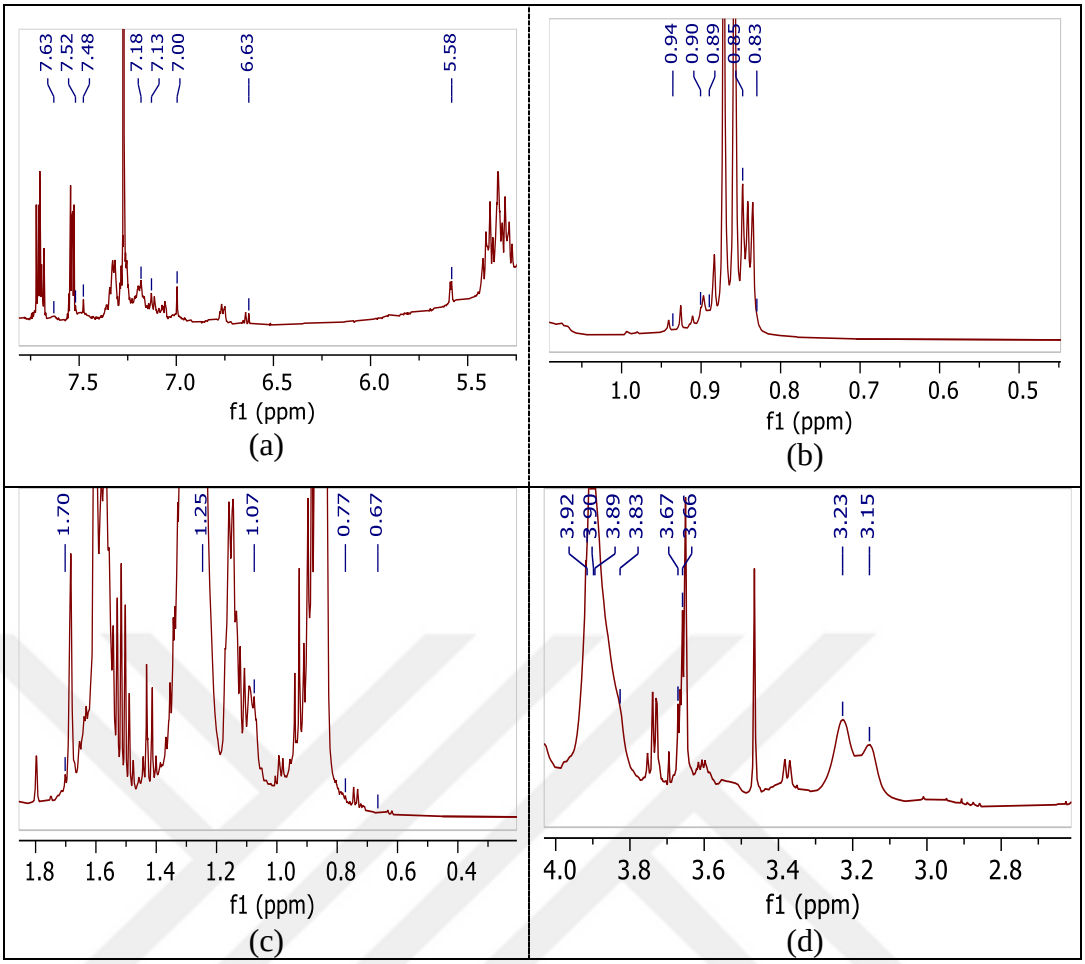

Figure 3.21 : ^{1}H spectra show expanded regions of the aromatic (a), aliphatic (b-c), multiple O-alkyl-type (d) proton signals.

The^{1}H NMR spectrum (500 MHz, $CDCl_3$) showed signals at δ 3.94–3.89 (m, 4H), 2.37 (s, 3H), 2.29 (s, 2H), 1.67–1.54 (m, 5H), 1.38–1.24 (m, 40H), 0.93 (s, 4H), 0.98–0.82 (m, 15H), and 0.08 (d, J = 3.4 Hz, 1H). Multiple signals in the olefinic region (δ 6.0–7.0 ppm) and multiple methyl resonances between δ 0.9–2.2 ppm are seen in the spectrum, which are indicative of a conjugated carotenoid/xanthophyll structure. Carotenoids' 1H NMR spectra have been reported to exhibit signals in the range of 1.2-1.6 ppm for alkyl chain CH_2 protons and 0.8-1.0 ppm for terminal CH_3 protons [80]. Figure 3.22- Figure 3.23 shows ^{13}C NMR (126 MHz, $CDCl_3$) spectra of the pigment isolated from *Rhodococcus fascians*.

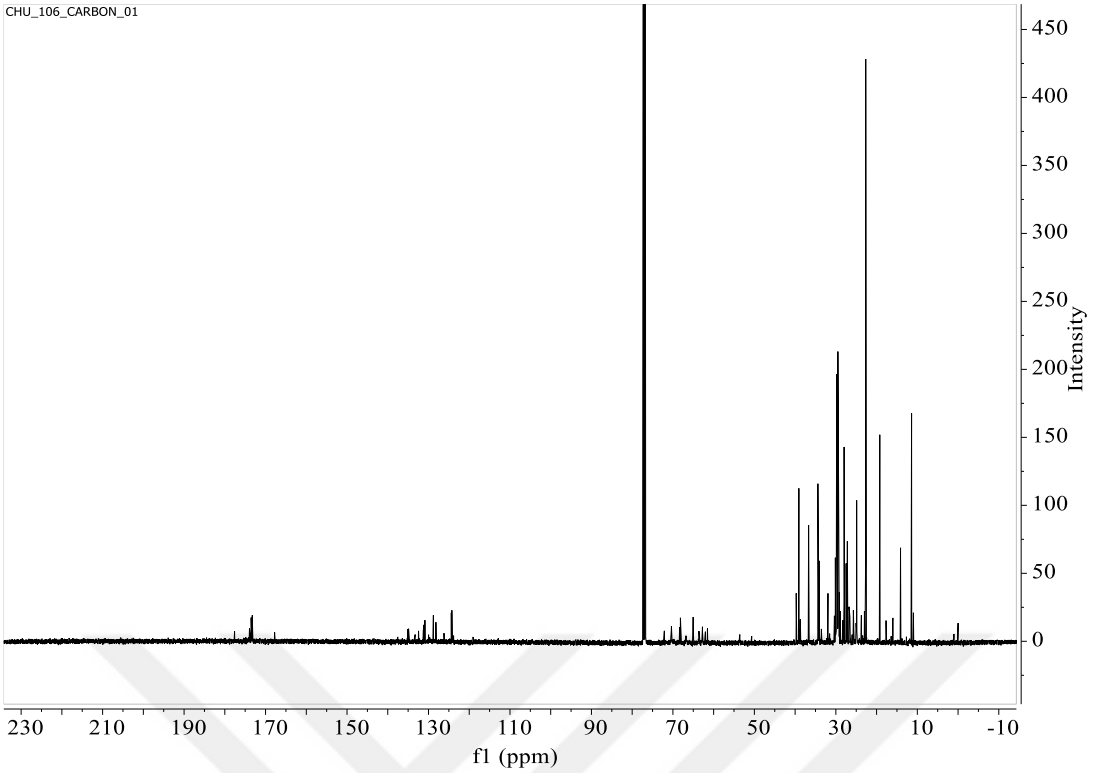

Figure 3.22 : ^{13}C NMR spectra of the pigment isolated from *Rhodococcus fascians.*

Resonances in the range of δ 15–40 ppm for aliphatic CH_3/CH_2 carbons, δ 60–75 ppm for oxygenated C–O carbons, δ 120–140 ppm for olefinic carbons of the conjugated polyene chain, and δ 167–178 ppm for carbonyl or ester-type C=O carbons were observed in the ^{13}C NMR spectrum (126 MHz, $CDCl_3$).

In xanthophylls such as zeaxanthin/lutein, C–OH carbons (alcoholic carbons) have a δ of 62–75 ppm. ^{13}C NMR supports the identification of the pigment as a xanthophyll-type carotenoid by detecting conjugated C=C carbons, oxygenated C–O carbons, and isoprenoid methyl carbons. Additionally, no distinct resonances attributable to aromatic carbons in the 110–120 ppm region were observed. This observation supports the linear carotenoid character of the pigment. The overall signal distribution and relative intensities are more consistent with C40 carotenoids. Furthermore, the 120–140 ppm range does not exhibit a regular pattern of intense signals; instead, the resonances are more consistent with conjugated C=C carbons.

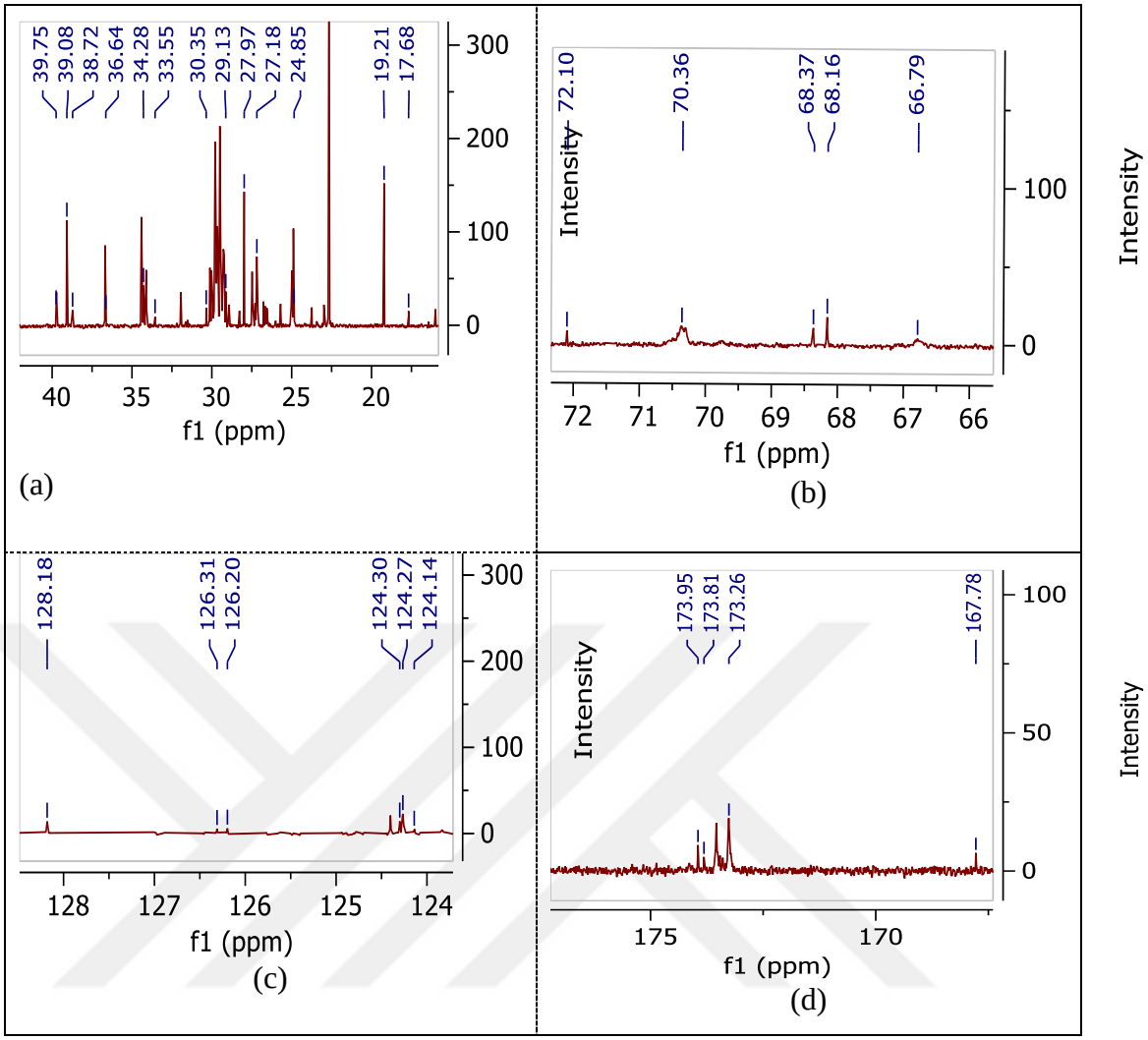

Figure 3.23 : ^{13}C NMR spectra shows expanded regions of the aliphatic (a), oxygen bound (b), olefinic- double bound (c), carbonyl-ester-group carbon signals.

3.2.9 Antibacterial activity test

The antimicrobial activity of the pigments was determined using the disk diffusion method in triplicate tests. Antimicrobial activity of the extracted pigment was tested against the human pathogens *Escherichia coli* (Gram-negative) and *Staphylococcus aureus* (Gram-positive). Trials were carried out in three parallel repetitions, all measurements were made in millimeters, and the results were used as mean ± SD (n = 3) in statistical evaluation. summarizes the inhibition zone diameters obtained through disk diffusion tests.

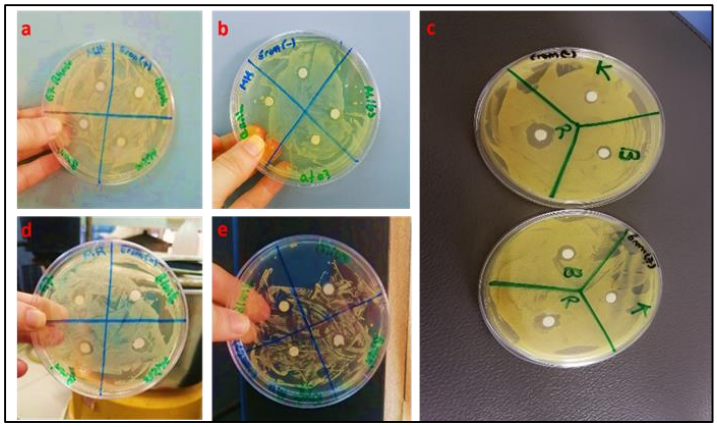

Figure 3.24 : Experimental images of the antibacterial activity of pigment extracts produced by *Rhodococcus fascians* (G7), *Brevibacterium* sp. (B), and *Microbacterium* sp. (M) against *E.coli* (Gram-) and *S.aureus* (Gram+) using the using the disk diffusion method.

Table 3.8 : Inhibition zone diameters of bacterial pigment extracts against Gram-positive and Gram-negative test strains (mm, mean ± SD, n = 3).

Microorganisms	Target	Rep1 (mm)	Rep2 (mm)	Rep3 (mm)	Average	SD	SE	Average±SD	Average±SE
R. fascians (G_7)	Gram (+)	8	9	6	7.667	1.528	0.882	7.667 ± 1.5275	7.667 ± 0.8819
R. fascians (G_7)	Gram (-)	10	11	8	9.667	1.528	0.882	9.667 ± 1.5275	9.667 ± 0.8819
Brevibacterium sp. (B)	Gram (+)	5	4	6	5.000	1.000	0.577	5 ± 1	5 ± 0.5774
Brevibacterium sp. (B)	Gram (-)	3	3	4	3.333	0.577	0.333	3.333 ± 0.5774	3.333 ± 0.3333
Microbacterium sp. (M)	Gram (+)	3	4	7	4.667	2.082	1.202	4.667 ± 2.0817	4.667 ± 1.2019
Microbacterium sp. (M)	Gram (-)	5	4	3	4.000	1.000	0.577	4 ± 1	4 ± 0.5774

The pigment fraction from *R. fascians* (G7) had the highest antibacterial activity, with zone diameters of 7.67 ± 1.53 mm for the Gram (+) test strain and 9.67 ± 1.53 mm for the Gram (-) strain (n = 3). The pigment extract from *Brevibacterium* sp. (B) showed moderate inhibition with 5.00 ± 1.00 mm for Gram (+) bacteria and 3.33 ± 0.58 mm for Gram (-). *Microbacterium* sp. pigment zone diameters were 4.67 ± 2.08 mm in the Gram (+) strain and 4.00 ± 1.00 mm in the Gram (-) strain.

4. CONCLUSION AND RECOMMENDATIONS

This study investigated the pigment biosynthetic potential of *Rhodococcus fascians*, *Brevibacterium* sp. and *Microbacterium* sp. strains isolated from ice and water samples from different regions of Antarctica. Antarctic microorganisms have become a notable biological resource for natural pigment production in recent years due to their unique adaptation mechanisms developed under extreme conditions. Therefore, optimization and characterization analyses were used to assess the pigment production potential of three distinct actinobacterial isolates. A Plackett-Burman Design (PBD) optimization study was carried out to examine the important media elements and environmental factors influencing pigment yield. For each of the three bacterial species, the optimal pH and temperature were determined, the critical media parameters affecting pigment production were identified, and the total amounts of carotenoid were calculated. (*R. fascians = 485,00 µg/g, Microbacterium* sp.*=179,89 µg/g, Brevibacterium* sp. *=63,62 µg/g*). Second place went to the *Microbacterium* sp. isolate, which had 179.89 µg/g. SEM analysis of pigments extracted from *Rhodococcus fascians* culture revealed micron-sized clusters with irregular, rough, and waxy surface morphologies in 20 µm and 50 µm images. This morphology is associated with the carotenoids combining through hydrophobic interactions during drying and accumulating as amorphous agglomerates without forming a crystalline structure. Furthermore, the absence of crystalline structures in the SEM image indicates good purity of the extracted pigment. The literature reports a wide range of specific pigment production values for strains of *Brevibacterium linens*. Guyomarc'h et al. reported a range of 0.20–0.60 mg/g, whereas Dufossé et al. found that pigment production among various strains ranged from 146 µg/g to 975 µg/g [50], [75].Research has suggested that variations in strain, culture yield, and medium composition could be the cause of this discrepancy. It is thought that variations in the amounts of medium components and the omission of casamino acid composition from this experimental procedure could be cause factors for the variation in yield when the culture compositions in these two articles were analyzed for study conditions. The highest pigment yield for *Microbacterium* sp. found in this investigation was 179.89 µg/g. Compared to the relatively high pigment yield of 7.5

mg/g obtained in a study by Ojha et al., glucose, in particular, was reported to negatively affect carotenoid yield, while sucrose and mannose increased pigment production [72]. The lower level of 179.89 μg/g obtained by *Microbacterium* sp. supports the inhibitory effect of glucose on carotenoid biosynthesis. This result suggests that the choice of carbon source is a determinant of pigment biosynthesis and that glucose may reduce yield by triggering metabolic repression mechanisms in some species.

Additionally, it was found that *Rhodococcus fascians* had a higher pigment yield (485.00 μg/g) than other *Rhodococcus* species reported in the literature. Specifically, it exhibits 4–8-fold higher pigment production than *R. sp. ANT_H53B* strain and approximately 30-fold higher than *Rhodococcus* sp. strains in Fe-supplemented medium [76] [77]. In contrast, a 2023 study found that *Rhodococcus aetherivorans* produced 6.4 mg/g of carotenoids in a glucose-containing medium and 3.0 mg/g in agricultural waste sources like straw hydrolysate [78]. This high production capacity is due to the strain's fully functioning MEP biosynthesis pathway.

The basic chromophore characteristics of the pigments were revealed by the UV-Vis results. UV-Vis analysis of the three isolates revealed a strong resemblance to the carotenoid/xanthophyll character of the *Rhodococcus fascians* pigment, the diaromatic carotenoid isorenieraten of the *Brevibacterium* sp. isolate, and the spectral peaks of neurosporene-derived pigments in *Microbacterium* sp. FTIR analyses also supported these findings. Three isolates' spectra showed aliphatic C-H stretches in the 2920-2850 cm^{-1} region, conjugated C=C bands in the 1600-1650 cm^{-1} region, and carbonyl signals in the 1700-1730 cm^{-1} range. These bands represent the polyene chain structure of carotenoids. When the pigment concentrations and biomass ratios of three different bacterial species were compared, pigment performances of 0.868 gr/L for *Rhodococcus fascians*, 0.836 mg/L for *Brevibacterium* sp., and 0.554 mg/L for *Microbacterium* sp. were obtained. Although the total pigment concentrations measured at pH 7 were comparable in *Rhodococcus fascians* and *Brevibacterium* sp. cultures (0.868 and 0.836 mg/L, respectively), there was a significant difference in specific yield. While the calculated pigment content in *R. fascians* was 0.482 mg/g, this value remained at 0.058 mg/g in *Brevibacterium* sp. This demonstrates that in *Brevibacterium* sp, the metabolic flux is primarily directed toward primary growth, with carotenoids synthesized in smaller amounts per cell. In other words, the higher specific pigment yield observed in *R. fascians* despite similar volumetric

concentrations indicates that carotenoid biosynthesis pathways are more strongly up-regulated in this species, whereas the carbon flux in *Brevibacterium* sp. is primarily directed to primary growth processes. The difference in absorbances can be attributed to two factors: quantity (total pigment concentration) and quality. *Rhodococcus fascians* and *Brevibacterium* sp. have very similar pigment concentration mg/L values, so the expected similar absorbance data is a physically reasonable result. *Microbacterium* sp. absorbs less because its total pigment content is lower. The second factor, the various pigment types, can be interpreted as the qualitative cause of this difference. In other words, pigment mixtures from different species differ in terms of conjugated system length and aromatic substitution level. This affects both the λ_max values and the molar absorption coefficient (ε) at the chosen wavelength. The number of conjugated double bonds in different carotenoid pigments, whether the rings are aromatic, and structures such as hydroxyl, keto, glycosyl, etc., at the end rings can all explain the differences in UV-Vis absorbances.

The *R. fascians* extract produced two distinct bands in TLC analysis used to determine pigment composition (*Rf: 0.84 and 0.31*). The β-carotene standard used for comparison had an Rf value of 0.92. The first band's migration near the standard indicates that the pigment has a carotenoid structure resembling that of β-carotene. The lower Rf value of the second band indicates the presence of polar components in the mixture. These findings suggested that rather than being a single molecule, *Rhodococcus fascians* pigments might be a combination of carotenoids. Analysis of *R. fascians* pigment using 1H and ^{13}C NMR provided compelling evidence for the existence of a carotenoid skeleton. The typical spectral characteristics of carotenoids are supported by the broad aliphatic region signals (δ 0.8-2.2 ppm), olefinic carbon signals in the range of 120-140 ppm in ^{13}C NMR, and vinylic proton signals between 5 and 7 ppm in 1H NMR. The pigment's polyene structure with long conjugated chains is confirmed by the prominent observation of different CH_2/CH_3 chains. Both Gram-positive and Gram-negative bacteria were inhibited by the pigments, according to antibacterial tests. Using the DPPH free radical scavenging test, the study also assessed *Rhodococcus fascians* pigment's antioxidant capacity. The pigment's DPPH inhibition increased from 17.46% to 84.99%, with an IC_{50} value of approximately 0.36 μg/μL calculated by linear regression, indicating a strong antioxidant effect. The calculated R^2 value of 0.8817 supports the validity of the model.

The IC_{50} value calculated for *Rhodococcus fascians* pigment in this study (0.36 μg/μL) appears relatively moderate compared to the very low values reported in the literature for some bacterial carotenoids. However, this difference is scientifically fully expected and methodologically consistent considering the purity level, chemical composition, and experimental conditions of the pigment sample used in this study. First, antioxidant analyses in this study were conducted using crude pigment extracts. Crude extracts contain not only the target pigment but also numerous impurities such as lipophilic membrane components, phospholipids, and protein residues. This dilutes the true concentration of the carotenoid molecule in solution, thereby reducing its DPPH radical scavenging capacity, resulting in an increase in the apparent IC_{50} value. In contrast, the vast majority of the lowest IC_{50} values reported in the literature were calculated on high-purity, chromatographically separated single carotenoid compounds.

This study demonstrates that bacteria isolated from various Antarctic regions have pigment-producing capacity. This potential is exciting for biotechnological applications. The UV resistance of these promising pigments should be evaluated, and their use in paint formulations and application to cold surfaces should be investigated in the future.

REFERENCES

[1] **F. Hund,** "Inorganic Pigments: Bases for Colored, Uncolored, and Transparent Products," *Angewandte Chemie International Edition in English*, vol. 20, no. 9, pp. 723–730, 1981, doi: 10.1002/anie.198107231.

[2] **S. Jose, D. Joshy, S. B. Narendranath, and P. Periyat,** "Recent Advances in Infrared Reflective Inorganic Pigments," *Solar Energy Materials and Solar Cells*, vol. 194, pp. 7–27, Jun. 2019, doi: 10.1016/j.solmat.2019.01.037.

[3] **T. Sen, C. J. Barrow, and S. K. Deshmukh,** "Microbial Pigments in the Food Industry—Challenges and the Way Forward," *Frontiers in Nutrition*, vol. 6, art. no. 7, Mar. 2019, doi: 10.3389/fnut.2019.00007.

[4] **B. Harrow,** "William Henry Perkin," *The Scientific Monthly*, vol. 9, no. 3, pp. 234–245, Sep. 1919.

[5] **A. Kumar, H. S. Vishwakarma, J. Singh, S. Dwivedi, and M. Kumar,** "Microbial Pigments: Production and Their Applications in Various Industries," *International Journal of Pharmaceutical, Chemical and Biological Sciences (IJPCBS)*, vol. 5, no. 1, pp. 203–212, 2015.

[6] **A. Das, S.-H. Yoon, S.-H. Lee, J.-Y. Kim, D.-K. Oh, and S.-W. Kim,** "An Update on Microbial Carotenoid Production: Application of Recent Metabolic Engineering Tools," *Applied Microbiology and Biotechnology*, vol. 77, no. 3, pp. 505–512, Dec. 2007, doi: 10.1007/s00253-007-1206-3.

[7] **G. D. López, G. Álvarez-Rivera, C. Carazzone, E. Ibáñez, C. Leidy, and A. Cifuentes,** "Bacterial Carotenoids: Extraction, Characterization, and Applications," *Critical Reviews in Analytical Chemistry*, vol. 53, no. 6, pp. 1239–1262, 2023, doi: 10.1080/10408347.2021.2016366.

[8] **W. N. Hunter,** "The Non-Mevalonate Pathway of Isoprenoid Precursor Biosynthesis," *Journal of Biological Chemistry.*, vol. 282, no. 30, pp. 21573–21577, 2007, doi: 10.1074/jbc.R700005200.

[9] **V. Ashokkumar, G. Flora, M. Sevanan, R. Sripriya, W. H. Chen, J.-H. Park, J. Rajesh Banu, and G. Kumar,** "*Technological Advances in the Production of Carotenoids and Their Applications—A Critical Review," Bioresource Technology*, vol. 367, art. no. 128215, Jan. 2023, doi: 10.1016/j.biortech.2022.128215.

[10] **P. D. Fraser, S. Romer, C. A. Shipton, P. B. Mills, J. W. Kiano, N. Misawa, R. G. Drake, W. Schuch, and P. M. Bramley,** "Evaluation of Transgenic Tomato Plants Expressing an Additional Phytoene Synthase in a Fruit-Specific Manner," *Proceedings of the National Academy of Sciences of the United States of America*, vol. 99, no. 2, pp. 1092–1097, Jan. 2002, doi: 10.1073/pnas.241374598.

[11] **C. U. Mussagy, J. Winterburn, V. C. Santos-Ebinuma, et al.,** "Production and Extraction of Carotenoids Produced by Microorganisms," *Applied Microbiology and Biotechnology*, vol. 103, no. 3, pp. 1095–1114, Feb. 2019, doi: 10.1007/s00253-018-9557-5.

[12] **J. Clotault, D. Peltier, V. Soufflet-Freslon, et al.,** "Differential Selection on Carotenoid Biosynthesis Genes as a Function of Gene Position in the Metabolic Pathway: A Study on the Carrot and Dicots," *PLoS ONE*, vol. 7, no. 6, art. no. e38724, Jun. 2012, doi: 10.1371/journal.pone.0038724.

[13] **S. Wagener, T. Völker, S. De Spirt, H. Ernst, and W. Stahl,** "3,3′-Dihydroxyisorenieratene and Isorenieratene Prevent UV-Induced DNA Damage in Human Skin Fibroblasts," *Free Radical Biology and Medicine*, vol. 53, no. 3, pp. 457–463, Aug. 2012, doi: 10.1016/j.freeradbiomed.2012.05.022.

[14] **D. B. Rodriguez-Amaya and M. Kimura,** HarvestPlus Handbook for Carotenoid Analysis, *HarvestPlus Technical Monograph* 2. Washington, DC and Cali, 2004, pp. 15, 31, 46."

[15] **F. P. Rattray and P. F. Fox,** "Aspects of Enzymology and Biochemical Properties of Brevibacterium linens Relevant to Cheese Ripening: A Review," *Journal of Dairy Science*, vol. 82, no. 5, pp. 891–909, 1999, doi: 10.3168/jds.S0022-0302(99)75308-7.

[16] **A. S. Benditkis, A. A. Ashikhmin, A. A. Moskalenko, and A. A. Krasnovsky,** "Photogeneration and Quenching of Singlet Molecular Oxygen by Bacterial C40 Carotenoids with Long Chain of Conjugated Double Bonds," *Photosynthesis Research*, vol. 159, no. 2–3, pp. 291–301, 2024, doi: 10.1007/s11120-023-01070-6.

[17] **J. Fiedor, A. Sulikowska, A. Orzechowska, L. Fiedor, and K. Burda,** "Antioxidant Effects of Carotenoids in a Model Pigment–Protein Complex," *Acta Biochimica Polonica*, vol. 59, no. 1, pp. 61–64, 2012, doi: 10.18388/abp.2012_2172.

[18] **M. C. P. P. Reis-Mansur et al.,** "Carotenoids from UV-Resistant Antarctic Microbacterium sp. LEMMJ01," *Scientific Reports*, vol. 9, art. no. 9554, 2019, doi: 10.1038/s41598-019-45840-6.

[19] **A. Baricz et al.,** "Investigating the Potential Use of an Antarctic Variant of Janthinobacterium lividum for Tackling Antimicrobial Resistance in a One Health Approach," *Scientific Reports*, vol. 8, no. 1, art. no. 15272, 2018, doi: 10.1038/s41598-018-33691-6.

[20] **N. Mojib, R. Philpott, J. P. Huang, M. Niederweis, and A. K. Bej,** "Antimycobacterial Activity In Vitro of Pigments Isolated from Antarctic Bacteria," *Antonie van Leeuwenhoek*, vol. 98, no. 4, pp. 531–540, 2010, doi: 10.1007/s10482-010-9470-0.

[21] **N. Órdenes-Aenishanslins, G. Anziani-Ostuni, M. Vargas-Reyes, J. Alarcón, A. Tello, and J. M. Pérez-Donoso,** "Pigments from UV-Resistant Antarctic Bacteria as Photosensitizers in Dye-Sensitized Solar Cells," *Journal of Photochemistry and Photobiology B: Biology*, vol. 162, pp. 707–714, 2016, doi: 10.1016/j.jphotobiol.2016.08.004.

[22] **J. M. Seddon,** "Dietary Carotenoids, Vitamins A, C, and E, and Advanced Age-Related Macular Degeneration: Eye Disease Case-Control Study Group," *Journal of the American Medical Association*, vol. 272, no. 18, pp. 1413–1420, 1994, doi: 10.1001/jama.272.18.1413.

[23] **X. Lyu, Y. Lyu, H. Yu, W. N. Chen, L. Ye, and R. Yang,** "Biotechnological Advances for Improving Natural Pigment Production: A State-of-the-Art Review," *Bioresources and Bioprocessing*, vol. 9, no. 1, art. no. 8, 2022, doi: 10.1186/s40643-022-00497-4.

[24] **H. O. Boo, S. J. Hwang, C. S. Bae, S. H. Park, B. G. Heo, and S. Gorinstein,** "Extraction and Characterization of Some Natural Plant Pigments," *Industrial Crops and Products*, vol. 40, no. 1, pp. 129–135, 2012, doi: 10.1016/j.indcrop.2012.02.042.

[25] **L. G. Buttle, V. O. Crampton, and P. D. Williams,** "The Effect of Feed Pigment Type on Flesh Pigment Deposition and Colour in Farmed Atlantic Salmon, Salmo salar L.," *Aquaculture Research*, vol. 32, no. 2, pp. 103–111, 2001, doi: 10.1046/j.1365-2109.2001.00536.x.

[26] **P. S. Hamano and B. V. Kilikian,** "Production of Red Pigments by Monascus ruber in Culture Media Containing Corn Steep Liquor," *Brazilian Journal of Chemical Engineering*, vol. 23, no. 4, pp. 443–449, 2006, doi: 10.1590/S0104-66322006000400002.

[27] **T. Sopandi, A. Wardah, T. Surtiningsih, A. Suwandi, and J. J. Smith,** "Utilization and Optimization of a Waste Stream Cellulose Culture Medium for Pigment Production by Penicillium spp.," *Journal of Applied Microbiology*, vol. 114, no. 3, pp. 733–745, 2013, doi: 10.1111/jam.12110.

[28] **J. Tinoi, N. Rakariyatham, and R. L. Deming,** "Simplex Optimization of Carotenoid Production by Rhodotorula glutinis Using Hydrolyzed Mung Bean Waste Flour as Substrate," *Process Biochemistry*, vol. 40, no. 7, pp. 2551–2557, 2005, doi: 10.1016/j.procbio.2004.11.005.

[29] **R. Chaib and M. Barone,** Chemicals in the Food Industry, SpringerBriefs in Molecular Science. Cham: *Springer International Publishing*, 2020, pp. 58–59, doi: 10.1007/978-3-030-42943-0.

[30] **M. P. Narsing Rao, M. Xiao, and W.-J. Li,** "Fungal and Bacterial Pigments: Secondary Metabolites with Wide Applications," *Frontiers in Microbiology*, vol. 8, art. no. 1113, 2017, doi: 10.3389/fmicb.2017.01113.

[31] **J. Garrido-Fernández, A. Maldonado-Barragán, B. Caballero-Guerrero, D. Hornero-Méndez, and J. L. Ruiz-Barba,** "Carotenoid Production in Lactobacillus plantarum," *International Journal of Food Microbiology*, vol. 140, no. 1, pp. 34–39, 2010, doi: 10.1016/j.ijfoodmicro.2010.02.015.

[32] **A. K. P. Harris et al.,** "The Serratia Gene Cluster Encoding Biosynthesis of the Red Antibiotic, Prodigiosin, Shows Species- and Strain-Dependent Genome Context Variation," *Microbiology*, vol. 150, no. 11, pp. 3547–3560, 2004, doi: 10.1099/mic.0.27222-0.

[33] **S. Jayaseelan, D. Ramaswamy, and S. Dharmaraj,** "Pyocyanin: Production, Applications, Challenges and New Insights," *World Journal of Microbiology and Biotechnology*, vol. 30, no. 4, pp. 1159–1168, 2014, doi: 10.1007/s11274-013-1552-5.

[34] **S. Ichiyama, K. Shimokata, and M. Tsukamura,** "Carotenoid Pigments of Genus Rhodococcus," *Microbiology and Immunology*, vol. 33, no. 6, pp. 503–508, 1989, doi: 10.1111/j.1348-0421.1989.tb01999.x.

[35] **A. Osawa, A. Kasahara, S. Matsuoka, S. Gassel, G. Sandmann, and K. Shindo,** "Isolation of a Novel Carotenoid, OH-Chlorobactene Glucoside Hexadecanoate, and Related Rare Carotenoids from Rhodococcus sp. CIP and Their Antioxidative Activities," *Bioscience, Biotechnology, and Biochemistry*, vol. 75, no. 11, pp. 2142–2147, 2011, doi: 10.1271/bbb.110441.

[36] **T. Correa and F. Abreu,** "Antarctic Microorganisms as Sources of Biotechnological Products," *Physiological and Biotechnological Aspects of Extremophiles*, 2020, pp. 269–284, doi: 10.1016/B978-0-12-818322-9.00020-4.

[37] **L. Núñez-Pons, C. Avila, G. Romano, C. Verde, and D. Giordano,** "UV-Protective Compounds in Marine Organisms from the Southern Ocean," *Marine Drugs*, vol. 16, no. 9, art. no. 336, 2018, doi: 10.3390/md16090336.

[38] **P. Akilandeswari and B. V. Pradeep,** "Exploration of Industrially Important Pigments from Soil Fungi," *Applied Microbiology and Biotechnology*, vol. 100, no. 4, pp. 1631–1643, 2016, doi: 10.1007/s00253-015-7231-8.

[39] **L. Liao et al.,** "Biosynthetic Potential of a Novel Antarctic Actinobacterium Marisediminicola antarctica ZS314T Revealed by Genomic Data Mining and Pigment Characterization," *Marine Drugs*, vol. 17, no. 7, art. no. 388, 2019, doi: 10.3390/md17070388.

[40] **T. R. E. Silva et al.,** "Pigments from Antarctic Bacteria and Their Biotechnological Applications," *Critical Reviews in Biotechnology*, vol. 41, no. 6, pp. 809–826, 2021, doi: 10.1080/07388551.2021.1888068.

[41] **D. N. Correa-Llantén, M. J. Amenábar, and J. M. Blamey,** "Antioxidant Capacity of Novel Pigments from an Antarctic Bacterium," *Journal of Microbiology*, vol. 50, no. 3, pp. 374–379, 2012, doi: 10.1007/s12275-012-2029-1.

[42] **D. H. Zhang, Y. K. Lee, M. L. Ng, and S. M. Phang,** "Composition and Accumulation of Secondary Carotenoids in Chlorococcum sp.," *Journal of Applied Phycology*, vol. 9, no. 2, pp. 147–155, 1997, doi: 10.1023/A:1007926528388.

[43] **M. Dieser, M. Greenwood, and C. M. Foreman,** "Carotenoid Pigmentation in Antarctic Heterotrophic Bacteria as a Strategy to Withstand Environmental Stresses," *Arctic, Antarctic, and Alpine Research*, vol. 42, no. 4, pp. 396–405, 2010, doi: 10.1657/1938-4246-42.4.396.

[44] **M. Dworkin, S. Falkow, E. Rosenberg, K.-H. Schleifer, and E. Stackebrandt, Eds.,** The Prokaryotes: Vol. 3: Archaea. Bacteria: Firmicutes, Actinomycetes, *3rd ed. New York, NY: Springer*, 2006, pp. 297, 1013, doi: 10.1007/0-387-30743-5.

[45] **G. Funke, A. von Graevenitz, J. E. Clarridge, and K. A. Bernard,** "Clinical Microbiology of Coryneform Bacteria," *Clinical Microbiology Reviews*, vol. 10, no. 1, pp. 125–159, 1997, doi: 10.1128/cmr.10.1.125.

[46] **C. Pascual and M. D. Collins,** "Brevibacterium avium sp. nov., Isolated from Poultry," *International Journal of Systematic Bacteriology*, vol. 49, no. 4, pp. 1527–1530, 1999, doi: 10.1099/00207713-49-4-1527.

[47] **B. Whitman, M. Goodfellow, P. Kämpfer, H.-J. Busse, M. E. Trujillo, K.-I. Suzuki, et al.,** Eds., Bergey's Manual of Systematic Bacteriology: Volume 5: The Actinobacteria, *2nd ed. New York, NY: Springer*, 2012, pp. 437, 685, doi: 10.1007/978-0-387-68233-4.

[48] **H. J. Nelis and A. P. De Leenheer,** "Reinvestigation of Brevibacterium sp. Strain KY-4313 as a Source of Canthaxanthin," *Applied and Environmental Microbiology*, vol. 55, no. 10, pp. 2505–2510, 1989, doi: 10.1128/aem.55.10.2505-2510.1989.

[49] **M.-A. Laneelle et al.,** "Biological and Chemical Bases for the Reclassification of Brevibacterium vitarumen (Bechdel et al.) Breed (Approved Lists, 1980) as Corynebacterium vitarumen (Bechdel et al.) comb. nov. and Brevibacterium liquefaciens Okabayashi and Masuo (Approved Lists, 1980) as Corynebacterium liquefaciens (Okabayashi and Masuo) comb. nov.," *International Journal of Systematic Bacteriology*, vol. 30, no. 3, pp. 539–546, 1980.

[50] **F. Guyomarc'h, A. Binet, and L. Dufossé,** "Production of Carotenoids by Brevibacterium linens: Variation Among Strains, Kinetic Aspects and HPLC Profiles," *Journal of Industrial Microbiology and Biotechnology*, vol. 24, no. 1, pp. 64–70, 2000, doi: 10.1038/sj.jim.2900761.

[51] **E. Stackebrandt, F. A. Rainey, and N. L. Ward-Rainey,** "Proposal for a New Hierarchic Classification System, Actinobacteria classis nov.," *International Journal of Systematic Bacteriology*, vol. 47, no. 2, pp. 479–491, 1997, doi: 10.1099/00207713-47-2-479.

[52] **E. Y. Epova et al.,** "Heterotrophic Microbiota from the Oligotrophic Waters of Lake Vostok, Antarctica," *International Journal of Environmental Research and Public Health*, vol. 19, no. 7, art. no. 4025, 2022, doi: 10.3390/ijerph19074025.

[53] **R. Koshti et al.,** "Evaluation of Antioxidant Potential and UV Protective Properties of Four Bacterial Pigments," *Microbiology and Biotechnology Letters.*, vol. 50, no. 3, pp. 375–386, 2022, doi: 10.48022/mbl.2205.05010.

[54] **E. Armadillo, E. Bozzo, M. Gambetta, and D. Rizzello,** "Impact of Human Activities on the Geomagnetic Field of Antarctica: A High-Resolution Aeromagnetic Survey over Mario Zucchelli Station," *Environment International*, vol. 47, pp. 1–7, 2012, doi: 10.1016/j.envint.2012.05.005.

[55] **T. H. Jukes and C. R. Cantor,** "Evolution of Protein Molecules," *Mammalian Protein Metabolism*, 1969, pp. 21–132, doi: 10.1016/B978-1-4832-3211-9.50009-7.

[56] **S. Kumar, G. Stecher, and K. Tamura,** "MEGA7: Molecular Evolutionary Genetics Analysis Version 7.0 for Bigger Datasets," *Molecular Biology and Evolution*, *vol*. 33, no. 7, pp. 1870–1874, 2016, doi: 10.1093/molbev/msw054.

[57] **F. Cappa, N. Suciu, M. Trevisan, S. Ferrari, E. Puglisi, and P. S. Cocconcelli,** "Bacterial Diversity in a Contaminated Alpine Glacier as Determined by Culture-Based and Molecular Approaches," *Science of the Total Environment*, vol. 497–498, pp. 50–59, 2014, doi: 10.1016/j.scitotenv.2014.07.094.

[58] **L. Butinar, I. Spencer-Martins, and N. Gunde-Cimerman,** "Yeasts in High Arctic Glaciers: The Discovery of a New Habitat for Eukaryotic Microorganisms," *Antonie van Leeuwenhoek*, vol. 91, no. 3, pp. 277–289, 2007, doi: 10.1007/s10482-006-9117-3.

[59] **P. Singh, M. Tsuji, S. M. Singh, U. Roy, and T. Hoshino,** "Taxonomic Characterization, Adaptation Strategies and Biotechnological Potential of Cryophilic Yeasts from Ice Cores of Midre Lovénbreen Glacier, Svalbard, Arctic," *Cryobiology*, vol. 66, no. 2, pp. 167–175, 2013, doi: 10.1016/j.cryobiol.2013.01.002.

[60] **S. J. Patil and A. S. Pendse,** "Optimization of Carotenoid Production from Microbacterium oleivorans SAA1517 and Its Application as Fish Feed," Biological Forum—*An International Journal*, vol. 15, no. 2, pp. 323–332, 2023.

[61] **T. R. Silva et al.,** "Pigments in an Iridescent Bacterium, Cellulophaga fucicola, Isolated from Antarctica," *Antonie van Leeuwenhoek*, vol. 112, no. 3, pp. 479–490, 2019, doi: 10.1007/s10482-018-1179-5.

[62] **E. Forgacs and T. Cserhati,** "Thin-Layer Chromatography of Natural Pigments: New Advances," *Journal of Liquid Chromatography & Related Technologies*, vol. 25, no. 10–11, pp. 1521–1541, 2002, doi: 10.1081/jlc-120005702.

[63] **K. Mishra, H. Ojha, and N. K. Chaudhury,** "Estimation of Antiradical Properties of Antioxidants Using the DPPH Assay: A Critical Review and Results," *Food Chemistry*, vol. 130, no. 4, pp. 1036–1043, 2012, doi: 10.1016/j.foodchem.2011.07.127.

[64] **S. B. Chaturwedi, S. Mainali, and R. Chaudhary,** "Antibacterial Activity of Pigment Extracted from Bacteria Isolated from Soil Samples," *BMC Research Notes*, vol. 17, no. 1, art. no. 169, 2024, doi: 10.1186/s13104-024-06834-4.

[65] **W. A. Ahmad, W. Y. W. Ahmad, Z. A. Zakaria, and N. Z. Yusof,** Application of Bacterial Pigments as Colorant: The Malaysian Perspective, SpringerBriefs in Molecular Science. *Berlin, Heidelberg: Springer*, 2012, doi: 10.1007/978-3-642-24520-6.

[66] **M. Fuciman, G. Keşan, A. M. LaFountain, H. A. Frank, and T. Polívka,** "Tuning the Spectroscopic Properties of Aryl Carotenoids by Slight Changes in Structure," *The Journal of Physical Chemistry B,* vol. 119, no. 4, pp. 1457–1467, 2015, doi: 10.1021/jp512354r.

[67] **F. Meddeb-Mouelhi, J. K. Moisan, J. Bergeron, B. Daoust, and M. Beauregard,** "Structural Characterization of a Novel Antioxidant Pigment Produced by a Photochromogenic Microbacterium oxydans Strain," *Applied Biochemistry and Biotechnology,* vol. 180, no. 7, pp. 1286–1300, 2016, doi: 10.1007/s12010-016-2167-8.

[68] **T. Neha, T. Shishir, and D. Ashutosh,** "Fourier Transform Infrared Spectroscopy (FTIR) Profiling of Red Pigment Produced by Bacillus subtilis PD5," *African Journal of Biotechnology,* vol. 16, no. 27, pp. 1507–1512, 2017, doi: 10.5897/ajb2017.15959.

[69] **G. D. López, G. Álvarez-Rivera, C. Carazzone, E. Ibáñez, C. Leidy, and A. Cifuentes,** "Bacterial Carotenoids: Extraction, Characterization, and Applications," *Critical Reviews in Analytical Chemistry,* vol. 53, no. 6, pp. 1239–1262, 2023, doi: 10.1080/10408347.2021.2016366.

[70] **D. Martin, A. M. Amado, A. G. Gonzálvez, M. P. M. Marques, L. A. E. Batista De Carvalho, and Á. G. Ureña,** "FTIR Spectroscopy and DFT Calculations to Probe the Kinetics of β-Carotene Thermal Degradation," *The Journal of Physical Chemistry A,* vol. 123, no. 25, pp. 5266–5273, 2019, doi: 10.1021/acs.jpca.9b02327.

[71] **P. D. Kolekar, S. S. Phugare, and J. P. Jadhav,** "Biodegradation of Atrazine by Rhodococcus sp. BCH2 to N-Isopropylammelide with Subsequent Assessment of Toxicity of Biodegraded Metabolites," *Environmental Science and Pollution Research,* vol. 21, no. 3, pp. 2334–2345, 2014, doi: 10.1007/s11356-013-2151-6.

[72] **S. Ojha, S. Kapoor, and S. Mishra,** "Carotenoid Production by a Novel Isolate of Microbacterium paraoxydans," *Indian Journal of Microbiology,* vol. 58, no. 1, pp. 118–122, 2018, doi: 10.1007/s12088-017-0686-9.

[73] **M. Aspinall-O'Dea, M. Wentworth, A. Pascal, B. Robert, A. Ruban, and P. Horton,** "In Vitro Reconstitution of the Activated Zeaxanthin State Associated with Energy Dissipation in Plants," *Proceedings of the National Academy of Sciences of the United States of America,* vol. 99, no. 25, pp. 16331–16335, 2002, doi: 10.1073/pnas.252500999.

[74] **R. M. Al-Ali, S. A. H. Al-Hilifi, and A.-E.-B. H. J. Al-Mossawi,** "Extraction of Lutein from Some Plant Source in Different Conditions and Application in Food System," *Plant Archives,* vol. 20, suppl. 1, pp. 1679–1685, 2020."

[75] **L. Dufossé, P. Mabon, and A. Binet,** "Assessment of the Coloring Strength of Brevibacterium linens Strains: Spectrocolorimetry versus Total Carotenoid Extraction/Quantification," *Journal of Dairy Science,* vol. 84, no. 2, pp. 354–360, 2001, doi: 10.3168/jds.S0022-0302(01)74484-0.

[76] **M. Styczynski, A. Rogowska, K. Gieczewska, M. Garstka, A. Szakiel, and L. Dziewit,** "Genome-Based Insights into the Production of Carotenoids by Antarctic Bacteria, Planococcus sp. ANT_H30 and Rhodococcus sp. ANT_H53B," *Molecules*, vol. 25, no. 19, art. no. 4357, 2020, doi: 10.3390/molecules25194357.

[77] **L. Ortega-Cabello, H. I. Pérez-Méndez, N. Manjarrez-Alvarez, A. Solís-Oba, and A. López-Luna,** "Effect of Iron Salts on Rhodococcus sp. and Gordonia sp. on Carotenoid Production," *Revista Mexicana de Ingeniería Química*, vol. 16, no. 1, pp. 1–10, 2017.

[78] **W. Jiang et al.,** "Carotenoids Production and Genome Analysis of a Novel Carotenoid Producing Rhodococcus aetherivorans N1," *Enzyme and Microbial Technology*, vol. 164, art. no. 110190, 2023, doi: 10.1016/j.enzmictec.2022.110190.

CURRICULUM VITAE

Name Surname **:** Gülden AÇIL

EDUCATION **:**

- **B.Sc.** **:** 2011, Çanakkale Onsekiz Mart University, Faculty of Art and Sciences, Department of Biology

PROFESSIONAL EXPERIENCE AND REWARDS:

- **Ms.C. Scholar** **:** 2025, TUBITAK 1001 Research Project *(#124G027)*
- **Erasmus Intership** **:** 2025, University of Camerino, Faculty of Biology and Veterinary Medicine
- **Polar Researcher** **:** 2024, TASE IV-Turkish Arctic Scientific Expedition

OTHER PUBLICATIONS, PRESENTATIONS AND PATENTS:

- **G. Açıl,** G. N. Özcan, S. Altun, S. N. Ogujuba, A. Vassallo, C. Miceli, and S. Pucciarelli, "Antarktika sularının renklerini ortaya çıkarmak: Ross Denizi'nden izole edilen pigment üreten bakteriler," *in Proc. 9th National Polar Sciences Symposium and 5th Polar Festival*, Nov. 5–6, 2025.